

## ABSTRACT

Title of Document: DESIGN AND SYNTHESIS OF AN ELECTRON RICH QUINONE METHIDE PRECURSOR FOR SEQUENCE –DIRECTED ALKYLATION OF DNA

Chengyun Huang, Doctor of Philosophy, 2012

Directed By: Professor Steven E. Rokita, Department of Chemistry and Biochemistry

Quinone methides (QM) can be delivered to alkylate specific sites with a single strand DNA through target promoted alkylation. Previous experimental results indicated that alkylation by DNA-QM self-adduct was too slow for application in a biological system. A new quinone methide precursor (QMP) with enhanced reactivity is necessary to accelerate the reaction.

Previous study showed that an electron donating group present in the QMP would facilitate the generation of QM from the precursor and its regeneration from the reversible alkylation adducts. Therefore, new QMPs with increased electron density were designed. An electron rich QMP2 was successfully synthesized through a benzylaldehyde derivative. As predicted, DNA-QM self-adduct formation was much faster using QMP2 than using the conventional precursor QMP1 without an electron donating group. Only 20 min was needed for QM2 to complete the conversion from DNA-QMP conjugate while QM1 needed 24 hrs to finish the same

conversion. The DNA-QM2 self-adduct also exhibited faster reaction for alkylation of the target single strand. A two-day incubation was necessary to achieve its maximal yield of 20% compared to 6 days required to achieve the maximal yield of 16% for DNA-QM1.

In order to target duplex DNA, QMP was coupled to triplex forming oligonucleotides (TFO) to deliver the QM to the major groove of DNA through triple helix formation. Alkylation products were observed with the DNA-QMP1 conjugate but not the DNA-QM1 self-adducts. An adjacent guanine in the sequence can increase alkylation yield from around 10% to up to 20%. QMP2 was also coupled to the TFO to generate the self-adduct DNA-QM2. Maximal duplex alkylation yield (15%) using DNA-QM2 self-adduct was achieved in 3 days if the triplex samples were incubated at room temperature. The alkylation yield increased to 20% with the DNA-QM2 self-adduct when samples were incubated at 37 °C. The DNA-QMP2 conjugate could even be activated at 37 °C without fluoride and resulted in an alkylation yield of up to 25%. The enhanced reactivity of the electron rich QMP2 improved the duplex alkylation effectiveness and prepared it for future *in vivo* application.

DESIGN AND SYNTHESIS OF AN ELECTRON RICH QUINONE METHIDE  
PRECURSOR FOR SEQUENCE –DIRECTED ALKYLATION OF DNA

By

Chengyun Huang

Dissertation submitted to the Faculty of the Graduate School of the  
University of Maryland, College Park, in partial fulfillment  
Of the requirements for the degree of  
Doctor of Philosophy  
2012

Advisory Committee:  
Professor Steven E. Rokita, Chair  
Professor Lyle Isaacs  
Professor Herman Sintim  
Professor Douglas Julin  
Professor Jeffrey DeStefano

© Copyright by  
Chengyun Huang  
2012

# **Dedication**

TO MY PARENTS

## Acknowledgements

First and foremost, I would like to thank Professor Steve Rokita to be my advisor for my Ph.D. life. Thank you so much for giving me the chance to work on this project. I would never get over all the difficulties during my graduate studies without your guidance and support. Your valuable suggestions and patient mentoring lead me to the way of a real chemist. I feel so lucky and honored to be your student.

I would like to thank for my committees, Professor Lyle Isaacs, Herman Sintim, Douglas Julin, and Jeffery DeStefano. Thank you for your advice and support for my research and dissertation. I learned a lot from your valuable thoughts.

Thanks so much to the past and present members of Rokita group. You guys are always helpful in various ways. I have spent wonderful times with you in the past 5 years.

Thanks to Dr. Yang Liu. We shared a lot of thoughts about research and life. You were always very patient when I brought you all kinds of questions. I really appreciate all the help and support I received from you. Thanks to Dr. Huan Wang, you taught me a lot of stuff about chemistry and also fun. Michael McCrane, You are always nice and thoughtful, I am very happy to share 2514 with you for almost 5 years. Good luck with your graduation and job hunting. Dr. Jen Buss, it is always nice talking to you. Although I am not biochemist, I still enjoyed your talk and thank you for making notes for the practice talks, those are really helpful.

Thanks also go to Dr. Amy Finch, Dr. Patrick Mctamney, Dr. Kostyantyn Bobyk, Jimin Hu, Petrina Abiola Boucher and AB Fakhari. It has been a pleasure to work with you all.

I would like to thank all my friends in Maryland. Thank you for being my companions during my Ph.D. journey. We had a lot of fun together. I will always remember those happy times. Wish everyone have a wonderful life.

I want to express my special thanks to my best friends Yin Liu and Dongke Yu. You witnessed all the happiness and sorrows of my life in the States. Your unconditional supports helped me get through those days that I once thought endless and helpless. Thank you for always being there for me. I am really looking forward to going back to stay together with you two. That will be very soon now!

Finally, I would like to thank my parents. Without your help and caring, I would never reach this stage. My dearest mom, thank you for taking good care of me for all these years. I cannot express how grateful I am of being your daughter. Your days with me in the State are the happiest days I have here. I love you mom and I am finally going home now.

# Table of Contents

Dedication .....	ii
Acknowledgements .....	iii
Table of Contents .....	v
List of Tables .....	vii
List of Figures .....	viii
List of Schemes .....	xi
List of Abbreviations .....	xii
Chapter 1: Introduction .....	1
1.1 Structure of DNA and DNA alkylation type .....	1
1.2 DNA alkylation agents .....	4
1.3 Quinone Methides (QMs) and reversible alkylation of DNA .....	7
1.4 Substituent's effect on the kinetics of QM alkylation .....	11
1.5 Target promoted alkylation by DNA-QMP conjugates .....	12
1.6 Triplex-forming oligonucleotides (TFO) as a delivery agent for alkylation of double strand DNA .....	13
Chapter 2: Design and synthesis of an electron rich quinone methide precursor .....	17
2.1 Introduction .....	17
2.2 Results and Discussion .....	19
2.2.1 Synthesis of QMP1 .....	19
2.2.2 Attempts for synthesis of QMP* .....	20
2.2.3 Attempts for synthesis of QMP2 .....	23
2.2.4 The final synthesis of QMP2 .....	27
2.3 Conclusion .....	29
2.4 Materials and methods .....	30
Chapter 3: DNA-QM self-adduct formation and its DNA single strand alkylation is accelerated by using an electron-rich quinone methide precursor (QMP2) .....	43
3.1 Introduction .....	43
3.2 Results and Discussion .....	44
3.2.1 Preparation of the DNA-QMP conjugates and DNA-QM self-adducts .....	44
3.2.2 DNA-QM self-adduct formation was promoted by the electron rich QMP2 .....	46
3.2.3 Single strand alkylation of DNA by DNA-QM self-adducts was accelerated by increased electron density of the QMP2 .....	50
3.3 Conclusion .....	52
3.4 Material and Methods .....	53
Chapter 4: Target duplex DNA sequences by DNA-QM species through triple helix formation .....	56
4.1 Introduction .....	56
4.2 Results and Discussion .....	60
4.2.1 Preparation of the DNA-QMP conjugate and DNA-QM self-adduct .....	60



4.2.2 ssDNA alkylation by TFO-QMP1 conjugate.....	60
4.2.3 Alkylation of the target duplex DNA by OD1-QMP1 conjugates.....	62
4.2.4 Sequence dependent alkylation by OD1-QMP1 conjugate.....	65
4.2.5 Modified TFO was used to enhance triplex binding.....	68
4.2.6 DNA-QM1 self-adduct showed limited ability to alkylate the target duplex .....	68
4.2.7 DNA-QM2 self-adducts showed good ability for duplex DNA alkylation	74
4.2.8 Concentration dependent alkylation by OD1-QM2 self-adduct .....	76
4.2.9 Sequence and temperature effect on alkylation of target duplex by OD1- QM2 self-adduct.....	78
4.3 Conclusion.....	82
4.4 Materials and Methods .....	84
Chapter 5: Conclusion.....	86
Appendix .....	90
References .....	107

## List of Tables

<b>Table 1.1</b> Reversible and irreversible adducts formed with deoxynucleotide by QMP.	11
<b>Table 2.1</b> Reaction conditions and results for FeCl <sub>3</sub> catalyzed TBDMS conversion reaction with compound <b>16</b> .	26
<b>Table 3.1</b> MALDI data of the purified DNA-QMP conjugates and DNA-QM self-adducts.	45

## List of Figures

<b>Figure 1.1</b> Structure of bases in DNA and DNA base pairing.	2
<b>Figure 1.2</b> Structure of double helical DNA and the position of major and minor groove.	2
<b>Figure 1.3</b> Mechanistic pathways for DNA alkylation by interstrand cross-linking agents.	4
<b>Figure 1.4</b> Structures of methyl iodide and dimethylsulfate.	5
<b>Figure 1.5</b> Structures of well known cyclopropyl alkylating agents.	7
<b>Figure 1.6</b> <i>O</i> - and <i>p</i> -quinone methide and general reaction mechanism.	8
<b>Figure 1.7</b> Methods of QM generation.	8
<b>Figure 1.8</b> Mechanism of Mitomycin C activation and alkylation.	9
<b>Figure 1.9</b> Activation of QMP and its function as alkylation reagent.	10
<b>Figure 1.10</b> Structures of substituted QMP and formation and decomposition of quinone methide adducts of dC N3.	12
<b>Figure 1.11</b> Target promoted alkylation by ssDNA linked QM.	13
<b>Figure 1.12</b> Schematic representation of DNA triplex formation.	14
<b>Figure 1.13</b> Hoogsteen and reverse Hoogsteen hydrogen bonding formed in the triplex.	15
<b>Figure 2.1</b> Structures of original (QMP1) and electron rich (QMP* and QMP2) quinone methide precursors.	18
<b>Figure 2.2</b> Synthesis route of QMP1.	19
<b>Figure 2.3</b> First attempt for synthesis of QMP*.	21
<b>Figure 2.4</b> Second attempt for synthesis of QMP*.	22

<b>Figure 2.5</b> First attempt for synthesis of QMP2.	24
<b>Figure 2.6</b> Intra-molecular hydrogen bond of compound <b>12</b> .	25
<b>Figure 2.7</b> Final synthesis of QMP2.	28
<b>Figure 3.1</b> Generation of a DNA-QMP conjugate and its DNA-QM self-adduct.	44
<b>Figure 3.2</b> OD1 sequence and RP-HPLC chromatography of OD1, OD1-QMP2 conjugate and OD1-QM2 self-adduct.	46
<b>Figure 3.3</b> Illustration of self-adduct formation using QMP1 as the model.	47
<b>Figure 3.4</b> HPLC chromatograph of self-adduct formation from both OD1-QMP1 and OD1-QMP2 conjugates.	48
<b>Figure 3.5</b> Plot of self-adduct yield over time.	49
<b>Figure 3.6</b> Target alkylation process of the single strand DNA using DNA-QM self-adduct.	50
<b>Figure 3.7</b> DNA sequences for alkylation of single stranded DNA.	50
<b>Figure 3.8</b> Alkylation of single stranded DNA by DNA-QM1 and DNA-QM2 self-adducts.	51
<b>Figure 3.9</b> Alkylation yield of single strand OD2 over time.	52
<b>Figure 4.1</b> Hydrogen bonding patterns for triplex formation with modified bases.	57
<b>Figure 4.2</b> Examples of applications based on triple helical structure.	58
<b>Figure 4.3</b> Alkylation of single strand DNA OD2 and OD3 by the OD1-QMP1 conjugate.	61
<b>Figure 4.4</b> Alkylation of target duplex OD4/OD5 by OD1-QMP1.	63
<b>Figure 4.5</b> Salt effects on alkylation and migration of DNA products through a denaturing gel.	64

<b>Figure 4.6</b> Alkylation of double strand DNA by OD1-QMP1.	65
<b>Figure 4.7</b> Sequence dependent alkylation by OD1-QMP1.	67
<b>Figure 4.8</b> Modified TFO sequences (TFO1) and alkylation of OD8/OD9 with TFO1 linked QMP1.	68
<b>Figure 4.9</b> Alkylation of duplex DNA by the TFO1-QM1 self-adduct.	69
<b>Figure 4.10</b> Possible folded structure of a TFO-QM1 self-adduct.	71
<b>Figure 4.11</b> Alkylation of duplex DNA by TFO2-QM1 self-adducts.	71
<b>Figure 4.12</b> Alkylation of the modified sequences.	73
<b>Figure 4.13</b> Alkylation of target duplex by OD1-QM2 and OD1-QM1 self-adducts.	75
<b>Figure 4.14</b> Alkylation over time plot with OD1-QM2 and [ <sup>32</sup> P]-OD8/OD9.	76
<b>Figure 4.15</b> Dosage dependent alkylation results.	77
<b>Figure 4.16</b> Alkylation of different duplex sequences by OD1-QM2.	79
<b>Figure 4.17</b> Alkylation of OD2 by OD1-QMP1 at different temperature.	80
<b>Figure 4.18</b> MALDI data of OD1-QMP2 conjugated after stored at -18 °C in water for 3 months.	81
<b>Figure 4.19</b> Temperature effect on duplex alkylation.	82

## List of Schemes

<b>Scheme 1.1</b> Cyclic and open chain $\beta$ -hydroxyacrolein adducts of dG.	6
<b>Scheme 4.1</b> <i>Hprt</i> gene target sequence.	59
<b>Scheme 4.2</b> TFO sequence OD1 and the single strand DNA sequences.	61
<b>Scheme 4.3</b> OD1-QMP1 sequence and target duplex sequence OD4/OD5.	62
<b>Scheme 4.4</b> New duplex sequences with adjacent guanine.	67
<b>Scheme 4.5</b> TFO1 sequence and target duplex sequences.	68
<b>Scheme 4.6</b> TFO2 sequences and its target duplex.	71
<b>Scheme 4.7</b> Modified duplex sequences for QM alkylation.	73

## List of Abbreviations

A - adenine

ATP - adenosine-5'-triphosphate

C - cytosine

CHO - chinese hamster ovary

dA - deoxyadenosine

dC - deoxycytidine

dG – deoxyguanosine

DMAP - 4-dimethylaminopyridine

DMF - dimethylformamide

DNA - deoxyribonucleic acid

dppp - 1,3-bis(diphenylphosphino)propane

dsDNA - double strand DNA

EDCI - 1-ethyl-3-(3'-dimethylaminopropyl)carbodiimide

EDTA - ethylenediaminetetraacetic acid

ESI - electrospray

G - guanine

HMBC - heteronuclear multiple bond correlation

HPLC - high Performance liquid chromatography

Hprt - hypoxanthine phosphoribosyl transferase

HSQC - heteronuclear single quantum coherence,

MALDI - matrix-assisted laser desorption/ionization

MDA - malondialdehyde

MES - 2-(N-morpholino)ethanesulfonic acid  
Mops - 3-(N-morpholino)propanesulfonic acid  
MS - mass spectrum  
PNA - peptide nucleic acid  
PNK - T4 polynucleotide kinase  
RNA - ribonucleic acid  
RP-HPLC - reverse phase high performance liquid chromatography  
QM - quinone methide  
QMP - quinone methide precursor  
ssDNA - single strand DNA  
T - thymine  
TBAF - *tetra*-n-butylammonium fluoride  
TBE - Tris-borate-EDTA  
TBDMSCl - *tert*-butyldimethylsilyl chloride  
TEA - triethylamine  
TFA - trifluoroacetic acid  
TFO - triplex forming oligonucleotide  
TLC - thinner Layer Chromatography  
U's - thiouracil  
UV-Vis - ultra-violet visible spectroscopy



# Chapter 1: Introduction

## *1.1 Structure of DNA and DNA alkylation type*

Double strand DNA structure was first identified in 1953. It contains two polynucleotide strands wound about the same axis as a right handed helix.<sup>1</sup> According to this Watson and Crick model, there are four types of nucleotides bases attached to the DNA backbone: adenine (A), guanine (G), cytosine (C) and thymine (T) (Figure 1.1a), which can form hydrogen bonding to anneal the two strands.<sup>2</sup> The backbone of the strand is the sugar-phosphate chains occupying the peripheral part to minimize the electrostatic repulsions between the two strands. In most cases, adenine forms a base pair with thymine through two hydrogen bonds and cytosine forms a base pair with guanine through three hydrogen bonds (Figure 1.1b). The hydrogen bond provides fixed conformations of the base pairs in DNA helical structure that result in very important differences of DNA major groove and minor groove (Figure 1.2). The DNA major groove is much wider than the minor groove and it also contains more functional groups and less hydrophobic than minor groove. These properties make the major groove an ideal place to interact with some small molecules like alkylating agents.

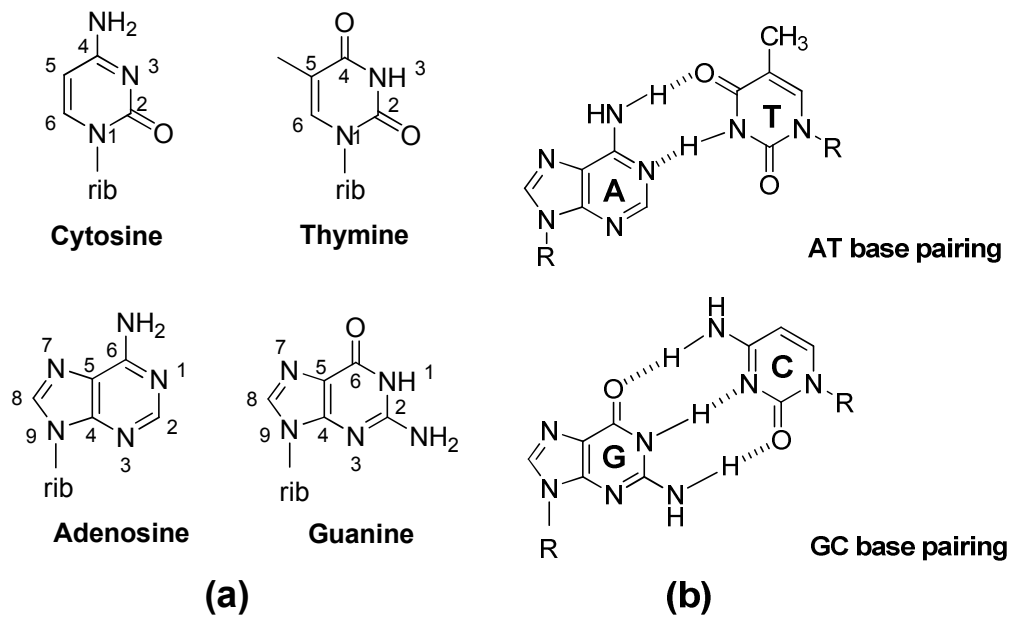


**Figure 1.1** (a) Structure and numbering of bases in DNA; (b) base pairings of DNA.

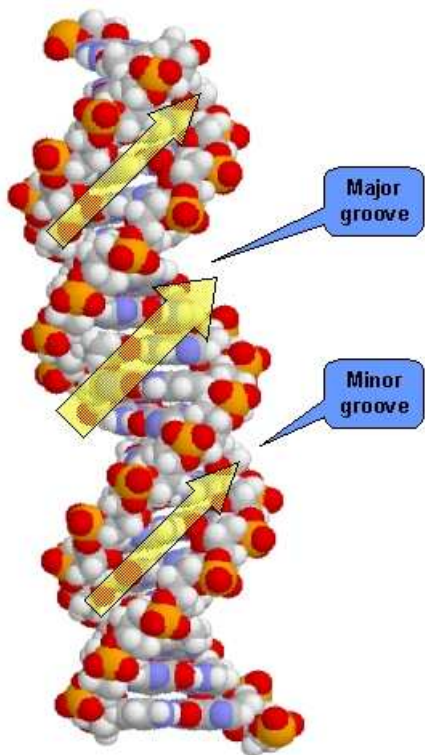


**Figure 1.2** Structure of double helical DNA and the position of major and minor groove (copied from reference 3).<sup>3</sup>

DNA is considered a very important target for biological study, because the double helical structure of DNA holds rich biological information of a living system. Its nucleotide sequence does not only code for protein and enzyme synthesis through transcription and translation, it also provides templates for RNA synthesis.<sup>4</sup> It is also found that DNA structures can be modified by a variety of chemicals which can interrupt normal base pairing, leading to mutations of genes or even cause death to cells. Thus, selective modification of DNA with encoding genes that cause disease can be an effective medical treatment. DNA alkylation is one type of these modifications.

DNA alkylation has attracted a lot of interest over the years because of its function as both carcinogens and anti-cancer agents. Some DNA alkylating agents are widely used as antitumor drugs in the clinic. Antitumor drugs usually involve both specific and non-specific interactions with a DNA duplex sequence, which codes for the protein related to the tumor, DNA repair, or transcription activation.<sup>5</sup> These interactions either affect the protein that is crucial to cell growth or directly influence DNA synthesis. However, alkylation agents can also cause serious toxic effects to the normal cells. Therefore, it becomes essential to understand the detailed mechanism and reactivity of alkylating agents.

There are three major types of DNA alkylation: monoalkylation, intrastrand crosslink, and interstrand crosslink (Figure 1.3). Monoalkylation is formed when alkylating agents have only a single reactive site and examples including small molecules like methyl iodide which will be introduced below. Alkylating agents with bifunctional groups to react with nucleophiles in the DNA can generate intra and

interstrand crosslinking depending on the position of the nucleophiles.<sup>6</sup> Of all three, interstrand cross-linking is the most toxic of all alkylation events since it results in seizure of the replication fork which completely shut down the replication.<sup>7</sup>

Therefore, the DNA interstrand cross-linking agents are significant clinical agents in the treatment of cancer and also other diseases such as psoriasis and various anemia.<sup>8</sup>

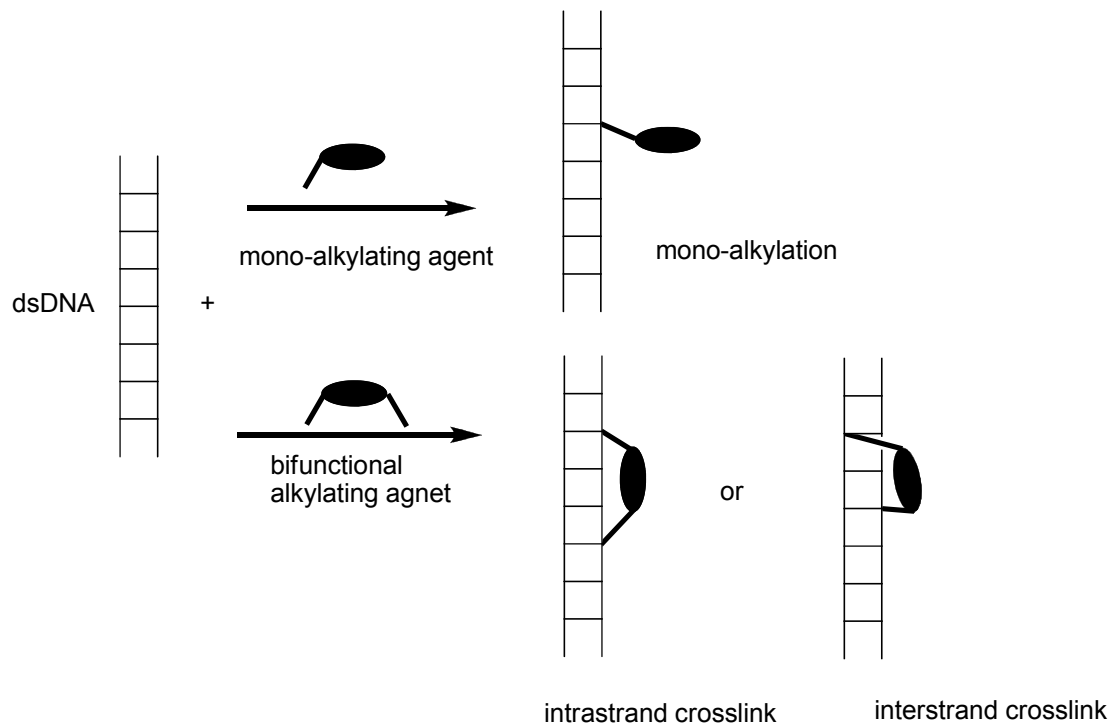


**Figure 1.3** Mechanistic pathways for DNA alkylation by interstrand cross-linking agents.<sup>5</sup>

### 1.2 DNA alkylation agents

DNA alkylating agents can be generated from a variety of biological and chemical process, or synthetic pathways.<sup>9,10</sup> Two most common examples of the alkylating agents are methyl iodide and dimethylsulfate, which can react through  $S_N2$  mechanisms (Figure 1.4). These compounds can react with most of the nucleophiles

in the DNA. Due to their high reactivity, these molecules usually lack specificity and reversibility and will lead to difficulties in controlling their reactions.

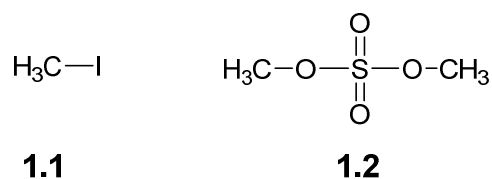
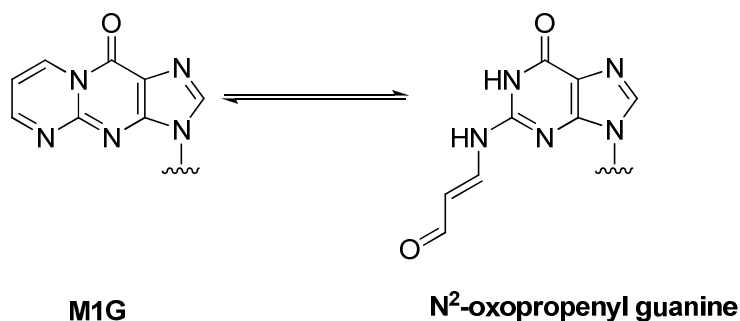


**Figure 1.4** Structures of methyl iodide (**1.1**) and dimethylsulfate (**1.2**)

DNA alkylating agents can also form reversible adducts with the nucleophiles in the DNA. Malondialdehyde (MDA), which is the mutagenic byproducts of lipid peroxidation, is such an example.<sup>10,11</sup> MDA can form adducts with adenine and cytosine, but it reacts most readily with guanine to form a 1:1 adduct, pyrimido[1,2- $\alpha$ ]purin-10-(3*H*)-one, termed M1G. NMR studies of M1G in oligonucleotides suggest that it exists as the ring-opened form, *N*<sup>2</sup>-oxopropenylguanine (Scheme 1.1).<sup>12</sup> But under heating condition, denaturation will initiate cyclization to form M1G again. Therefore, the products exist in an equilibrium between the ring closed and ring opened forms. The generation of this reversible alkylation product increased the toxicity of the alkylation process to the cell. Because the structures of the two adducts are so different, it is assumed that they have a significant difference in cytotoxicity. Thus, different pathways are required for DNA to repair this type of damage. As a result, chances become larger repair of DNA during replication and mutation fail caused of the alkylation will harm the cells.



**Scheme 1.1** Cyclic and open chain  $\beta$ -hydroxyacrolein adducts of dG.<sup>13</sup>

Cyclopropyl alkylating agents is another example that could form reversible alkylation adducts. These include members such as the duocarmycins and CC-1065 (Figure 1.5). The bases of DNA react with these compounds by nucleophilic attack on the cyclopropyl ring. It then opens the ring and restores the aromaticity to an adjacent ring system. In the case of duocarmycins, alkylation reaction is reversible. This near thermal neutral reaction was stabilized by extensive noncovalent binding interactions derived from hydrophobic binding and van der Waals contacts.<sup>14</sup> The reversible alkylating agents are believed to have more potential applications than irreversible alkylating agents because the reversible alkylating agent can be regenerated and realkylate the DNA after its adducts are excised from DNA.<sup>15,16</sup> Therefore, study of the alkylating agent that can react reversibly is very important and is also the focus of this dissertation.

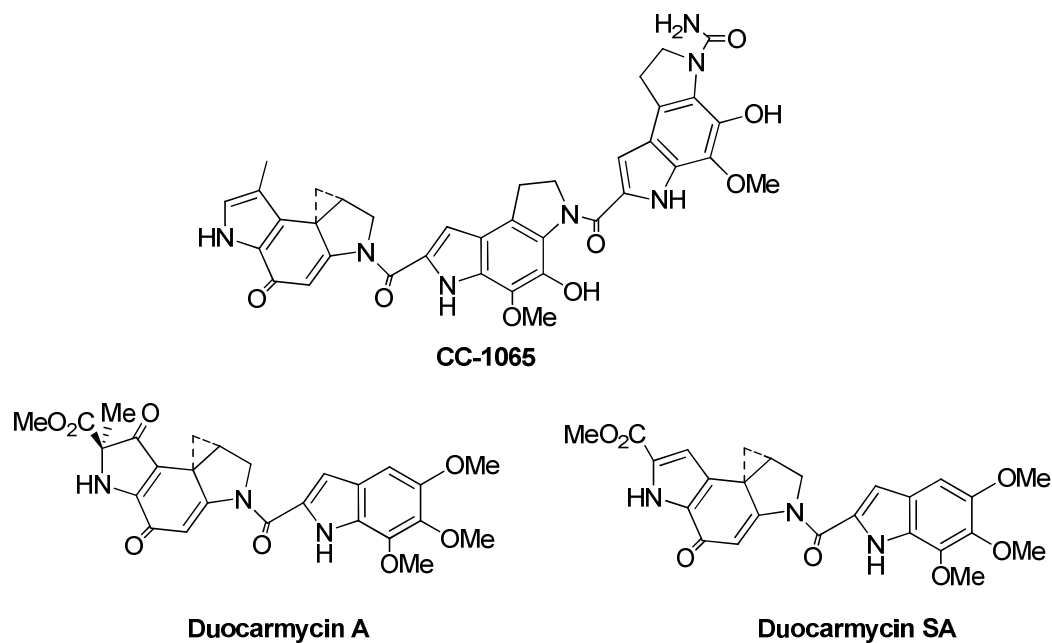


**Figure 1.5** Structures of well known cyclopropyl alkylating agents.

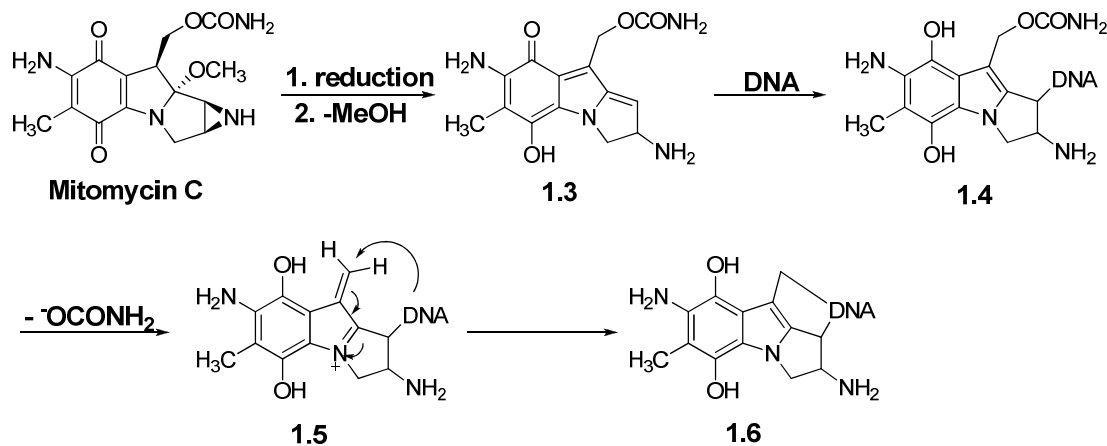
### ***1.3 Quinone Methides (QMs) and reversible alkylation of DNA***

Quinone methide (QM) and its derivatives are a class of reactive intermediates that widely occur in phenol chemistry and biological metabolism.<sup>17</sup> QMs are structurally related to benzoquinones with one of the carbonyl oxygens replaced by a methylene group. This structural change makes them highly electrophilic intermediates and the exo-double bond readily reacts with nucleophiles. There are generally two types of quinone methides: *o*-QM and *p*-QM (Figure 1.6). These transient intermediates can be generated through activation of quinone methide precursors (QMP). Methods of activation include heat,<sup>18</sup> UV radiation,<sup>19-21</sup> oxidation<sup>22,23</sup> and through biological processes (Figure 1.7).<sup>24,25</sup>



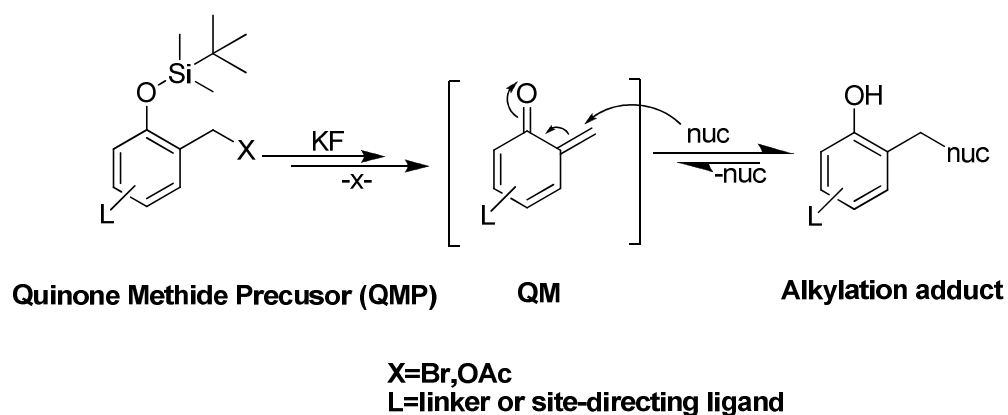


from DNA react with the electrophilic site yielding a mono-adduct (Compound **1.4**). After releasing another leaving group, the nucleophilic sites in the DNA react with the newly formed double bond to form a cross-linking product (Compound **1.6**).<sup>26</sup> Mitomycin C usually alkylates DNA at dG N7 position.<sup>27</sup> However, toxic side effects have also been observed mainly caused by non-specific reactions.<sup>27,28</sup>



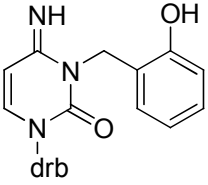
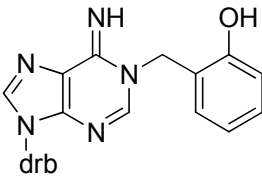
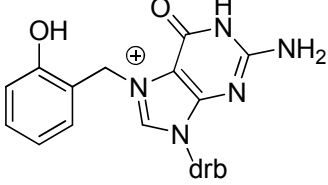
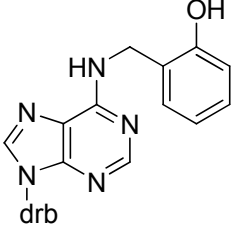
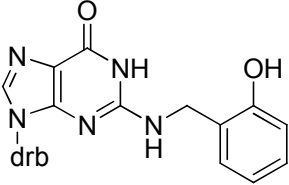
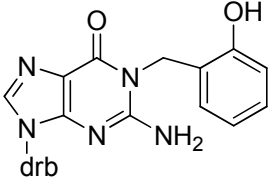
**Figure 1.8** Mechanism of Mitomycin C activation and alkylation.

A series of silyl ether protected quinone methide precursors was developed by the Rokita lab. These QMPs can be activated in the presence of fluoride ion (Figure 1.9).<sup>29,30</sup> The *o*-QM precursor usually has a bromide or an acetate group as the leaving group. The QMP can be delivered to the specific target site by coupling to the site-directing ligand to improve the alkylation specificity.<sup>31</sup> This alkylation process will be discussed in detail later in this chapter.



**Figure 1.9** Activation of QMP and its function as alkylation reagent.

Comprehensive studies have been performed in Rokita lab to investigate the reactivity and selectivity of QM with nucleophilic sites in the DNA. Experimental results showed that the formation of the QM alkylation adduct may be actually reversible.<sup>32</sup> Model QM studies showed that QM reacts with strong nucleophiles such as dA N1 and dG N7 quickly but reversibly.<sup>29</sup> The quickly formed adducts are not stable and will regenerate QM readily. The reactions of QM with weak nucleophiles such as dG N1, dG N<sup>2</sup> and dA N6 are slow but irreversible (Table 1).<sup>33</sup> The reversibility of the alkylation by QM is significant because reversible alkylating agents can be regenerated from the non-specific binding adducts and finally associate with target nucleophiles to form the thermodynamic products. The reversibility of the alkylation increases the half life of this highly transient intermediate in the reaction solution.<sup>34</sup> It also provides us an alternative way to generate the QM without using any chemicals or energy source.

<b>Reversible adducts</b>	 dC N3 adduct	 dA N1 adduct	 dG N7 adduct
<b>Irreversible adducts</b>	 dA N <sup>6</sup> adduct	 dG N <sup>2</sup> adduct	 dG N1 adduct

**Table 1.1** Reversible and irreversible adducts formed with deoxynucleotide by QMP.

#### 1.4 Substituent's effect on the kinetics of QM alkylation

To further understand the alkylation activity of the QMP with deoxynucleotides, aromatic substituent effects were studied. Alkylation adducts were generated with QMP containing different substitution groups and the stability of the adducts were tested.<sup>35</sup> The dC adduct formed by QMP with an electron donating methyl substituent reached its maximal yield in less than 1 hour, while the half life of releasing dC was around 5 hours (Figure 1.10).<sup>35</sup> In the contrast, an electron-withdrawing group present in the quinone methide precursor suppresses both initial formation of the QM and regeneration of QM from its dC adduct. The methyl ester QM was generated over 40 hours and the formed dC adduct was stable for more than 24 hours. Unsubstituted QMP-dC adducts showed a moderate stability, with the half life of decomposition of 24 hours.<sup>35</sup> These results are consistent with the electron

deficient property of the QM intermediate. Therefore, QMP with an electron donating group should accelerate its reaction with the nucleophiles which are studied in later chapters.

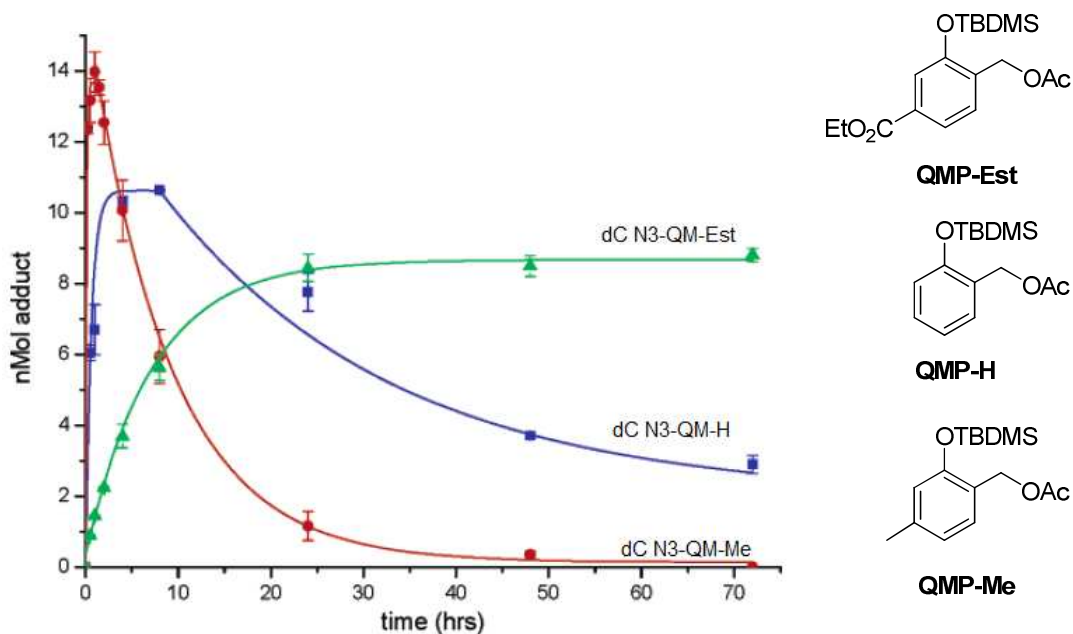


**Figure 1.10** Structures of substituted QMP and formation and decomposition of quinone methide adducts of dC N3. Plot was taken from the literature.<sup>36</sup>

### 1.5 Target promoted alkylation by DNA-QMP conjugates

Selective alkylation of DNA by QM can be achieved by coupling the QMP to a site-directing agent.<sup>31</sup> This target promoted alkylation process was designed based on the reversible reaction of QM with nucleobases. The QMP was first coupled to a single strand DNA. Then the QM was generated from a precursor by adding fluoride. The QM then reacted with bases in the DNA strand to form QM-oligonucleotide self-adducts. When a complementary strand (the target sequence) was added to this QM-oligonucleotide self-adduct, the QM could be regenerated from the reversible self-adduct and began to alkylate the other strand as two strands anneal together to

produce the interstrand cross-linking adduct (Figure 1.11). This process allows QM to be selectively delivered to a specific target sequence for alkylation and minimize toxicity caused by alkylation agents lacking of selectivity. Previous results showed that the cross-linking of this process is very specific. However, maximal alkylation requires a 7 days incubation.<sup>31</sup>

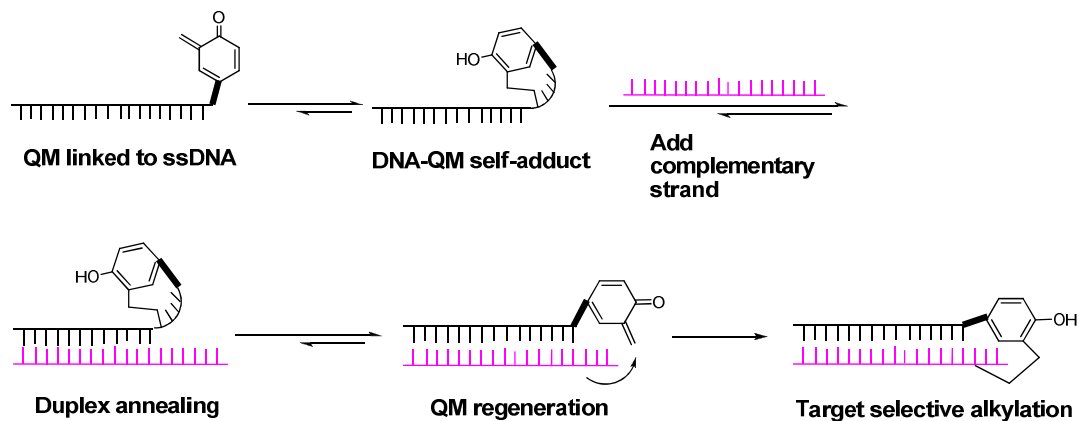


**Figure 1.11** Target promoted alkylation by ssDNA linked QM.

### ***1.6 Triplex-forming oligonucleotides (TFO) as a delivery agent for alkylation of double strand DNA***

DNA duplex can form a stable structure with a third strand. The formation of such a triple-helical nucleic acid structure was first observed in 1957.<sup>37</sup> It happens when a single strand DNA/RNA binds to a homopurine or homopyrimidine region of the duplex DNA. The third strand is normally described as a triplex-forming oligonucleotide (TFO) and binds specifically in the major groove of the duplex DNA (Figure 1.12). The structure is stabilized through Hoogsteen or reverse Hoogsteen hydrogen bonding between the third strand and the purine strand (Figure 1.13).

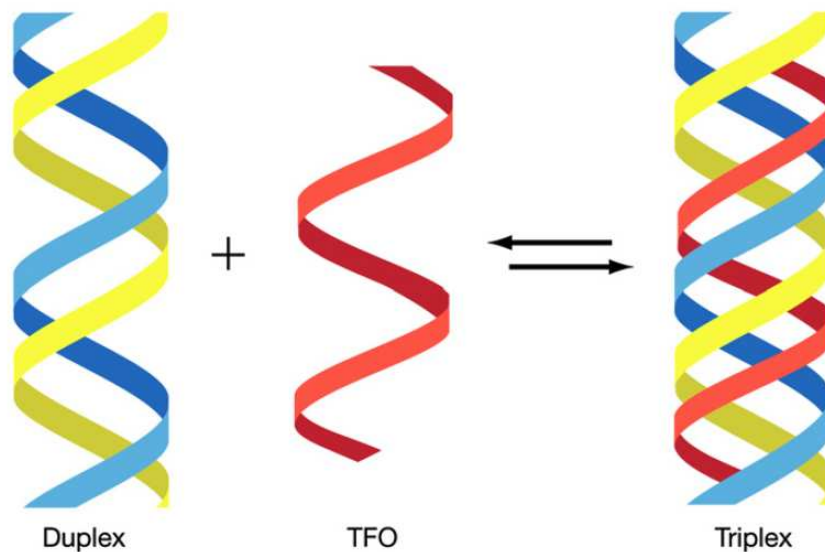


**Figure 1.12** Schematic representation of DNA triplex formation. The purine and pyrimidine strands are shown in blue and yellow respectively. The TFO indicated in red binds to the purine-rich strand of the target duplex through the major groove. Figure was copied from the literature.<sup>38</sup>

A TFO can be either a poly-pyrimidine or a poly-purine sequence. The TFO that consists of cytosines (C) and thymines (T) binds parallel to the purine-rich strand of DNA through Hoogsteen bonds. In this case, the cytosines in the third strand need to be protonated at N3 position for hydrogen bond with N7 of guanine. Therefore, this type of triplex only occurs under acidic condition. It could not bind to double strand DNA under physiologic condition without further modification.<sup>39</sup> The purine motif binds to the purine rich strand in an antiparallel orientation. The binding is through reverse Hoogsten base pair and no base protonation is required.<sup>40</sup> Thus, this triplex formation is largely pH independent.

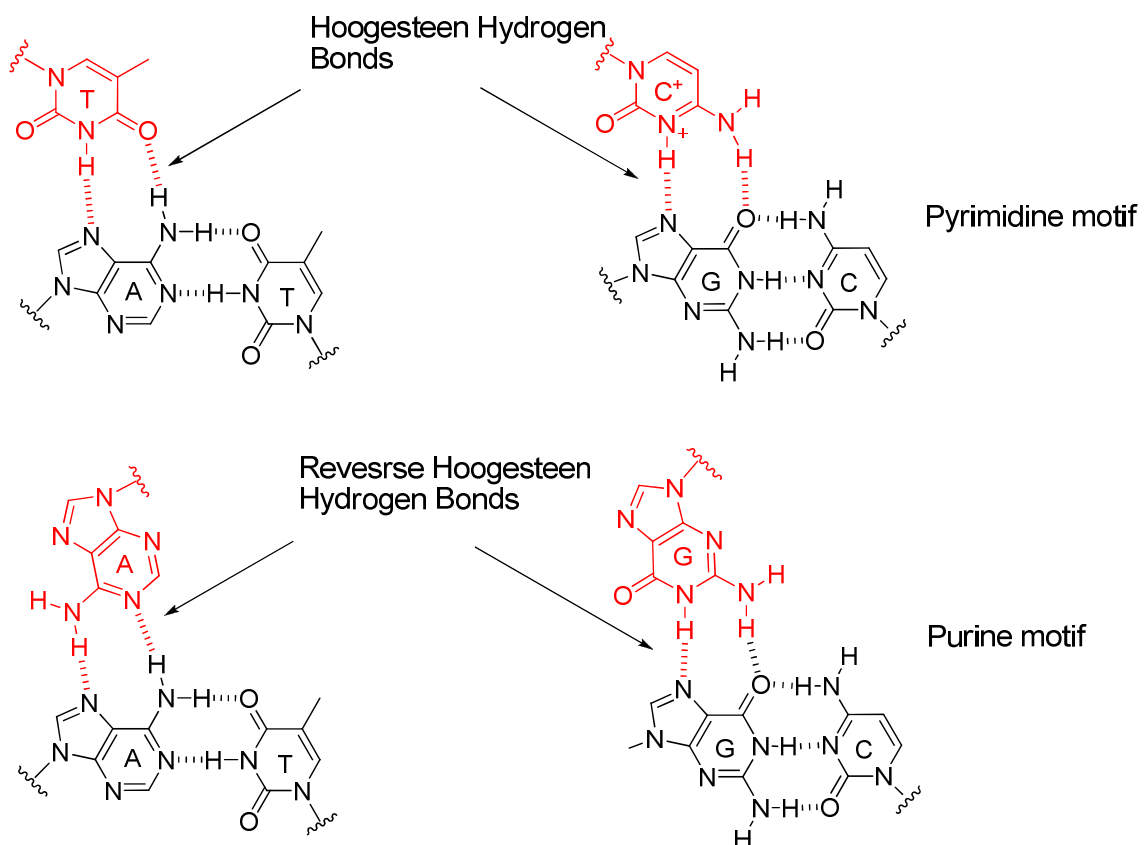


**Figure 1.13** Hoogsteen and reverse Hoogsteen hydrogen bonding formed in the triplex.

Triplex formation is sequence and length dependent. Studies showed that at least 12-14 uninterrupted purines are needed to achieve adequate triplex binding.<sup>41</sup> A single interruption in the polypurine sequence can significantly destabilize triplex formation. However, once the triple helix structure is formed in the homopurine/pyrimidine region, it is quite stable in the presence of divalent cations such as  $Mg^{2+}$ ,  $Ca^{2+}$ ,  $Zn^{2+}$  and naturally occurring polyamines which reduce the electrostatic repulsive forces between the negatively charged strands.<sup>37,42</sup> As a result, TFO is considered as an effective tool in gene targeting based on its stability and specific binding. TFO can bind to the selected site of a target gene to affect its expression, or mutate and

inactivate it. There are abundant TFO binding sites in mammalian genomes and a lot of them are in the promoter and/or transcribed gene regions.<sup>43</sup> A variety of chemical modifications of the DNA strands are also available to improve a strand's affinity for the duplex DNA. Therefore, the triple helical structure provides an effective tool to manipulate duplex DNA.

One example of this application is to use TFO as a site delivery agent for alkylation agents to the target duplex DNA. Seidman's group reported an *Hprt* knock-out assay to measure the activity of TFOs linked to the DNA cross-linker psoralen.<sup>44</sup> The photo-activated molecule successfully cross-linked the target duplex sequence through triplex formation and the subsequent mutation activity of that specific gene was analyzed.

In order to apply QMs for alkylating duplex DNA, a reactive QMP must be produced to speed up the alkylation process. Currently, alkylation of the DNA is too slow to take effect in the biological system. This dissertation will focus on design and synthesis of a more reactive QMP with increased electron density compared to the conventional QMP. Both QMPs were coupled to single strand DNA and their DNA-QM self-adducts formation was investigated and compared. Alkylation of the single strand DNA target and double strand DNA target using both self-adducts was studied. The electron rich QMP improved alkylation efficiency of the target promoted alkylation process. It also prepared the QM for further application of its alkylation activity in vivo.



## Chapter 2: Design and synthesis of an electron rich quinone

### methide precursor

#### 2.1 Introduction

Inspired by the reversible nature of QM alkylation,<sup>45,46</sup> a DNA-QM complex was delivered to a specific DNA sequence for alkylation. Previous results indicated that the yield of the single strand alkylation by the DNA-QM complex reached its maximal after a 7-day incubation.<sup>31</sup> This indicated a slow process of DNA alkylation by the DNA-QM self-adduct. As a result, the current QM will not be very efficient if developed to treat disease. The slow reaction speed will also limit the QM alkylation ability of a target DNA in the biological system because DNA repair may fix the cross-linking part before it affects the DNA activity. Therefore, it is necessary to design a more reactive QMP than the previous one to speed up the alkylation. The increased alkylation rate would help optimize the QM alkylation ability for a biological application.

The structure of the original quinone methide precursor (QMP1) used by our group is showed in Figure 2.1. In this precursor, an acetate group is the leaving group for QM formation. The N-hydroxysuccinimide ester included in the molecule is designed to activate the carboxylic acid group for coupling to the terminal amine linker of a synthetic DNA. Kinetic study of QMP1 indicated that the rate determining step of QM generation from its precursor was the elimination of the acetate group after deprotecting the TBDMS (*tert*-butyldimethylsilyl) group.<sup>31</sup> So the rate of QM

generation can be increased by speeding up the elimination step which will eventually accelerate the target promoted alkylation. According to previous results, an electron-donating group present in the molecule will facilitate the generation of the QM from the precursor and its regeneration from the reversible alkylation adduct.<sup>35</sup> Therefore, a pair of electron rich quinone methide precursors were designed and their structures are showing below (Figure 2.1, QMP\* and QMP2). QMP\* has the same structure as QMP1 except for a methoxy group on the *para* position with respect to the benzylic acetate group. In QMP2, the ester linker is moved to the *para* position to the acetate group and an oxygen atom is used to replace a carbon of the linker. These modifications can increase the electron density of the molecule to facilitate the elimination of the acetate group and maintain the alkylation function of the molecule. Multiple synthesis routes were tried to produce QMP\* and QMP2. This chapter will focus on the design and synthesis work and towards these two desired QMPs.

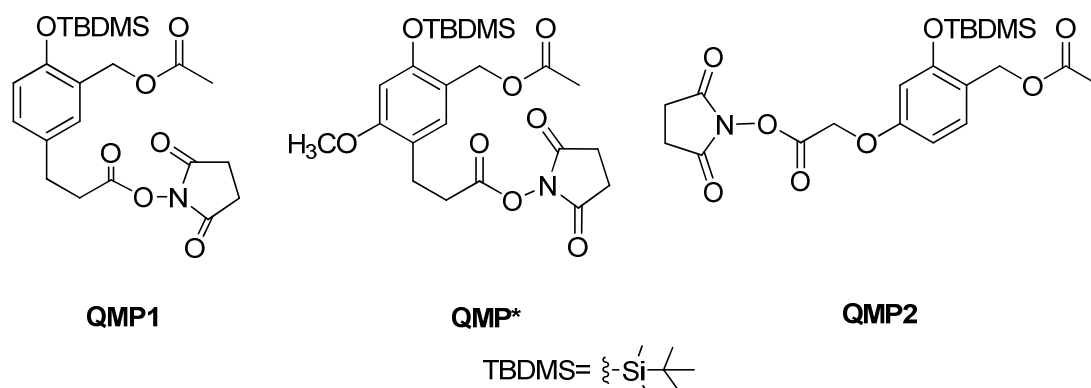


**Figure 2.1** Structures of original (QMP1) and electron rich (QMP\* and QMP2) quinone methide precursors.

## 2. 2 Results and Discussion

### 2.2.1 Synthesis of QMP1

QMP1 was previously synthesized in our laboratory.<sup>31</sup> The synthetic procedure was followed with slight modification (Figure 2.2). In the original literature, compound **1** was generated in sodium salt form and was used directly for the next step without any purification. The overall yield for the two steps was 13%.<sup>31</sup> Modification was made to this step because salt form of sodium salt form of **1** had similar polarity with compound **2** which made the separation of the protection reaction difficult. Therefore, compound **1**(acid form) was produced and purified after the first step. Separation of protected product **2** from the reactant **1** was easy to achieve due to their different polarity without influencing the yield (15% for two steps). Finally, QMP1 was isolated and characterized by proton NMR to confirm its formation.

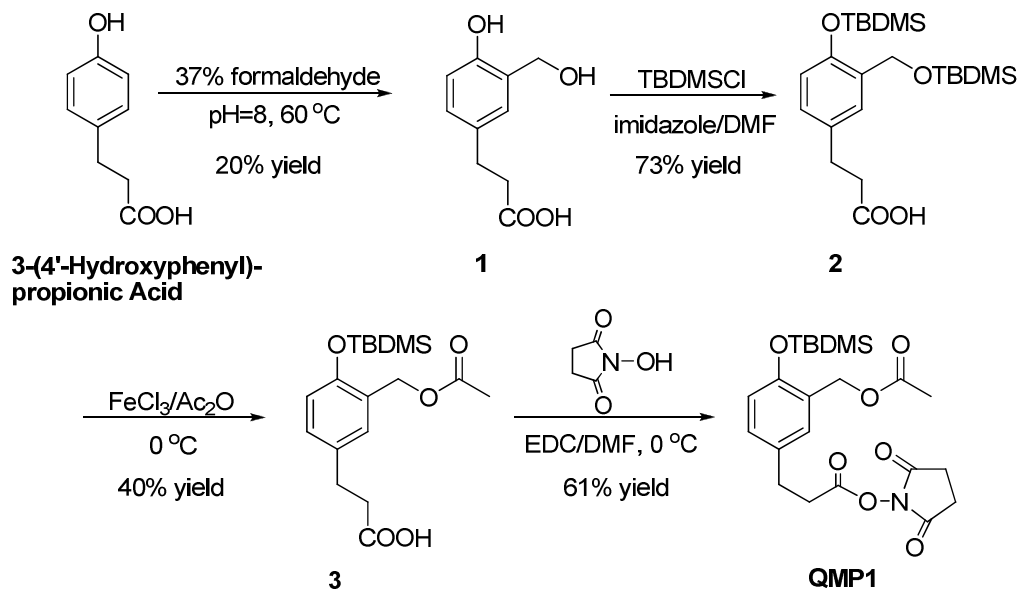
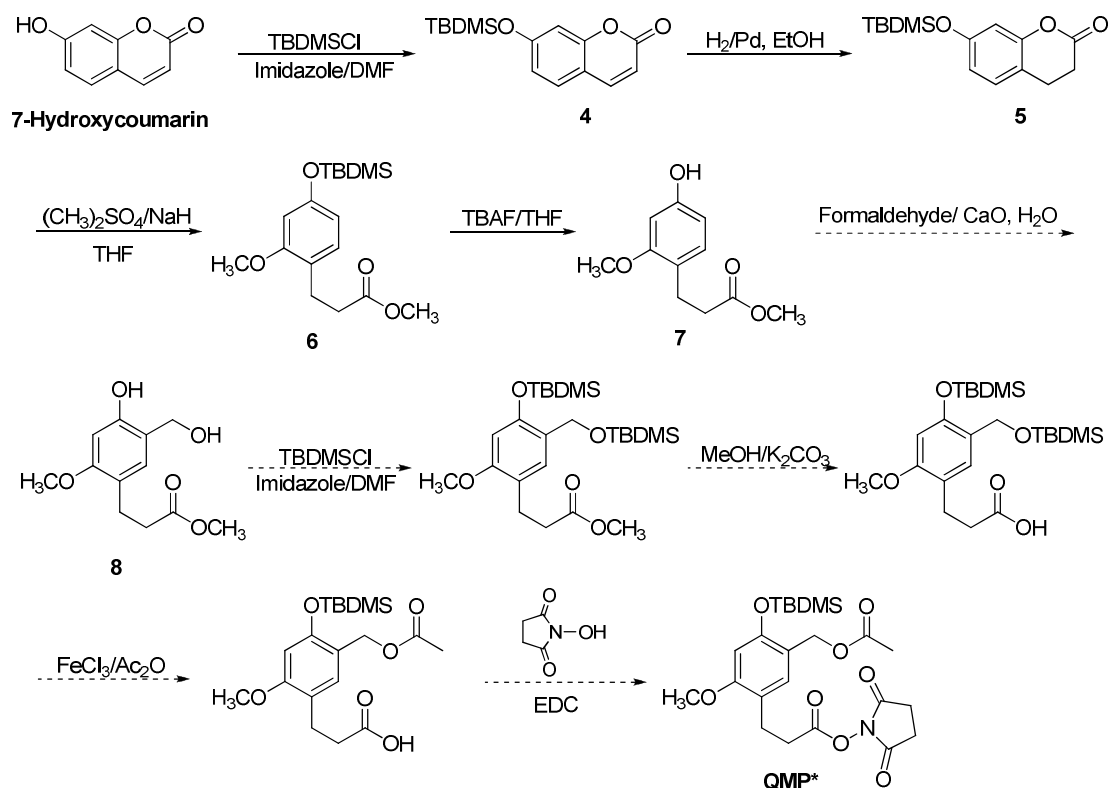


Figure 2.2 Synthesis route of QMP1.

### 2.2.2 Attempts for synthesis of QMP\*

QMP\* was initially designed as the electron rich target molecule. An electron donating methoxy group was added to QMP1 to increase the electron density of the molecule while the rest of the structure stayed the same to function as a QMP. Several attempts to synthesize this compound have been made. In the first attempted synthesis (Figure 2.3), 7-hydroxycoumarin was used as the starting material. This molecule could provide the substitutions on the desired positions of the benzene ring to construct the target molecule after the lactone ring was opened. The hydroxyl group was first protected by reacting with TBDMSCl in the DMF (dimethylformamide) following a standard procedure<sup>47</sup> (72% yield), the double bond of the lactone ring of compound **4** was reduced through hydrogenation to yield compound **5** in 87%. Ring opening and methylation of the nascent hydroxyl group was achieved in one step using dimethyl sulfate and sodium hydride.<sup>48</sup> Reaction was completed within 4 hours under room temperature to produce compound **6** with a 52% yield. Then compound **6** was deprotected with *tetra*-*n*-butylammonium fluoride (TBAF) under standard conditions<sup>49</sup> to yield compound **7** in 86%. The removal of the phenol protecting group was necessary since the coupling of benzylic hydroxyl group can only be achieved with the phenol substrate **7** rather than compound **6**. Previously, this step was accomplished by heating up the phenol substrate 3-(4'-hydroxyphenyl)-propionic acid with formaldehyde under basic condition.<sup>31</sup> Compound **1** was produced as the major product. However, the reaction worked differently in the presence of methoxy group on the starting material. No desired product (compound **8**) was ever detected when compound **7** was heated with the formaldehyde mixtures using the same condition.

TLC (Thin Layer Chromatography) results indicated that the starting material was quickly consumed during the reaction without forming any major products. Polymerization was likely under this condition since this reaction could evolve into chain reaction to produce Phenol-Formaldehyde resins (PF resins).<sup>50</sup> The same reaction was repeated without heat and using mild base CaO. This eliminated the formation of the byproducts, but no desired product was observed either.<sup>51</sup>



**Figure 2.3** First attempt for synthesis of QMP\*.

In order to avoid the difficulty brought by adding the methyl alcohol group to the electron rich substrate, a second synthetic route was designed starting with a benzyl aldehyde substrate (Figure 2.4). In this case, the target benzyl alcohol group could be constructed by reducing its aldehyde precursor instead of directly adding it

to the benzene. The commercially available 2-hydroxy-4-methoxybenzaldehyde was first brominated to produce compound **9**. Product was purified through recrystallization resulted in a final yield of 81%. A Heck reaction was then used to couple methyl acrylate to the benzene ring to construct the linker. Palladium acetate and 1,3-bis(diphenylphosphino)propane (dppp) were used as catalysts and triethylamine as the base for this coupling. The reaction mixture had to be maintained under inert gas with anhydrous reagents to produce the product in a 21% yield. The next step was to reduce the double bond of compound **10**. However, the aldehyde group was also reduced to methyl group under hydrogenation for double bond reduction. Thus, this synthesis attempt failed too.

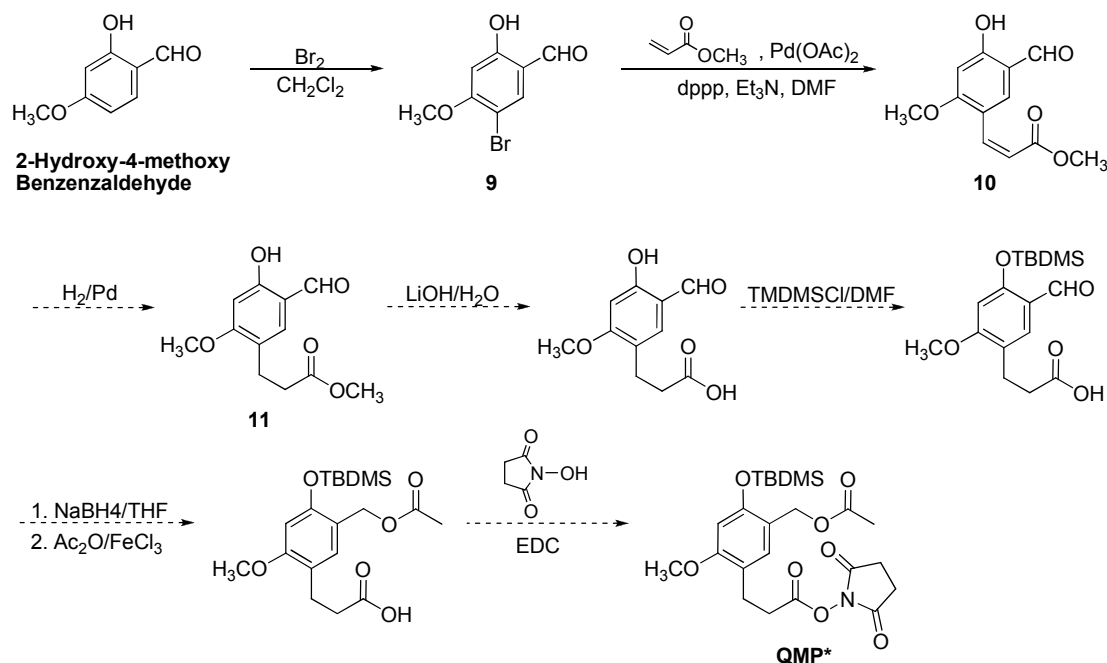


**Figure 2.4** Second attempt for synthesis of QMP\*.

### 2.2.3 Attempts for synthesis of QMP2

Based on my synthetic work, it was difficult to produce the model QMP structure in the presence of the added methoxy group. Upon Dr. Isaacs's suggestion, we modified our target molecule to simplify the synthetic process by eliminating the extra functional group on the benzene ring. A second electron rich quinone methide precursor (QMP2) was designed using oxygen atom to replace the carbon atom of the ethyl carbon chain of the linker. The QM linker was moved to the *para* position away from the benzylacetate group. As a result, the electron density of the molecule was increased without adding an extra functional group. Reposition of the linker would not affect its function to attach the precursor to a site-directing ligand.

The initial synthesis of QMP2 started with commercially available 2,4-dihydroxybenzaldehyde and its reaction with methyl bromoacetate to couple the linker to the 4-hydroxy group of the ring (Figure 2.5).<sup>52</sup> This reaction was selective for the 4-hydroxy group. The isolated mono-alkylation product was confirmed as methyl 2-(4-formyl-3-hydroxyphenoxy)acetate (compound **12**) by 2D NMR showing all corresponding C-H (Heteronuclear Single Quantum Coherence, HSQC) and C-C (Heteronuclear Multiple Bond Correlation, HMBC) correlations. This selectivity was likely to be the result of the hydrogen bonding between the oxygen atom of the carbonyl group and the proton of its neighboring phenol hydroxyl group (Figure 2.6). The increased pKa of the 2-hydroxyl proton made it hard to be removed compared to the proton of the 4-position hydroxyl group.<sup>28</sup> This hydrogen bonding was also indicated by correlation between the carbonyl carbon and the phenol proton showed in the HMBC spectrum of the product (Appendix, Figure 4, and Page 93). If reaction

was refluxed for more than 6 hours, there was still starting material left but the disubstituted product started to appear based on TLC. The disubstituted product was less polar than compound **12** and its structure was confirmed by proton NMR. So 1 equivalent of methyl bromoacetate was used minimize the formation of disubstituted byproducts and the desired compound **12** was yielded in 40%. If the unreacted starting material was recovered during purification, the yield can increase to 56%.

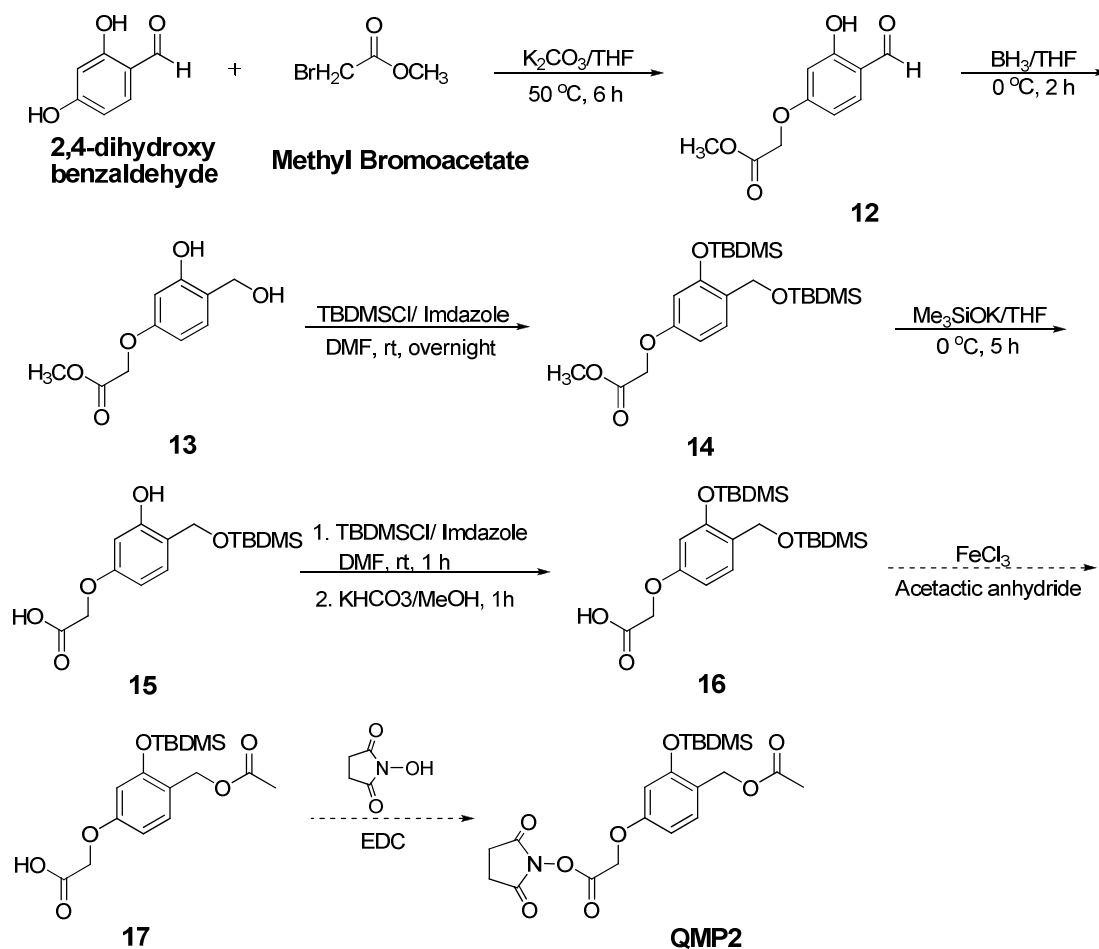


**Figure 2.5** First attempt for synthesis of QMP2.



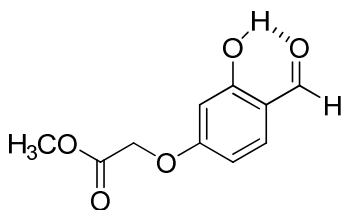


**Figure 2.6** Intra-molecular hydrogen bonding of compound **12**.

The reduction of the aldehyde of compound **12** was carried out using borane-tetrahydrofuran (BH<sub>3</sub>-THF) complex. This reducing reagent was selected because it would not affect the carbonyl group of the methyl ester. A single product **13** was produced through this reaction in a 83% yield. The hydroxyl groups were then protected by TBDMS through a standard procedure.<sup>47</sup> The methyl ester in the linker was then hydrolyzed to the desired carboxylic acid group. Potassium carbonate was first tried for this reaction since it appeared to be inert to the TBDMS group when synthesizing compound **2**. However, multiple products were evident by TLC resulting in very polar product. This indicated the TBDMS group was also removed during the hydrolysis. Potassium trimethylsilylanolate was then used for the hydrolysis. This mild base showed to be very inactive towards the silyl protecting group because of the steric hindrance of this bulky nucleophile.<sup>53</sup> However, compound **15** was produced in 65% instead of the expected compound **16** and confirmed by the NMR data with a missing set of TBDMS peak. This result indicated that the TBDMS group in this electron rich substrate was very sensitive to hydrolysis. The phenol group required protection again to form compound **16**. This was accomplished by a literature procedure using TBDMSCl with a 64% yield.

The next step was to replace the benzylic TBDMS with the acetate. Previously, this step was realized using ferric chloride with acetic anhydride, a

reaction that was developed by the Ganem's group.<sup>54</sup> This method was applied in QMP1 synthesis to produce compound **6** successfully. The reaction was tried on the electron rich substrate **16** using various reaction conditions (Table 2.1). The desired compound **17** was never identified but the starting material **16** could be isolated from the reaction mixture. This result indicated that compound **16** did not react with the acetic anhydride to form the target compound in the presence of iron chloride. A different Lewis acid Cu(OTf)<sub>2</sub> was also tried without yielding the expected polar product on the TLC. Therefore, the synthesis route had to be modified to avoid the formation of the benzylic acetate group from its TBDMS precursor.

Catalyst equivalent	Reagent/Solvent	Reaction Temperature	Reaction time	Results
0.15	Acetic anhydride (Ac <sub>2</sub> O)	0 °C	30 min	No product spot observed on TLC
0.3	Ac <sub>2</sub> O	0 °C	30 min	No product spot observed on TLC
Excess	Ac <sub>2</sub> O	0 °C	1 h	No product spot observed on TLC
Excess	Ac <sub>2</sub> O	-40 °C	4 h	Starting material remained, no product spot observed on TLC
Excess	Ac <sub>2</sub> O/CH <sub>2</sub> Cl <sub>2</sub>	-40 °C	4 h	Starting material remained, no product spot observed on TLC;
Excess	Ac <sub>2</sub> O	-15 °C	4 h	Starting material remained, no product spot observed on TLC
Excess	Ac <sub>2</sub> O	20 °C	4 h	Starting material remained, no product spot observed on TLC
Excess	Ac <sub>2</sub> O	40 °C	overnight	No starting material left, no product spot observed on TLC

**Table 2.1** Reaction conditions and results for FeCl<sub>3</sub> catalyzed TBDMS conversion reaction with compound **16**.

#### 2.2.4 The final synthesis of QMP2

The final synthesis plan (Figure 2.7) also started with 2,4-dihydroxy benzaldehyde to generate compound **12** by reacting with methyl bromoacetate. Different from the synthesis route discussed above, the aldehyde group was reduced in the later stage after the phenol group was protected. Then the resulting hydroxyl group was converted to acetate through esterification. This avoids the Lewis acid catalyzed conversion from the TBDMS protected hydroxyl group to acetate.

The methyl ester group of compound **12** was hydrolyzed using potassium trimethylsilylanolate to yield a single product **18** in 75%.<sup>55</sup> In the initial synthesis plan for this target molecule, the ester group was kept until the final stage for convenient handling during purification. However, we found that the phenol TBDMS protecting group was very unstable to hydrolysis. Thus, the carboxylic acid derivative was generated at an early stage and used for later reactions. The acid compound **18** was prepared by hydrolyzing its ester precursor **12**, which required two steps from the commercially available starting material, rather than coupling the acetic acid derivative directly to 2,4-dihydroxybenzaldehyde which required only one. This was because direct coupling yielded multiple products; the desired product could never be isolated. After purifying compound **18** by recrystallization, the phenol hydroxyl group was protected by TBDMS group using triethylamine (TEA) as the base and 4-dimethylaminopyridine (DMAP) as the catalyst to produce compound **19**.<sup>56</sup> Standard condition for the protecting reaction that included imidazole as the base but this only resulted in a less than 10% yield of **19**. This low yield might be caused by the increased pKa value of the phenol proton as discussed before compared to phenol

without an intermolecular hydrogen bonding. The reaction mixture was stirred in dry DMF under room temperature and nitrogen atmosphere for 20 hours. Compound **19** was then isolated after column purification in a yield of 42%. In addition to the higher conversion yield using this catalytic protecting condition compared to the standard condition, this condition also showed an interesting selectivity by not producing the TBDMS-ester intermediate observed previously.<sup>57</sup> The hydroxyl group of the carboxylic acid was also protected with TBDMS under standard condition when synthesizing compound **2**. This ester bond was labile and could be hydrolyzed under acidic condition. In that case, the crude product had to be treated with acid to remove the unwanted protecting group. Protection reaction using DMAP and TEA did not require this extra step since TBDMS group was selectively added to the phenol group.

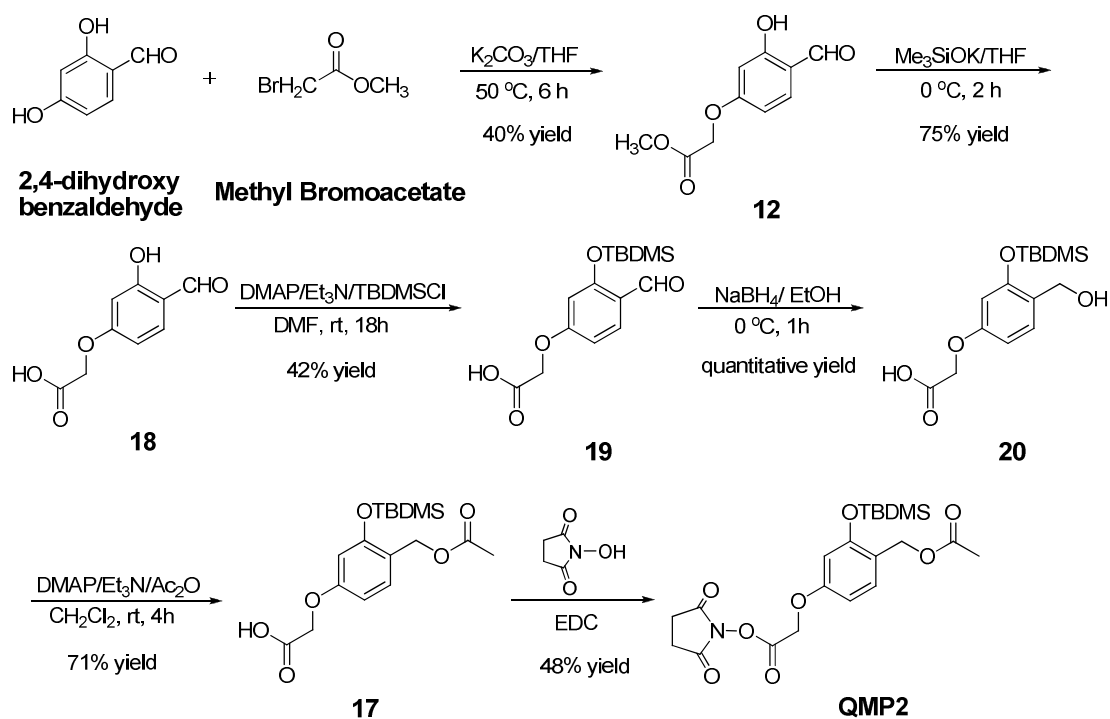


**Figure 2.7** The final synthesis of QMP2.

Sodium borohydride was then used to reduce the aldehyde group. The reducing agent was chosen to avoid possible reaction with the carbonyl group of the carboxylic acid. Compound **20** was formed quantitatively and the crude material was ready to use for the next reaction.<sup>56</sup> The acetate group was introduced through esterification of the benzylic alcohol with acetic anhydride using DMAP as the catalyst to form compound **17** in a yield of 71%. Finally, the N-hydroxysuccinimide was coupled to compound **17** following a procedure published previously.<sup>31</sup> The target electron rich quinone methide precursor QMP2 was isolated with a yield of 48% (single step yield) and ready to couple to DNA sequences.

### ***2.3 Conclusion***

In order to increase the alkylation speed efficiency by a DNA-QM species, two electron rich quinone methide precursors were designed. The increased electron density from the electron donating group can promote generation of the QM from its precursor.<sup>35</sup> As a result, subsequent alkylation should also be accelerated. Two synthetic plans were tried to construct the target molecule QMP\* but neither were successful. The major difficulty in this synthesis derived from constructing the benzyl alcohol structure and handling this reactive intermediate. Although hydroxymethylation proceeded easily for a substrate without electron donating groups, all attempts to repeat this procedure with an electron rich substrate (compound **7**) failed. Multiple products were evident and the desired product was never isolated. Another precursor QMP2 was then designed to simplify the synthetic procedure. Two more synthetic routes were planned for this molecule. First, the aldehyde functional group was included in the commercially available starting material

for later conversion to benzyl alcohol through reduction. This design avoided the step of directly adding the methylhydroxyl group to the molecule. The first synthetic attempt for QMP2 failed at the final stage, for which the TBDMS group protected benzyl hydroxyl could not be converted to the desired acetate using a Lewis acid catalyzed reaction. To avoid this particular reaction, a second synthetic route was designed. In this plan, the acetate group was produced through esterification of the methyl hydroxyl group with acetic anhydride. This modification in the synthetic plan finally led to the successful synthesis of the target molecule QMP2.

## ***2.4 Materials and methods***

### **General materials**

Reagents, starting materials, solvents and salts of the highest commercial grade were used without further purification. All aqueous solutions were prepared with distilled, deionized water with a resistivity of 18.0 M $\Omega$ . Silica gel (230-400 mesh) for column chromatography was purchased from EM Sciences. All deuterated solvents for NMR spectroscopy were purchased from Cambridge Isotope Laboratories.

### **General methods**

Melting points were measured with a Thomas-Hoover Unimelt apparatus that was not corrected. NMR spectra were recorded on a Bruker AM400 spectrometer and Bruker DRX-500 high resolution spectrometer and referenced to residual protons in the deuterated solvents. Chemical shifts ( $\delta$ ) are reported in parts per million (ppm). Coupling constants ( $J$ ) are reported in hertz (Hz). Mass spectra were determined using electrospray ionization on a JEOL AccuTOF-CS spectrometer.

## Synthetic Procedures

Synthetic procedure of QMP1 was adapted from the original preparation method in the literature with modification in purification step. All the compounds were characterized by proton NMR and the data were consistent with the literature.<sup>31,57</sup>

**3-[3-Hydroxymethyl-4-hydroxyphenyl]propionic acid (1).** A aqueous solution of NaOH (10%, 5 ml) was added to 3-(4-hydroxyphenyl)propionic acid (2.0 g, 12 mmol) solid to adjust the pH to 8. Then, a formaldehyde aqueous solution (37%, 5 mL) was added dropwise, and the mixture was heated at 60° C for 16 hours. The reaction mixture was cooled to room temperature and 1 M HCl was added to adjust the pH to 3. The resulted solution was extracted with ether (3×50 ml). The organic layer was collected, dried over sodium sulfate and evaporated with a rotoevaporator. The crude product was purified by silica gel chromatography (hexane : ethyl acetate = 2 : 1 and 0.5% HOAc) and yielded product **1** as a faint white solid (491 mg, 21.2%).  
<sup>1</sup>H NMR (400 MHz, D<sub>2</sub>O) δ 2.52 (d, *J*=8, 2H), 2.72 (t, *J*=8, 2H), 4.48 (s, 2H), 6.72 (d, *J*=8, 1H), 6.96 (d, *J*=8, 1H), 7.04 (s, 1H).

**3-[3-*tert*-Butyldimethylsilyloxymethyl-4-*tert*-butyldimethylsilyloxyphenyl]-propionic acid (2).** To a solution of compound **1** (490 mg, 2.52 mmol) in DMF (5 ml), *t*-butyldimethylsilyl chloride (TBDMSCl, 2.26 g, 15.1 mmol) and imidazole (2.03 g, 30.2 mmol) were added and stirred under room temperature for 18 hours. Brine was then added to dilute the solution which was extracted by diethyl ether (3×15ml). The combined organic phases were dried over sodium sulfate and filtered out. Solvent

was then filtered and evaporated to yield crude product. The crude was redissolved in 10 ml MeOH and potassium carbonate (556 mg, 4.03 mmol) was added. The solution was stirred under room temperature for 3 hours. Upon completion of reaction, 0.1 M HCl was added to adjust the solution to pH 3. The mixture was then diluted with water and extracted with ether (50 ml  $\times$ 3). The organic phases were combined, washed with brine, dried over NaSO<sub>4</sub>, and concentrated under reduced pressure. The residue was purified by silica gel chromatography (hexane: ethyl acetate= 5:1) to yield **2** as a colorless oil (770 mg, 73%). <sup>1</sup>H NMR (400 MHz, CDCl<sub>3</sub>)  $\delta$  0.09 (s, 6H), 0.18 (s, 6H), 0.94 (s, 9H), 0.98 (s, 9H), 2.63 (t,  $J$ = 8, 2H), 2.87 (t,  $J$ = 8, 2H), 4.71 (s, 2H), 6.66 (d,  $J$ = 8 1H), 6.92 (d,  $J$ = 8, 1H), 7.26 (s, 1H).

**3-[3-Acetoxymethyl-4-*tert*-butyldimethylsilyloxyphenyl]propionic acid (3).** Solid ferric chloride (9 mg, 0.06 mmol) was added to a solution of **2** (191 mg, 0.452 mmol) in acetic anhydride (3 mL) at 0 °C. The reaction mixture was stirred for 30 minutes and then diluted with 30 ml ether. The resulted solution was washed with water and saturated aqueous NaHCO<sub>3</sub>. The organic phase was dried over NaSO<sub>4</sub>, and concentrated under reduced pressure. The residue was subjected to silica gel column chromatography (hexane: ethyl acetate= 3:1) and yielded **3** as a colorless liquid (63 mg, 40%). <sup>1</sup>H NMR (400 MHz, CDCl<sub>3</sub>)  $\delta$  0.18 (s, 6H), 0.94 (s, 9H), 2.06 (s, 3H), 2.69 (t,  $J$ = 8.0, 2H), 2.86 (t,  $J$ = 8.0, 2H), 5.03 (s, 2H), 6.70 (d,  $J$ = 8.0, 1H), 6.99 (d,  $J$ = 8, 1H), 7.09 (s, 1H).

***N*-Succinimidyl-3-(3-acetoxymethyl-4-*tert*-butyldimethylsilyloxyphenyl)**

**propionate (QMP1).** *N*-Hydroxysuccinimide (34 mg, 0.32 mmol) was added to a DMF solution (2 mL) of compound **6** (63 mg, 0.18 mmol). This mixture was cooled



to 0 °C in ice and 1-ethyl-3-(3'-dimethylaminopropyl)carbodiimide (EDCI, 48 mg, 0.25 mmol) was added in one portion. The mixture was first stirred under 4 °C for 2 hours and then warmed up and maintained at room temperature for 21 hours. After the reaction completed, the solution was diluted with brine and extracted with ether (3×15 ml). The organic phases were collected, dried over NaSO<sub>4</sub> and concentrated under reduced pressure. The residue was purified by silica gel column chromatography (hexane: ethyl acetate=3:1) to yield QMP1 as a clear oil (49 mg, 61%). <sup>1</sup>H NMR (400 MHz, CDCl<sub>3</sub>) δ 0.18 (s, 6H), 0.94 (s, 9H), 2.06 (s, 3H), 2.62 (s, 4H), 2.69 (t, *J*= 8.0, 2H), 2.86 (t, *J*= 8.0, 2H), 5.03 (s, 2H), 6.70 (d, *J*= 8.0, 1H), 7.00 (d, *J*= 8, 1H), 7.10 (s, 1H).

**7-*tert*-Butyl(dimethylsily)oxycoumarin (4).**<sup>47</sup> To a solution of 7-hydroxycoumarin (1.6 g, 10 mmol) in DMF (25 ml), *t*-butyldimethylsilyl chloride (TBDMSCl, 1.8 g, 12 mmol) and imidazole (1.6 g, 24 mmol) were added and stirred under room temperature for 6 hours. Brine was then added to dilute the solution. The mixture was washed using ether (3×15ml). The organic layer was collected and dried with sodium sulfate. Solvent was then evaporated to yield crude solid product. The product was purified using silica gel chromatography with hexane and ethyl acetate (5:1) to afford a white solid in 72% yield. <sup>1</sup>H NMR (400 MHz, CDCl<sub>3</sub>) δ 0.23 (s, 6H), 0.97 (s, 9H), 6.24 (d, *J*=9.6, 1H), 6.75 (m, 2H), 7.31 (d, *J*=8.0, 1H), 7.61 (d, *J*=9.6, 1H); <sup>13</sup>C NMR (100 MHz, CD<sub>3</sub>CN) δ -4.9, 18.3, 25.3, 107.8, 113.6, 113.9, 129.7, 144.1, 156.0, 159.4, 161.0; *m/z* (ESI+): 277.9, calculate (M+H<sup>+</sup>): 277.1; m.p.: 64~66 °C.

**7-*tert*-Butyl(dimethylsily)oxy-(2H, 3H)coumarin (5).** The procedure was adapted from the literature with modification.<sup>58</sup> Compound **4** (1.10 g, 4.03 mmol) was

dissolved in 60 ml absolute ethanol and then 10% palladium/carbon (0.50 g) was added to the solution. The mixture was shaken under hydrogen atmosphere (50 psi) in the Parr hydrogenator at room temperature for 22 h, after which the catalyst was filtered off and washed with ethanol. The filtrate was concentrated in vacuo and crude product was purified through silica gel chromatography using a mixture of hexane and ethyl acetate (7:1) as eluent to afford a white solid in 87% yield. <sup>1</sup>H NMR (400 MHz, DMSO-*d*<sub>6</sub>) δ0.17 (s, 6H), 0.95 (s, 9H), 2.74 (t, *J*=7.1, 2H), 2.91 (t, *J*=7.1, 2H), 6.55 (m, 2H), 6.99 (d, *J*=8, 1H); <sup>13</sup>C NMR (100 MHz, DMSO-*d*<sub>6</sub>) δ-3.7, 18.8, 23.0, 26.4, 29.6, 108.7, 116.5, 117.0, 129.7, 153.0, 155.5, 169.1; m.p.: 40~42 °C.

**Methyl 3-(2-methoxy-4-*tert*-butyl(dimethylsilyloxybenzen)propionate (6).** The procedure was adapted from the literature with modification.<sup>48</sup> To a solution of **5** (0.83 g, 2.5 mmol) in THF (25 ml) was added sodium hydride (60% in mineral oil, 1.0 g). The mixture was stirred at room temperature for 1 hour and then dimethylsulfate (2.37 ml, 14.1 mmol) was added. After stirring the mixture for another 3 hours at room temperature, 20 ml water was added to dilute the solution. Chloroform was used for extraction (3×15ml) and the collected organic phase was washed with 10% aqueous NaOH. Magnesium sulfate was used to dry the organic phase. Product was concentrated in vacuo yielding a yellow oil. Purification was achieved through silica gel chromatography with hexane and ethyl acetate (7:1) to afford a transparent liquid in 52% yield. <sup>1</sup>H NMR (400 MHz, DMSO-*d*<sub>6</sub>) δ0.14 (s, 6H), 0.90 (s, 9H), 2.45 (m, overlap with solvent peak), 2.67 (d, *J*=7.6, 2H), 3.53 (s, 3H), 3.70 (s, 3H), 6.29 (dd, *J*=8, 2, 1H), 6.35 (d, *J*=2, 1H), 6.93 (d, *J*=8, 1H); <sup>13</sup>C

NMR (100 MHz, DMSO-*d*<sub>6</sub>)  $\delta$ -3.6 18.8, 25.7, 26.5, 34.4, 52.1, 56.1, 104.1, 111.7, 121.9, 130.6, 155.6, 158.7, 173.8.

**Methyl 3-(2-methoxy-4-hydroxybenzen)propionate (7).** The procedure was adapted from the literature.<sup>49</sup> To a solution of **6** (0.572 g, 1.58 mmol) in THF (6 ml) was added TBAF/THF (1.0 M, 4 ml). The mixture was stirred for 1 hr at room temperature and then diluted with water. Ethyl acetate (3×10 ml) was used to extract the mixture and the collected organic phases were dried with magnesium sulfate. After removing the solvent under reduced pressure, product was purified with silica gel chromatography using hexane and ethyl acetate (7:1). The purified product was isolated as clear oil in 87% yield. <sup>1</sup>H NMR (400 MHz, DMSO-*d*<sub>6</sub>)  $\delta$ 2.43 (m, overlap with solvent peak), 2.64 (t, *J*=8, 2H), 3.52 (s, 3H), 3.67 (s, 3H), 6.21 (dd, *J*=8.2, 2.2, 1H), 6.32 (d, *J*=2.4Hz, 1H), 6.83 (d, *J*=8Hz, 1H).

**5-Bromo-2-hydroxy-4-methoxybenzaldehyde (9).**<sup>51</sup> 2-Hydroxy-4-methoxybenzaldehyde (0.91 g, 6.1 mmol) was dissolved in methylene chloride (8 ml) and cooled in an ice/water bath. Bromine (1.0 g, 6.6 mmol) in methylene chloride solution (0.3 ml) was added to the cooled solution dropwise. The solution was stirred in an ice bath for 3 hours and then warmed to room temperature and stirred for another hour. Sodium bicarbonate solution (10%) was then used to wash the organic phase (3×10 ml). Then the organic layer was dried with sodium sulfate and concentrated to a yellow solid 0.93 g. After recrystallization (ethyl acetate/hexane, 1:10), a white solid was obtained in 81% (1.12 g). <sup>1</sup>H NMR (400 MHz, CDCl<sub>3</sub>)  $\delta$  3.93 (s, 3H), 6.46 (s, 1H), 7.66 (s, 1H), 9.67 (s, 1H), 11.42 (s, 1H); *m/z* (ESI<sup>+</sup>): 230.9,

232.9, Calculated ( $M^+$ : 231.0); m.p.: 118~120 °C. Data agreed with the literature value.

**Methyl 3-(2-methoxy-4-hydroxy-5-formylphenyl)acrylate (10).** The procedure was adapted from the literature with modification in the amount of reagent used.<sup>59</sup>

Compound **9** (0.28 g, 1.0 mmol), Pd(OAc)<sub>2</sub> (0.022 g, 0.010 mmol) and 1,3-bis(diphenylphosphino)propane (0.082 g, 0.020 mmol) were dissolved in anhydrous DMF (2 ml, purchased from Aldrich) in a round bottom flask. Distilled triethylamine (0.45 ml) and methyl acrylate (0.26 mg, 3.0 mmol) were then added to the solution. The reaction was heated to 110 °C for 20 hours under N<sub>2</sub> gas. Ethyl acetate was added to the mixture after completion of the reaction (15 ml) to dilute the mixture and 2N HCl was added to make the mixture acidic (pH~3). The organic phase was washed with brine (3×25 ml), dried over sodium sulfate and evaporated to remove the solvent. The residue was subject to silica gel chromatography (Hexane: Ethyl acetate=5:2) to yield a white solid 0.051 g (21%). <sup>1</sup>H NMR (400 MHz, CDCl<sub>3</sub>) δ 3.78 (s, 3H), 3.93 (s, 3H), 6.46 (d, *J*=16, 2H), 6.44 (s, 1H) ( these two peaks are overlapped), 7.83 (d, *J*=16, 2H), 9.74 (s, 1H), 11.59 (s, 1H); <sup>13</sup>C NMR (100 MHz, CDCl<sub>3</sub>) δ 52.0, 56.6, 99.8, 115.3, 117.5, 117.9, 135.4, 139.0, 165.5, 166.0, 168.2, 194.9; *m/z* (ESI+): 237.0, calculate ( $M+H^+$ ): 237.2; m.p.: 128~136 °C

**Methyl 2-(4-formyl-3-hydroxyphenoxy)acetate (12).** To a solution of 2,4-dihydroxybenzaldehyde (1.38 g, 9.98 mmol) in THF (50 ml), potassium carbonate (1.38 g, 9.98 mmol) was added in one portion. The mixture was kept at 0 °C in an ice bath and methyl bromoacetate (1.0 ml, 10 mmol) in THF (5 ml) was added to the solution dropwise over 3 minutes while stirring. The mixture was then heated to 60

°C for gentle reflux for 6 hours. Potassium carbonate was removed through filtration and solvent evaporated to yield a green oily liquid. Purification was carried out through silica gel chromatography with methylene chloride and ethyl acetate (20: 1) to afford a white solid in 40% yield. <sup>1</sup>H NMR (400 MHz, CDCl<sub>3</sub>) δ 3.80 (s, 3H), 4.66 (s, 2H), 6.36 (d, *J*=2.4, 1H), 6.57 (dd, *J*=2.4, 8.4, 1H), 7.45 (d, *J*=8.8, 1H), 9.72 (s, 1H), 11.43 (s, 1H); <sup>13</sup>C NMR (400 MHz, CDCl<sub>3</sub>) δ 52.9, 65.4, 101.8, 108.9, 116.2, 135.9, 164.7, 165.0, 168.6, 195.0; *m/z* (M+H<sup>+</sup>): 211.08, calculated 211.06; melting point: 91-92 °C. 2D NMR results are also available (HSQC and HMBC). All corresponding carbon hydrogen correlations of this molecule are showing in the spectra, which are attached as Figure 3 and Figure 4 in the appendix (Page 92, 93).

**Methyl 2-(3-hydroxy-4-(hydroxymethyl)phenoxy)acetate (13).** To a solution of **12** (631 mg, 3.00 mmol) in THF (20 ml), borane-THF complex (1.0 M, 3 ml) was added dropwise. The mixture was stirred on ice bath for 2 hours. Water (20 ml) was added in one portion to the solution to consume the excess borane. Ethyl ether (3×15 ml) was used to extract the solution and the combined organic phases were washed with brine (2×15 ml), dried over sodium sulfate and concentrated under reduced pressure to yield clear oil. This crude product was used directly and immediately for the next step. Crude yield: 1.1 g, 84%. <sup>1</sup>H NMR (400 MHz, CDCl<sub>3</sub>) δ 3.78 (s, 3H), 4.58 (s, 2H), 4.78 (2H), 6.38 (dd, *J*=4, 8, 1H), 6.44 (d, *J*=4, 1H), 6.91 (d, *J*=8, 1H), 7.4 (s, 1H); <sup>13</sup>C NMR (400 MHz, CDCl<sub>3</sub>) δ 52.7 (CH<sub>3</sub>), 64.6 (CH<sub>2</sub>), 65.6 (CH<sub>2</sub>), 103.5 (C), 106.6 (C), 118.6 (C), 129.0 (C), 157.8 (C), 159.3 (C), 169.7 (C).

**Methyl 2-(3-*tert*-butyldimethylsilyloxy-4-(*tert*-butyldimethylsilyloxymethyl)-phenoxy)acetate (14).**<sup>60</sup> Imidazole (1.62 g, 23.8 mmol) was added to a solution of

*tert*-butyldimethylsilyl chloride (TBDMSCl, 1.52 g, 10.1 mmol) and crude product **13** (1.1 g) in DMF (8 ml). The mixture was stirred under room temperature for 17 hours. Then brine (30 ml) was added to dilute the solution and ether (3×15 ml) was used for extraction. The combined organic phases were dried over sodium sulfate and concentrated under reduced pressure. The residue was then purified by silica gel chromatography (hexane: ethyl acetate, 4:1) to yield compound **17** as a clear oil (692 mg, 52.4% over two steps). <sup>1</sup>H NMR (400 MHz, CDCl<sub>3</sub>) δ 0.06 (s, 6H), 0.19 (s, 6H), 0.91 (s, 9H), 0.97 (s, 9H), 3.78 (s, 3H), 4.57 (s, 2H), 4.65 (s, 2H), 6.34 (d, *J*=4, 1H), 6.47 (dd, *J*=4, 8, 1H), 7.30 (d, *J*=8, 1H); <sup>13</sup>C NMR (400MHz, CDCl<sub>3</sub>) δ -4.9, -3.8, 18.84, 18.85, 52.6, 60.6, 65.9, 106.2, 106.7, 126.2, 128.2, 153.3, 157.7, 169.9

**2-(3-Hydroxy-4-(*tert*-butyldimethylsilyloxymethyl)phenoxy)acetic acid (15).**<sup>61</sup> To a solution of **14** (202 mg, 0.458 mmol) in THF (3 ml), potassium trimethylsilylanolate (118 mg, 0.921 mmol dissolved in 2 ml THF) was added. The mixture was stirred in ice bath for 4 hours. Then 0.1 M citric acid solution was used to adjust the pH to 3. Water (10 ml) was then added to dilute the solution. The mixture was extracted with ether (3×10 ml), dried over sodium sulfate and concentrated under reduced pressure. The residue was then purified by silica gel chromatography (hexane: ethyl acetate, 1:1) to afford the product as white solid. (265 mg, 64.8%). <sup>1</sup>H NMR (400 MHz, CDCl<sub>3</sub>) δ 0.11 (s, 6H), 0.90 (s, 9H), 4.62 (s, 2H), 4.83 (s, 2H), 6.38 (dd, *J*=4, 8, 1H), 6.44 (d, *J*=4, 1H), 6.84 (s, *J*=8, 1H); mass data was collected using negative ionization method; *m/z* (ESI): 311.0 (M-H<sup>+</sup>), calculated: 311.1

**2-(3-*tert*-Butyldimethylsilyloxy-4-(*tert* butyldimethylsilyloxymethyl)phenoxy)-acetic acid (16).** Imidazole (343 mg, 5.04 mmol) was added to a solution of *tert*-

butyldimethylsilyl chloride (TBDMSCl, 379 mg, 2.53 mmol) and product **15** (203 mg, 0.650 mmol) in DMF (5 ml). The mixture was stirred under room temperature for 1 hour. Brine (25 ml) was then added to dilute the solution and ether (3×10 ml) was used for extraction. The combined organic phases were dried over sodium sulfate and concentrated under reduced pressure. The residue was then dissolved in methanol (5 ml) and potassium bicarbonate (65 mg) was added in one portion. The solution was stirred at room temperature for one hour and neutralized with 1M HCl. The mixture was diluted with water and extracted with ether (3×10 ml). The combined organic phases were washed with brine, dried over sodium sulfate and concentrated under reduced pressure. The residue was purified by silica gel chromatography (hexane: ethyl acetate, 2:1) to afford the acid product as white solid. (172 mg, 64%). <sup>1</sup>H NMR (400 MHz, CDCl<sub>3</sub>) δ 0.06 (s, 6H), 0.19 (s, 6H), 0.90 (s, 9H), 0.91 (s, 9H), 4.59 (s, 2H), 4.65 (s, 2H), 6.36 (d, *J*=2.4, 1H), 6.50 (dd, *J*=2.4, 8.8, 1H), 7.32 (d, *J*=8.4, 1H); <sup>13</sup>C NMR (400 MHz, CDCl<sub>3</sub>) δ -4.9, -3.8, 18.6, 18.8, 60.6, 65.4, 106.2, 106.7, 123.7, 128.3, 153.4, 157.2. No significant carbonyl carbon peak was observed around 160-200 ppm range due to the weak signal of the *sp*<sup>2</sup> carbon on the spectrum.

**2-(4-Formyl-3-hydroxyphenoxy)acetic Acid (18).** This procedure was adapted from the literature using a modified recrystallization procedure.<sup>62</sup> Compound **12** (1.02 g, 4.76 mmol) was first dissolved in THF (40 ml) and cooled to 0 °C in an ice bath. Potassium trimethylsilylanolate (1.83g, 14.3 mmol) was then added to the solution. The mixture was stirred on an ice bath for 4 hours until all of the starting material was consumed as monitored by TLC. Aqueous citric acid (0.1 M) was next used to adjust the pH to 2. The mixture was extracted with ether (3×15 ml), dried over sodium

sulfate and concentrated under reduced pressure. The crude solid was recrystallized in hexane/ethanol (10: 1) to yield pure compound **2** as a white solid (0.694 g, 74.4%).

$^1\text{H}$  NMR (400 MHz,  $\text{CD}_3\text{CN}$ )  $\delta$  4.72 (s, 2H), 6.43 (d,  $J=2.4$ , 1H), 6.60 (dd,  $J=2.4$ , 8.6, 1H), 7.59 (d,  $J=8.5$ , 1H), 9.75 (s, 1H), 11.34 (s, 1H);  $^{13}\text{C}$  NMR (125 MHz,  $\text{CD}_3\text{CN}$ )  $\delta$  65.9, 102.9, 109.4, 117.2, 137.4, 165.3, 166.2, 169.8, 197.0;  $m/z$  ( $\text{M}+\text{H}^+$ ): 197.04, calculated 197.04; melting point: decomposed at 130 °C

**2-(3-*tert*-Butyldimethylsilyloxy-4-formylphenoxy)acetic Acid (19).** To a solution of compound **18** (0.250 g, 1.27 mmol) in DMF (4 ml), triethylamine (0.90 ml, 6.4 mmol) and DMAP (0.039 g, 0.32 mmol) were added. *tert*-Butyldimethylsilyl chloride (TBDMSCl, 1.12 g, 7.61 mmol) was then added to the solution. The mixture was stirred at room temperature under  $\text{N}_2$  atmosphere for 20 hours. Then the reaction was diluted with water (20 ml) and extracted with ether (3×15 ml). The combined organic phases were washed with brine (25 ml), dried over sodium sulfate and concentrated under reduced pressure. The crude product was purified through silica gel chromatography with hexanes and ethyl acetate (2: 1, 1% acetic acid) to yield a white powder (42%, 0.167 g).  $^1\text{H}$  NMR (400 MHz,  $\text{CD}_3\text{CN}$ )  $\delta$  0.26 (s, 6H), 1.00 (s, 9H), 4.70 (s, 2H), 6.37 (d,  $J=2.4$ , 1H), 6.63 (dd,  $J=2.4$ , 8.8, 1H), 7.68 (d,  $J=8.8$ , 1H), 10.23 (s, 1H);  $^{13}\text{C}$  NMR (125 MHz,  $\text{CD}_3\text{CN}$ )  $\delta$  -3.8, 19.4, 26.4, 66.1, 107.1, 110.4, 123.3, 131.2, 161.8, 165.2, 170.1, 189.3;  $m/z$  ( $\text{M}+\text{H}^+$ ): 311.14, calculated 311.12; melting point: 114-115 °C

**2-(3-*tert*-Butyldimethylsilyloxy-4-(hydroxymethyl)phenoxy)acetic Acid (20).**<sup>53</sup>

Compound **19** (0.11 g, 0.35 mmol) was first dissolved in EtOH (5 ml) and cooled to 0 °C on an ice bath. Sodium borohydride (0.013 g, 0.35 mmol) was then added to the



solution in one portion. The mixture was stirred in an ice bath for 2 hours until all the starting material was consumed as monitored by TLC. The solution was diluted with water (5 ml) and then placed under reduced pressure to remove EtOH. The resulting aqueous solution was first washed with ether and aqueous phase was acidified using citric acid solution (1 M). Then ether (3×15 ml) was used to extract the aqueous solution again. The combined organic phases were dried over sodium sulfate, and the solvent was removed under reduced pressure to yield a white solid 92.5 mg (92.6%). The yielded product appeared as a single spot on TLC and single compound in proton NMR. So it required no further purification and was used for the next step immediately to avoid decomposition. <sup>1</sup>H NMR (400 MHz, CD<sub>3</sub>CN) δ 0.21 (s, 6H), 0.99 (s, 9H), 4.48 (s, 2H), 4.59 (s, 2H), 6.34 (d, *J*=2.4, 1H), 6.50 (dd, *J*=2.4, 8.5, 1H), 7.23 (d, *J*=8.7, 1H). *m/z* (M+H<sup>+</sup>-H<sub>2</sub>O): 295.15, calculated (M+H<sup>+</sup>-H<sub>2</sub>O):312.14; melting point: 115-116 °C

**2-(3-*tert*-Butyldimethylsilyloxy-4-(acetoxymethyl)phenoxy)acetic Acid (20).** This procedure was adapted from literature using a modified procedure for purification s.<sup>63</sup> To a solution of compound **23** (0.070 g, 0.22 mmol) in CH<sub>2</sub>Cl<sub>2</sub> (5 ml), triethylamine (0.10 ml, 0.66 mmol) and DMAP (0.008 g, 0.07 mmol) were added. The mixture was stirred under room temperature for 2 hours after acetic anhydride (0.04 ml, 0.4 mmol) was added to the solution,. The mixture was then diluted with water (15 ml), and extracted with CH<sub>2</sub>Cl<sub>2</sub> (3×10 ml). The organic phases were combined and dried over sodium sulfate and concentrated under reduced pressure. The crude product was purified with silica gel chromatography with hexanes and ethyl acetate (1: 1) to afford a product as white solid (56 mg, 71%). <sup>1</sup>H NMR (400 MHz, CDCl<sub>3</sub>) δ 0.23 (s, 6H),

0.97 (s, 9H), 2.04 (s, 3H), 4.62 (s, 2H), 5.02 (s, 2H), 6.42 (d,  $J=2.4$ , 1H), 6.46 (dd,  $J=2.6$ , 8.5, 1H), 7.21 (d, overlapped with solvent peak);  $^{13}\text{C}$  NMR (125 MHz,  $\text{CDCl}_3$ )  $\delta$  -4.0, 18.4, 21.2, 25.8, 62.3, 65.6, 106.4, 106.5, 120.7, 131.9, 155.7, 158.7, 171.4, 173.1.  $m/z$  ( $\text{M}+\text{H}^+-\text{AcOH}$ ): 295.16, calculated ( $\text{M}+\text{H}^+-\text{AcOH}$ ):295.14; melting point: 98-99 °C

**N-Succinimidyl-2-(3-*tert*-butyldimethylsilyloxy-4-(acetoxymethyl)phenoxy)-acetate (QMP2)**<sup>57</sup>. N-hydroxysuccinimide (0.017 g, 0.15 mmol) and 1-ethyl-3-(3-dimethylaminopropyl)carbodiimide (EDC, 29 mg, 0.15 mmol) were added to a DMF (2 ml) solution of **20** (0.040 mg, 0.11 mmol). The mixture was then stirred for 20 hours under room temperature, diluted with brine and extracted with ether (3×15 ml). The organic phases were combined and dried over sodium sulfate and concentrated under reduced pressure. The resulting residue was purified by silica gel chromatography with hexanes and ethyl acetate (1: 1) to yield the desired activated ester of compound **3** as a colorless oil (22 mg, 48%).  $^1\text{H}$  NMR (400 MHz,  $\text{CDCl}_3$ )  $\delta$  0.23 (s, 6H), 0.97 (s, 9H), 2.02 (s, 3H), 2.83 (s, 4H), 4.90 (s, 2H), 5.00 (s, 2H), 6.43 (d,  $J=2.4$ , 1H), 6.48 (dd,  $J=2.4$ , 8.6, 1H) 7.22 (d, overlapped with solvent peak);  $^{13}\text{C}$  NMR (125 MHz,  $\text{CDCl}_3$ )  $\delta$  -4.3, 18.1, 20.9, 25.5, 25.5, 61.8, 63.3, 106.2, 106.5, 120.9, 131.6, 155.4, 158.3, 164.4, 168.4, 170.9;  $m/z$  ( $\text{M}+\text{H}^+-\text{AcOH}$ ): 393.10, calculated ( $\text{M}+\text{H}^+-\text{AcOH}$ ): 393.23

## **Chapter 3: DNA-QM self-adduct formation and its DNA single strand alkylation is accelerated by using an electron-rich quinone methide precursor (QMP2)**

### ***3.1 Introduction***

A quinone methide precursor can be delivered to a specific sequence for alkylation through a target promoted alkylation process discussed in the first chapter. The desired conjugates were prepared by coupling an activated ester form of a quinone methide precursor to a site directing ligand. The site directing ligand can be single strand DNA or peptide nucleic acid (PNA)<sup>64</sup> that can specifically bind to the target sequence. After the ligand-QMP conjugate was treated with fluoride to generate the quinone methide intermediate, the QM quickly reacted with the nearby nucleophiles, such as the bases within the single strand DNA to produce the DNA-QM self-adduct (Figure 3.1). Previous study demonstrated that the QM regenerates spontaneously from its reversible adduct to react with other bases.<sup>31</sup> The use of a DNA-QM self-adduct for alkylation may find more applications than the DNA-QMP conjugate because QM can be generated from the reversible self-adduct without the need for an additional chemical signal (like fluoride). This avoids potential side effects caused by a triggering compound when applying this process in a biological system. In this chapter, both the conventional QMP1 and an electron rich QMP2 were coupled to the chosen single strand DNA. DNA-QM self-adduct formation and the subsequent single strand DNA alkylation process were tested to study the effect of increased electron density on alkylation. Formation of the self-adduct can be

monitored on HPLC (High Performance Liquid Chromatography) since the loss of the TBDMS group from the DNA-QMP conjugate greatly increases the polarity of the complex allowing it to be eluted sooner on reverse phase HPLC compared to the conjugate. According to previous study,<sup>31</sup> the DNA-QMP1 conjugate completely converted to the corresponding self-adduct in 24 hours. The cross-linking product formed by alkylation of the ssDNA using DNA linked QM could be detected with a denaturing gel. The maximal alkylation yield of a complementary single strand required a 7 days incubation using the DNA-QM1 self-adduct. By using the electron rich QMP2, we expect that the formation of the self-adduct will be much faster and the maximal alkylation yield will be achieved in a shorter time compared with QMP1. This increased reaction rate should make the alkylation process effective in a biological system.

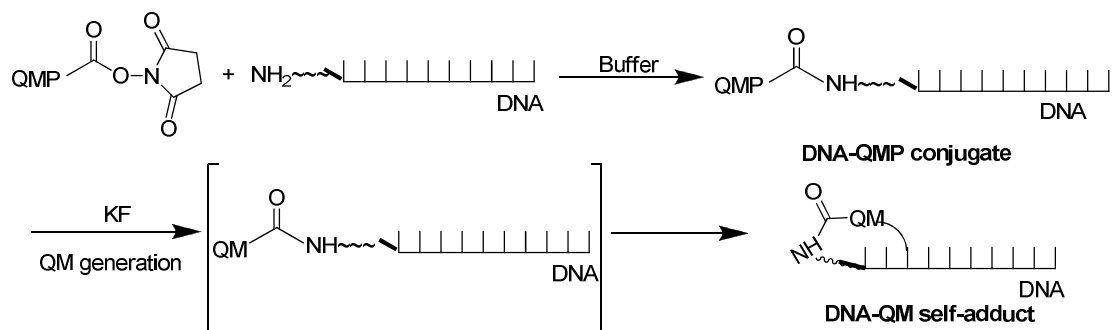


**Figure 3.1** Generation of a DNA-QMP conjugate and its DNA-QM self-adduct.

### 3.2 Results and Discussion

#### 3.2.1 Preparation of the DNA-QMP conjugates and DNA-QM self-adducts

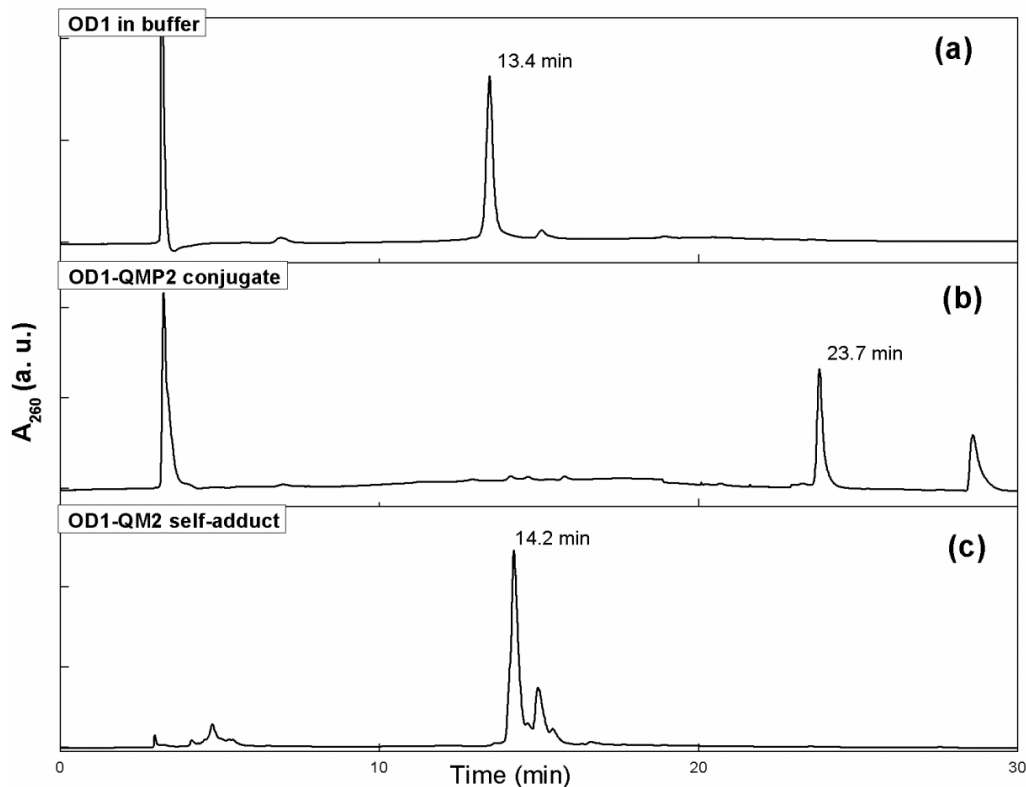
Both the DNA-QMP1 and the DNA-QMP2 conjugates were prepared following the same procedure by incubating the quinone methide precursor succinidyl esters with a 5'-aminohexyloligonucleotide OD1 (sequence listed in

figure 3.2).<sup>31</sup> After a 24 hours incubation at room temperature, the conjugates were purified by reverse phase HPLC. Both OD1-QMP1 and OD1-QMP2 have very similar retention times (around 24 min) on reverse phase HPLC using the same elution gradient due to their similar polarity (Figure 3.2 and appendix Figure 17, Page 105). The corresponding conjugates were collected and characterized by MALDI (Table 3.1). After confirming the formation of the conjugates by MALDI, the DNA-QM self-adducts were generated by incubating the corresponding conjugates with potassium fluoride. These products were also purified by HPLC. The retention time of the self-adducts were around 14 min (Figure 3.2c). This change in retention time resulted from the loss of the very non-polar TBDMS group from the quinone methide precursor.<sup>31</sup> The collected products were characterized and confirmed MALDI (Table 3.1 and appendix Figure 15, 16, Page 104).

<b>Product</b>	<b>Calculated Mass</b>	<b>Observed Mass</b>
<b>OD1-QMP1 conjugate</b>	<b>5562.5</b>	<b>5561.8</b>
<b>OD1-QM1 self-adduct</b>	<b>5388.7</b>	<b>5389.2</b>
<b>OD1-QMP2 conjugate</b>	<b>5564.5</b>	<b>5564.9</b>
<b>OD1-QM2 self-adduct</b>	<b>5392.7</b>	<b>5390.8</b>

**Table 3.1** MALDI data of the purified DNA-QMP conjugates and DNA-QM self-adducts.

**OD1 sequence:** 5' NH<sub>2</sub>~TTTCTCTTTTCTTCT



**Figure 3.2** OD1 sequence and RP-HPLC chromatography of (a) the pure oligonucleotide (OD1); (b) OD1-QMP2 conjugate; (c) OD1-QM2 self-adduct. Samples were eluted with a linear gradient of 10-55% acetonitrile in aqueous triethylammonium acetate (50 mM, pH 5.0) at 1 ml/min over 30 min.

### 3.2.2 DNA-QM self-adduct formation was promoted by the electron rich QMP2

As showed above, the DNA-QMP conjugates and DNA-QM self-adducts have very distinct retention time when eluting through HPLC. Therefore, HPLC can be used to monitor self-adduct formation over time and quantify the product yield with the corresponding peak area. After treating the conjugates with fluoride, the TBDMS protecting group is removed and the acetate derivative intermediate is generated (Figure 3.3). Then quinone methide intermediate is generated upon the left of the acetate group. This is the rate determining step for the QM generation reaction<sup>46</sup> and

the acetate derivative can be observed to accumulate on HPLC.<sup>31</sup> QM will react with a proximal nucleophilic base in the DNA sequence. As a result, a DNA-QM self-adduct is produced (Figure 3.3).

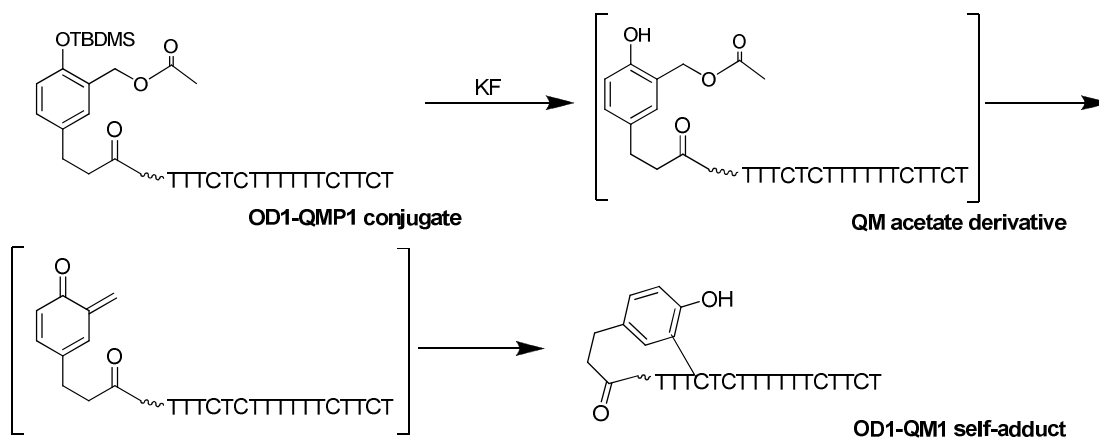


**Figure 3.3** Illustration of self-adduct formation using QMP1 as the model. The noted complex/intermediates are able to be detected on the HPLC.

The purified DNA-QMP conjugates were deprotected by addition of KF. The mixture was incubated at room temperature and separated by HPLC over different incubation time. According to the chromatography, both conjugates showed up around 24 min at the beginning of the reaction (0 min) (Figure 3.4a, b). After KF was added, the area of conjugate signal was decreased and new product corresponding to the acetate derivative (Figure 3.4a) and self-adduct (Figure 3.4a, b) appeared around 14 min. The acetate derivative was consistent with previous observation.<sup>31</sup> The self-adduct was confirmed by MALDI during preparation discussed above. Finally, all the conjugates were converted to the self-adduct since it is the only signal in the chromatograph with only self-adduct (15 min) showed up in the spectrum (Figure 3.4a, b).

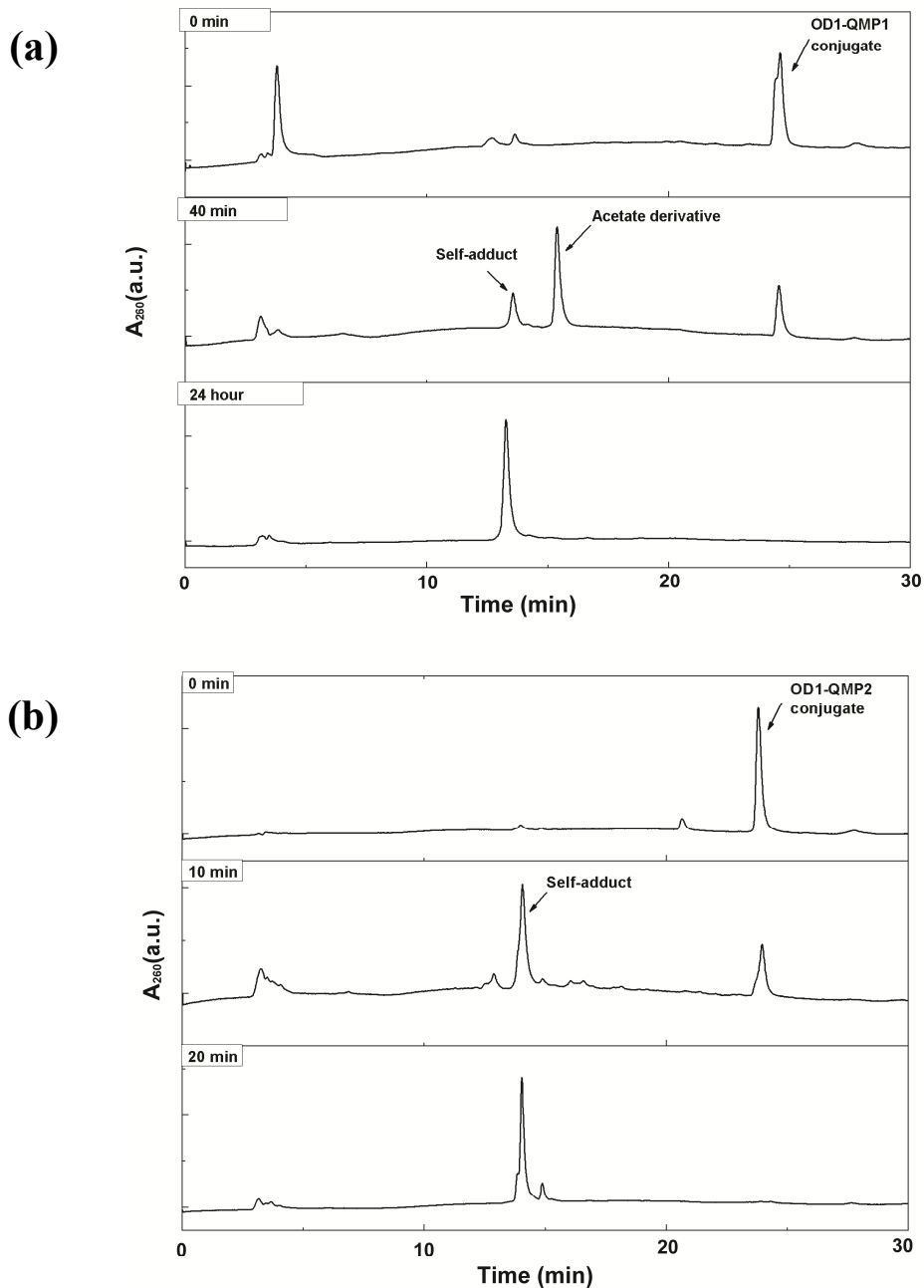


**Figure 3.4** (a) HPLC chromatograph of OD1-QMP1+KF in 0, 40 minutes and 24 hours; (b) HPLC spectrum of OD1-QMP2+KF in 0, 10, 20 minutes. Both conjugates samples were prepared with the same concentration ( $6.6 \mu\text{M}$ ) and incubated at room temperature. Equal amount of the reaction solution was injected to the HPLC at the indicated time. Samples were eluted with a linear gradient of 10-55% acetonitrile in aqueous triethyl-ammonium acetate (50 mM, pH 5.0) at 1 ml/min in 30 min.



Only around 20% OD1-QM1 self-adduct was formed after a 20 min incubation (Figure 3.4b) while OD1-QMP2 was completely consumed within that period of time and formed the OD1-QM2 self-adduct (Figure 3.4a). The OD1-QM1 generation yield over time was consistent with the previous results where the acetate derivative was clearly observed on the HPLC.<sup>31</sup> However, no acetate derivative peak was ever observed during OD1-QMP2 incubation. This observation agreed with our expectation that the generation of QM from QMP2 would be very fast and it might be hard to trap the acetate intermediate. These results suggested that generation of QM was promoted with the electron donating group in the molecule. The reaction half life was around 60 min with QMP1 but less than 5 min with QMP2 (Figure 3.5). This acceleration also suggested that regeneration of QM from the reversible self-adduct would also be faster for DNA-QM2 compared with DNA-QM1.

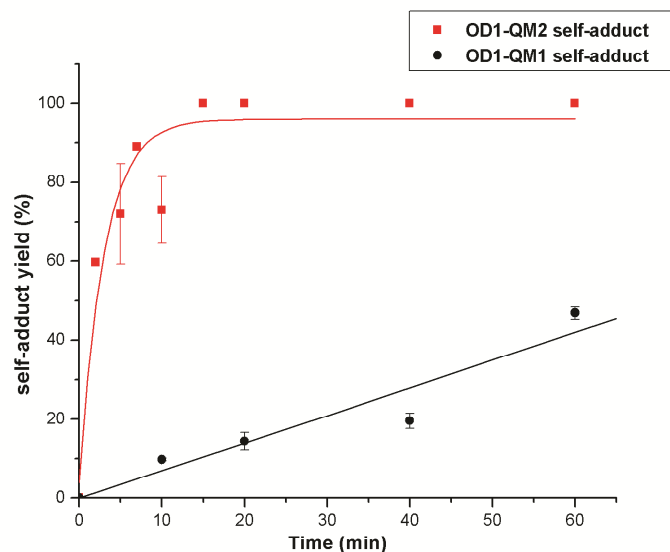


**Figure 3.5** Product yield of OD1-QM1 self-adduct (black) and OD1-QM2 self-adduct (red) generation over time. The data in the plot with error were the average of two experimental results. Data without error showed in the plot was one time result. The errors represent the range.

### 3.2.3 Single strand alkylation of DNA by DNA-QM self-adducts was accelerated by increased electron density of the QMP2

Quinone methides can alkylate a target single strand DNA sequence using a complementary single stranded DNA as the site-directing agent (Figure 3.6). In order to investigate the effect of the electron donating group on QMP alkylation, OD1-QM self-adduct generated from correspond conjugate was incubated with single strand OD2 (Figure 3.7). OD2 is complementary to OD1 sequence and has three more bases at the 3' end. The overhang was added to provide the non-base pairing nucleophiles for reaction to QM. Both OD1-QM1 and OD1-QM2 self-adducts were generated *in situ* and incubated with  $^{32}\text{P}$  radiolabeled OD2 at room temperature for up to 6 days (Figure 3.8).

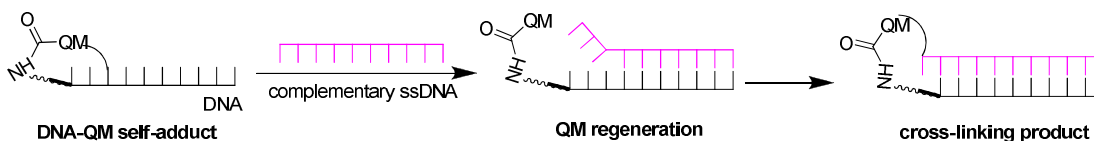


**Figure 3.6** Target alkylation process of the single strand DNA using DNA-QM self-adduct.

OD1: 5' NH<sub>2</sub>~~~ TTTCTCTTTTTTCTTCT  
 OD2: 3'..... AGAAAAGAGAAAAAAGAAGA

**Figure 3.7** DNA sequences for alkylation of single stranded DNA.

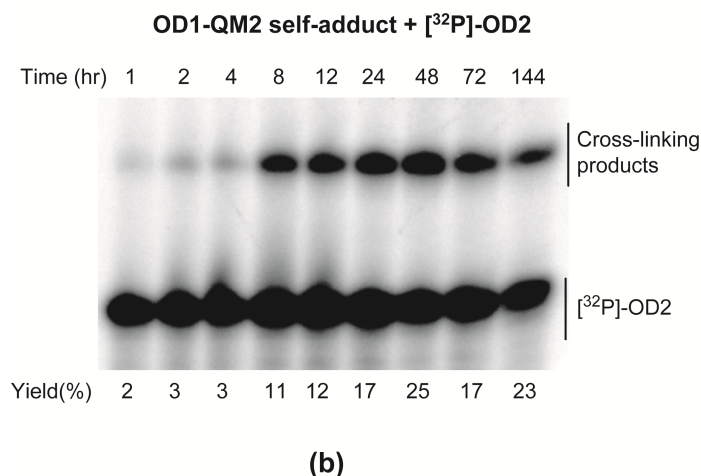
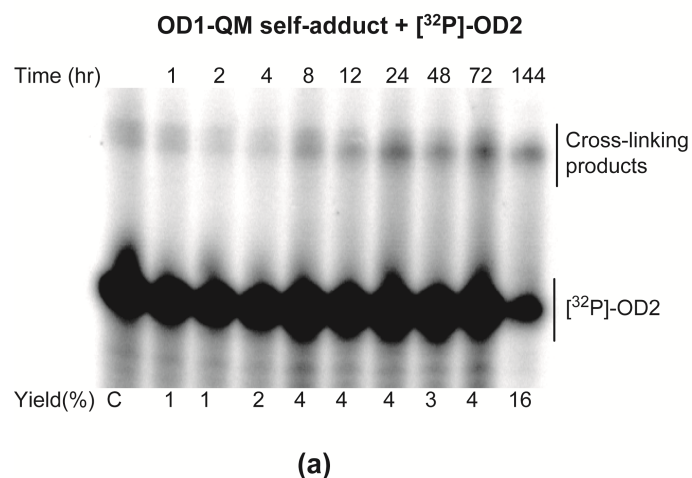


**Figure 3.8** Alkylation of single stranded DNA by DNA-QM1 (a) and DNA-QM2 (b). OD1-QM self-adducts were generated *in situ* by adding KF (100 mM) to the purified conjugates (6.6  $\mu$ M). <sup>32</sup>P radiolabeled OD2 was added to the sample after the conjugate incubated with KF for 24 hours. The samples were incubated under room temperature in MES buffer (20 mM, pH 7) for different periods of time. The final concentration of self-adduct was 3.3  $\mu$ M and OD2 was 3  $\mu$ M. The samples were then analyzed by 20% polyacrylamide denaturing gel. Alkylation yield was quantified based on the radioactivity of the product bands over the whole sample.

Maximal alkylation yield (20%) of OD2 was reached using the OD1-QM2 self-adduct within 2 days. However, it took at least 4 days for the OD1-QM1 self-adduct to achieve its maximal alkylation yield of 15% (Figure 3.9). This result

confirmed our earlier prediction that the use of the electron rich quinone methide precursor could accelerate DNA alkylation. However, in the previous report, single strand alkylation yield can reach 20% using the self-adduct formed by QMP1.<sup>31</sup> My self-adduct provided a lower average yield of alkylation. This difference probably came from the different sequence QM1 forms self-adduct with. Previously, a mixed base sequence was used. In my experiment, OD1 consists of pyrimidines and only the cytosine in the sequence would form alkylation adduct with the QM. This decreased the efficiency of self-adduct formation and thus limited its subsequent alkylation of the single strand DNA.

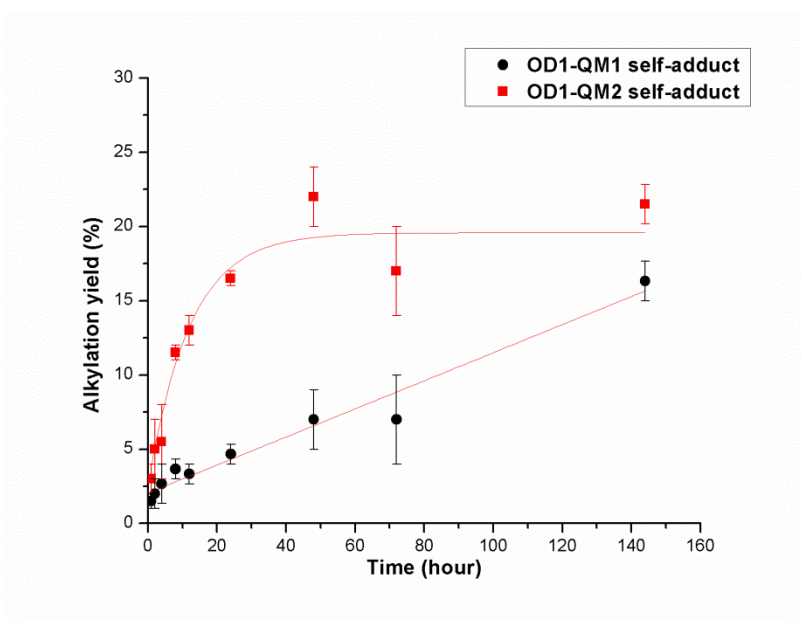


**Figure 3.9** Alkylation yield of OD2 over time. The alkylation yield in the plot is the average value of at least 3 experimental results. The error in the plot represents the range.

### 3.3 Conclusion

In order to investigate the effect of increased electron density on QM formation and alkylation, the electron rich quinone methide precursor QMP2 was

coupled to a DNA sequence OD1 to generate a self-adduct and alkylate single strand targets. The OD1-QMP1 conjugate which lacked the electron donating group was also used as a comparison. Twenty-four hours were necessary to completely convert OD1-QMP1 conjugate to the self-adduct but only 20 minutes were needed for OD1-QMP2 to complete the same process. The single strand alkylation process was also accelerated by using OD1-QM2 self-adduct. The maximal yield was achieved within the time (2 days) that OD1-QM1 needed (4 days). In conclusion, the electron donating group of QMP2 enhanced the alkylation ability of the QM by accelerating its QM generation process. This improvement on QM alkylation may be useful when applying to the biological system. The alkylation agents can form the cross-linking products in a short time before possible degradation happens by nuclease present in the system. Quick generation of QM might also help increase the reaction yield as discussed in the following chapter.

### ***3.4 Material and Methods***

#### **Materials**

All the reagents and materials used were obtained from the same source as stated in chapter 2. Aqueous buffer solutions were prepared with distilled, deionized water with a resistivity of 18.0 M $\Omega$ . T4 polynucleotide kinase (PNK) was obtained from New England Biolabs (Ipswich, MA). [ $\gamma$ -<sup>32</sup>P]-ATP was purchased from Perkin-Elmer (Waltham, MA).

#### **General HPLC method**

Oligonucleotides, their conjugates and self-adducts were all purified by reverse-phase (C-18, Varian Microsorb-MV, 300 A pore, 250 mm) HPLC using a gradient (30 min,

1 ml/min) of 10-55% acetonitrile in aqueous triethylammonium acetate (50 mM, pH 5.0) as controlled by a Jasco PU-2080 plus system (Jasco, Easton, MD). Samples were manually collected during elution from the HPLC and dialyzed against water to remove the salt. The purified product was analyzed by MALDI-TOF in the mass spectrometry facility of the Chemistry and Biochemistry Department.

**Preparation of DNA-QMP conjugates:** The conjugates were formed by combining the quinone methide activated succinidyl ester (1 mg) in CH<sub>3</sub>CN/DMF (2:1, 300  $\mu$ L) with the 5'aminohexyloligonucleotide (OD1, 15 nmol) in 3-(N-morpholino)-propanesulfonate buffer (MOPS, 250 mM, pH 7.5, 300  $\mu$ L) and incubating the mixture for 24 hours at room temperature. The above mixture was then purified by HPLC using the gradient above. Pure conjugate was collected in around 55% yield (8.5 nmol). The collected portion was dialyzed against water, lyophilized and store at -20 °C for future use.

**Formation of the self-adducts from the conjugates:** Self-adducts were formed by desilylating the TBDMS group of DNA-QMP conjugates (6.6  $\mu$ m) with KF (0.1 M) in 4-morpholineethanesulfonate buffer (MES, 20 mM, pH 7.0) and incubated at room temperature for 24 hours. The formation of self-adduct was monitored by HPLC. The mixture was incubated for 24 hours to allow the self-adduct to form and it could be used directly for alkylation study without further purification.

### **Target promoted alkylation and gel electrophoresis**

Target oligonucleotides were <sup>32</sup>P-labeled at their 5' terminus with 5'-[ $\gamma$ -<sup>32</sup>P]-ATP (Perkin Elmer Life Sciences, 5 mCi/ml), T4 polynucleotide kinase buffer (70 mM

Tris-HCl, 10 mM MgCl<sub>2</sub>, 5 mM dithiothreitol) and T4 polynucleotide kinase (New England Biolabs) using standard protocols. Self-adduct were generated *in situ* as mentioned above. 5'-[<sup>32</sup>P] target oligonucleotides solution (6 μL, 6 μM) was added to self-adduct solution (6 μL, 6 μM in MES: 20 mM, pH 7.0) generated equivalently. The mixture remained at room temperature for up to 7 days before analyzed by denaturing gel. After incubation, the samples were added to a loading buffer (0.05% bromophenol blue and 0.05% xylene cyanol FF in formamide, 1:1, V/V) and then analyzed by denaturing gel electrophoresis (20% acrylamide/7 M urea). The gel was exposed to a phosphorimager plate over night then scanned using a Molecular Dynamics Storm Phosphorimager (Sunnyvale, CA). Products were quantified using ImageQuant 5.2 software. The product yield was calculated using the radioactivity of the alkylation material divided by the overall radioactivity of the sample. This result indicated the percent of the radiolabeled strand that was cross-linked by the alkylating agent. The above experiments were repeated and the final yield was determined by averaging from at least 3 experimental results.

## **Chapter 4: Target duplex DNA sequences by DNA-QM species through triple helix formation**

### ***4.1 Introduction***

Double stranded DNA in the cell contains all of the genetic information necessary for life's processes. The primary nucleic acid sequence defines the genetic code and its secondary structure also has great effect on gene expression and regulation. Duplex DNA is considered an important target for developing therapeutic treatment because of its leading role in controlling cell activity.

Triple-helical DNA is one type of multi-stranded DNA structure that can affect regular cellular functions. It can be formed with a third strand (triplex forming oligonucleotide, TFO) binding to the major groove of the duplex sequence. A poly-pyrimidine/ poly-purine sequence is required for this binding.<sup>65</sup> The triplex binding is specific and stable through Hoogsteen hydrogen bonding. Modifications of the base and backbone of the TFO can further improve its binding affinity. For example, in the parallel pyrimidine triplex motif, substitution of cytosine with a 5-methylcytosine or N<sup>6</sup>-methyl-8-oxo-2-deoxyadenosine has been used to reduce the pH dependence of triplex formation (Figure 4.1).<sup>66,67</sup> Since regular cytosine in the TFO needs to be protonated around pH 5 to form hydrogen bonding with guanine, this modification allows the triplex formed and stabilized at neutral pH which makes it applicable in the biological system. Although the pKas of cytosine and methylcytosine are almost the same ( $4.4 \pm 0.2$ ), the 5-methylcytosine as may stabilize triple helix through enhanced base stacking.<sup>66</sup> 2'-O-Methylribose (2'-OMe) and 2'-O-aminoethylribose (2'-AE)



modified oligonucleotide were used to induce mutations in the cell<sup>68</sup> and also increased the binding affinity of the third strand to the duplex *in vitro* compared to the regular ribose backbone.<sup>69</sup> Triplex formed by a 2'-OMe modified third strand require less distortion of the TFO with the binding duplex.<sup>70</sup>

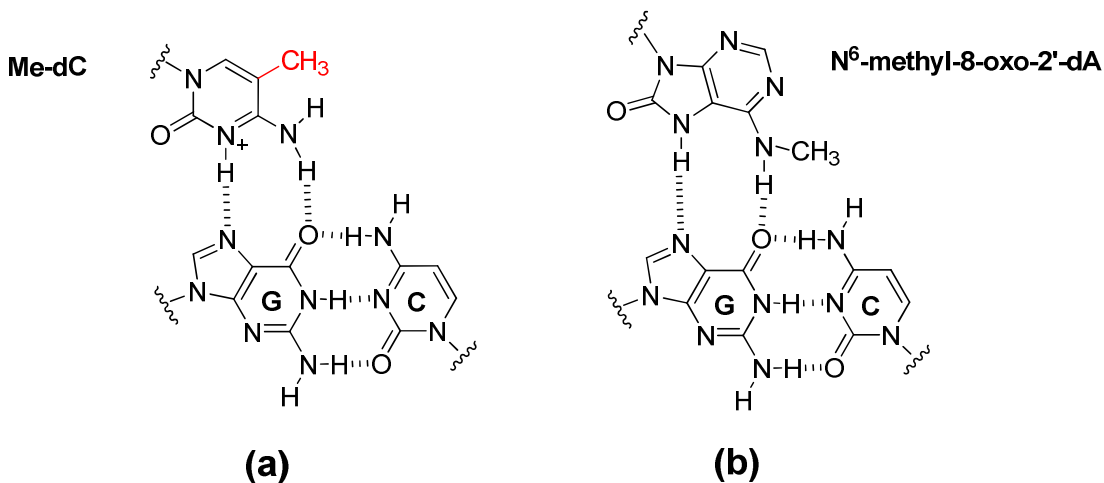


**Figure 4.1** Hydrogen bonding patterns for triplex formation with modified bases (a) 5-methylcytosine and (b) N<sup>6</sup>-methyl-8-oxo-2'-deoxyadenosine in the pyrimidine motif.

Small molecules can be attached to the TFO for delivery to a desired site to manipulate gene expressing.<sup>71</sup> One example of this is coupling a gene cleaver to the TFO for sequence specific cleavage. Common gene cleavers include Fe-EDTA<sup>72</sup> and biologically active enzymes like micrococcal nuclease.<sup>73</sup> These conjugates cleaved the DNA at the specific site and produce DNA fragments for gel electrophoretic analysis (Figure 4.2a).<sup>72</sup> Oligonucleotide clamping is another example of gene targeting through triple helix formation. A single oligonucleotide was designed with two parts of a sequence connected by a linker (Figure 4.2b). Of the two DNA sequence parts, one part binds first to the homopurine<sup>74</sup> or homopyrimidine<sup>75</sup> target through Watson-Crick bonds and then the other part folds back to bind to the newly

formed duplex to generate a triplex structure. This “clamp” structure inhibited chain elongation during DNA replication of a single stranded template *in vitro* by DNA polymerase.<sup>76</sup> Psoralen is another molecule that has been coupled to the TFO. Psoralen intercalates into the major groove of double strand DNA while the TFO binds to the major groove. The intercalation helps stabilize the triplex structure. Psoralen can also be activated through UV radiation to form DNA cross-links (Figure 4.2c). Psoralen reacts at AT base pairs and cross-links thymine. This light activated molecule allows control of the timing for damage and reduces non-specific damage to the rest of the genome.<sup>64</sup>

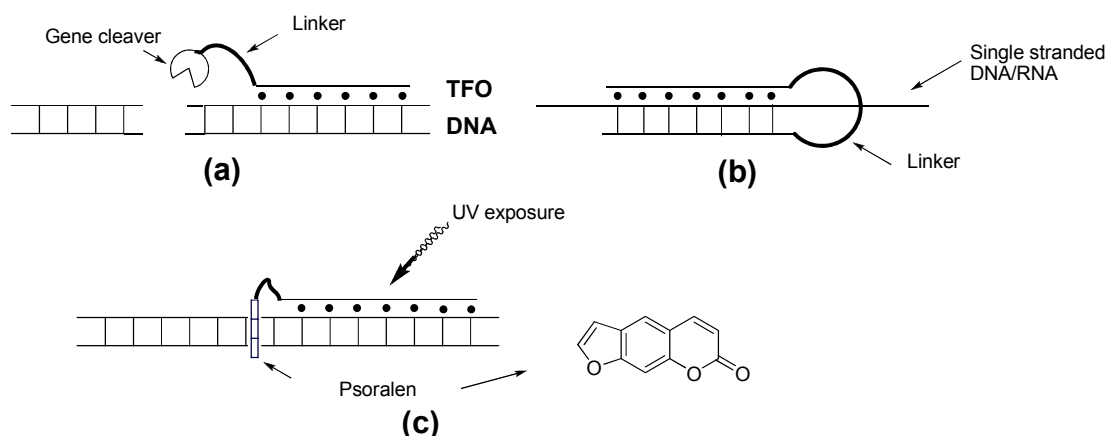
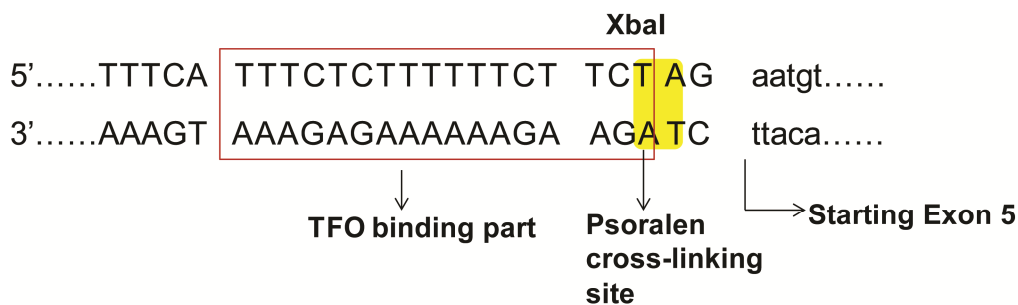


**Figure 4.2** Examples of applications based on triple helical structure. (a) Strand scission by TFO coupled with a cleaving agent. (b) Oligonucleotide clamping on a single stranded nucleic acid. (c) Site specific alkylation by psoralen linked TFO. Diagram was adapted from literature.<sup>71</sup>

Seidman’s group developed a gene targeting method using psoralen-linked TFO.<sup>44,77</sup> The target sequence selected was in the fourth intron next to exon 5 of the CHO *Hprt* gene (Scheme 4.1). This sequence contains a 17-base polypurine: polypyrimidine sequence with a 5’-TA base at the end which was used as a cross-linking site of psoralen. Mutagenesis by this TFO in the living cell was observed. Various modified TFO were test for the mutation and the TFO with a 2’-O-

aminoethyl substitution showed the best activity.<sup>78</sup> Around 20~30% of the cross-linking adducts formed by the TFO-psoralen conjugate induced mutation (>5% mutation frequency) indicating an effect target binding and mutagenesis by TFOs in living cell.

Inspired by this application of a DNA cross-linker in gene targeting, our quinone methide reagents should be tested in this system leading to mutations. Instead of using the photo-active molecule psoralen, quinone methide could be generated from DNA-QM self-adducts and react with the bases without any chemical or light initiation. The use of QM could avoid possible side reactions that might be induced by light.



**Scheme 4.1** *Hprt* gene target sequence. This sequence contains a recognition site for restriction enzyme XbaI (TCTAG) which was used for digestion purpose to analyze the cross-linking products.<sup>44</sup>

In this chapter, conditions to alkylate the target duplex DNA *in vitro* were optimized. Both DNA-QMP conjugates and DNA-QM self-adducts were prepared for alkylation study. The TFO sequence was also modified to promote the alkylation by enhancing triplex binding. Various target sequences were also tested to find the optimal sequence for QM alkylation. The electron rich quinone methide precursor (QMP2) was also coupled to the TFO to study its alkylation ability. Duplex alkylation

should be accelerated with QMP2 and its enhanced reactivity should also help increase the alkylation efficiency.

## ***4.2 Results and Discussion***

### **4.2.1 Preparation of the DNA-QMP conjugate and DNA-QM self-adduct**

The DNA-QMP conjugate and DNA-QM self-adduct species used for alkylation in this chapter were prepared following the procedure provided in Chapter 3. The DNA-QM self-adducts were generated by adding KF to the corresponding conjugates. They were either generated *in situ* for alkylation or purified through HPLC prior to incubate with the duplex as indicated in the specific experiment.

### **4.2.2 ssDNA alkylation by TFO-QMP1 conjugate**

The target duplex sequence chosen for the alkylation was adapted from the CHO *Hprt* gene introduced above. The TFO sequence (OD1) is listed below (Scheme 4.2). It is a 17-base long poly-pyrimidine sequence that binds to the poly-purine part of the target duplex to form a triplex structure. In order to ensure that only the QM formed cross-linking with target sequence through triplex formation, OD1-QMP1 conjugate was first incubated with selected single strand DNA (OD2 or OD3, Scheme 4.2) to check for the alkylation products.

Alkylation of a single strand DNA is expected when a target strand anneals to the delivery strand to form duplex. Incubation of the OD1-QMP1 conjugate with OD2, which was complementary to OD1, was used as a positive control to confirm its alkylation ability. OD3 represents polypurine sequence of the target duplex (red box of the purine strand in Scheme 4.1). OD1 was designed to bind to this sequence only

when it formed double strand DNA. So the sequence of OD3 was complementary to OD1 through Hoogsteen base pairs in a parallel direction. We expected no cross-linking between two strands because they should not form duplex. OD1-QMP1 was incubated with radiolabeled OD3 in MES 20 mM, pH 7 at room temperature and KF was added to initiate reaction. Alkylation products of OD2 by the OD1-QMP1 conjugate were detected by gel electrophoresis and the maximal yield around 68% was achieved within 24 hours (Figure 4.3a). Less than 5% alkylation was observed for OD3 using OD1-QMP1. This result agreed with our expectation that the OD1-QMP1 conjugate could not alkylate a target that could not form a duplex. Therefore, any cross-linking products observed with OD1 and this type of parallel complementary purine strand could only result from triplex formation (Figure 4.3b).

OD1: 3'..... TTTCTCTTTTTTCTTCT ~~~NH<sub>2</sub>  
 OD2: 5'..... AAAGAGAAAAAAGAAGAAGA  
 OD3: 5'..... AGAAGAAAAAAGAGAAA

**Scheme 4.2** TFO sequence OD1 and the single strand DNA sequences (OD2 and OD3). The 5' amino group linker in OD1 was used couple to QMP.

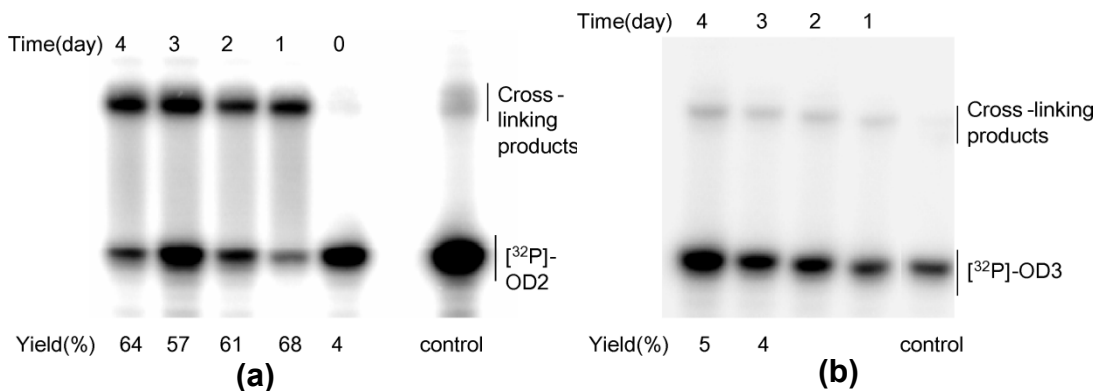
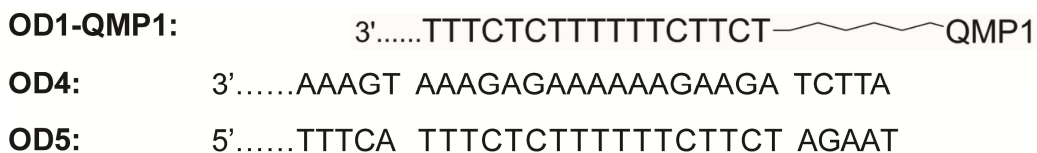


**Figure 4.3** Alkylation of single strand DNA OD2 (a) and OD3 (b) by the OD1-QMP1 conjugate. OD1-QMP1 (3.3 μM) and radiolabeled single strand DNA (3.0 μM) were incubated in MES (20 mM, pH 7). KF (100 mM) was added to initiate the reaction. The samples incubated at room temperature for 0-4 days. Then the samples were subject to analysis by 20% polyacrylamide denaturing gel electrophoresis.

### 4.2.3 Alkylation of the target duplex DNA by OD1-QMP1 conjugates

A target duplex DNA was prepared by annealing complementary single strands OD4 and OD5. The dsDNA sequence was adapted from the target *Hprt* gene. It contained the 17-base long homopurine/pyrimidine section for TFO binding (Scheme 4.3). Duplex OD4/OD5 was designed with 5 additional base pairs at both termini of the homopurine/pyrimidine region to stabilize the double helical structure. These bases also provided nucleophiles from beyond the triplex binding region so that QM could alkylate bases without destabilizing the triplex structure. OD1-QMP1 conjugate was incubated with OD4/OD5 and reaction was initiated with fluoride. Samples were incubated in MES (20 mM, pH 5) with MgCl<sub>2</sub> (10 mM). Divalent cation like Mg<sup>2+</sup> stabilizes the triplex by reducing the electrostatic repulsive forces between the negatively charged phosphate backbones of the three strands.<sup>65</sup> The cross-linking product was not observed consistently on the gel (Figure 4.4). Although we did see a high molecular weight product in less than a 10% yield (3 days and 4 days sample in the gel of figure 4.4), the DNA tended to migrate irregularly on the gel and lacked a distinct single band (1 day and 2 days sample in same gel). This irregular migration was observed repeatedly.



**Scheme: 4.3** OD1-QMP1 sequence and target duplex sequence OD4/OD5.

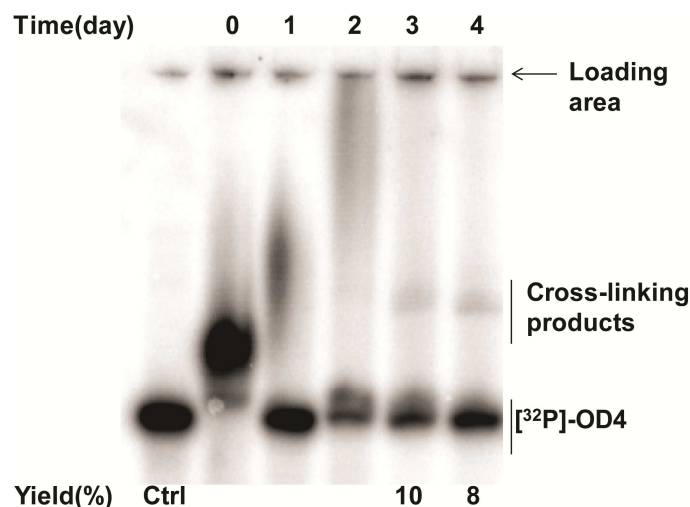


**Figure 4.4** Alkylation of target duplex OD4/OD5 by OD1-QMP1. [<sup>32</sup>P]-OD4/OD5 (0.1 μM) was pre-annealed in MES buffer. OD1-QMP1 (10.0 μM) was added to the duplex (0.05 μM) and KF (100 mM) was used to activate the QM. The sample was incubated in MES buffer (20 mM, pH 5) with NaCl (150 mM) and MgCl<sub>2</sub> (10 mM) under ambient conditions for 0~4 days. Samples were analyzed by 20% polyacrylamide denaturing gel without any further treatment. Ctrl: single strand [<sup>32</sup>P]-OD4 in the incubation buffer.

Various methods were tested to solve the inconsistent mobility issue of the DNA. Ultimately, the fluoride and magnesium in the sample solution were found responsible for disturbed proper migration of the cross-linked material on the gel (Figure 4.5, lane 2). Ethylenediaminetetraacetic acid (EDTA) was added to the solution to help solve this problem. EDTA could chelate Mg<sup>2+</sup> to prevent possible precipitation caused by Mg<sup>2+</sup> and F<sup>-</sup>. With the addition of EDTA, the cross-linking products reappeared on the gel (Figure 4.5, lane 3). However, use of EDTA did not help with the triplex samples and the still no distinct alkylation band was observed. Data for this looked similar to Figure 4.4 and is included in the appendix Figure 18 (Page 105).

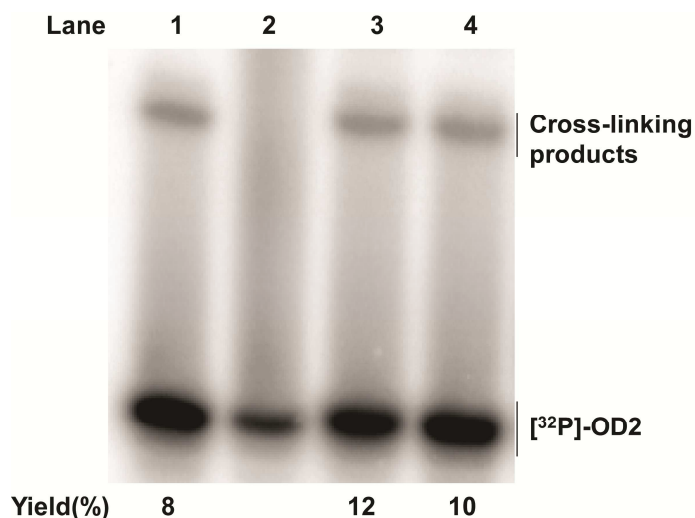


**Figure 4.5** Salt effects on alkylation and migration of DNA products through a denaturing gel. OD1-QMP1 (3.3  $\mu$ M), [ $^{32}$ P]-OD2 (3.0  $\mu$ M) and KF (100 mM) were incubated in MES (20 mM, pH 6) with different salt concentrations. Lane 1: No salt added; Lane 2: NaCl (150 mM) and MgCl<sub>2</sub> (10 mM); Lane 3: NaCl (150 mM) and MgCl<sub>2</sub> (10 mM) with EDTA (10 mM); Lane 4: NaCl (150 mM).

Finally, samples had to be desalted using P6 columns to remove the ions in the solution before analysis by the denaturing gel. Single distinct high molecular weight signals representing the cross-linking products were observed on the gel after samples were desalted (Figure 4.6). OD1-QMP1 conjugates was incubated with [ $^{32}$ P]-OD4/OD5 in MES (20 mM, pH 5) with 150 mM NaCl, 2.5 mM MgCl<sub>2</sub> and 100 mM KF at room temperature. Lower concentration of MgCl<sub>2</sub> was used here than used in the previous sample (10  $\mu$ M) to minimize its effect on DNA migration on the gel. The above buffer concentration is regarded as the standard condition for duplex alkylation and was used for all the following triplex samples for incubation or otherwise specified.



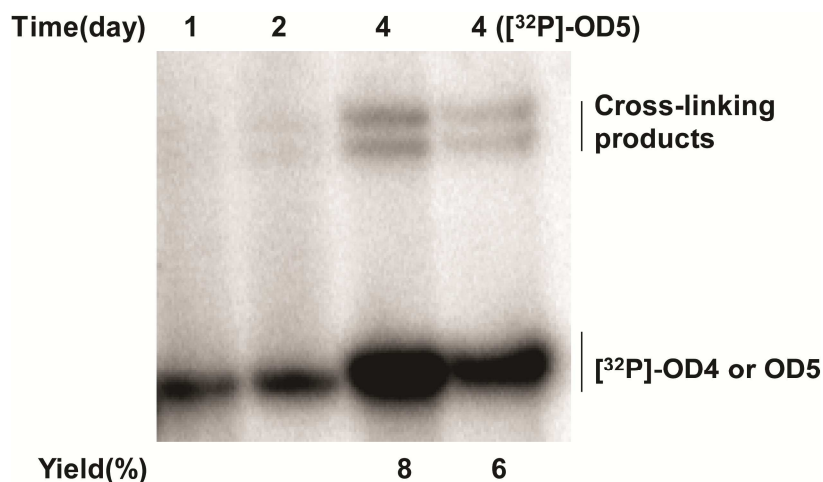


**Figure 4.6** Alkylation of double strand DNA by OD1-QMP1. Double strands [<sup>32</sup>P]-OD4/OD5 (samples without specification) and OD4/[<sup>32</sup>P]-OD5 (specified in the figure) were pre-annealed in MES buffer (20 mM, pH 5) with NaCl (150 mM) and MgCl<sub>2</sub> (2.5 mM). OD1-QMP1 (10.0 μM) was added to the duplex (0.05 μM) and KF (100 mM) was used to initiate the reaction. The samples were incubated under ambient conditions for 1~4 days. Samples were desalted using P6 columns before analyzed by the 20% polyacrylamide denaturing gel.

Only around 10% alkylation product was formed with the polypurine binding strand (OD4) after a 4-day incubation by observing the cross-linking products with radiolabeled purine strand. The cross-linking yield with the polypyrimidine strand (OD5) was even lower (6%). These yields are too low for alkylation to make an effect in a biological system. Efforts discussed below were made to improve the alkylation yield.

#### 4.2.4 Sequence dependent alkylation by OD1-QMP1 conjugate

One way to increase the alkylation yield of DNA is to provide the QM with nucleophiles that are preferred to react with. Previous study of QM alkylation through triplex formation showed that QM preferred to react with adjacent guanine to the binding strand of the duplex to form cross-linking products.<sup>79</sup> Therefore, new target

duplexes were designed with guanines adjacent to the binding site of TFO next to QM. The new targets were modified from OD4/OD5 by deleting the AT base pair adjacent to the binding region and next to QMP to place a guanine at the adjacent site (Scheme 4.4). OD1 can still bind to the duplex and would be adjacent to guanine to promote QM alkylation. The guanine was placed in the pyrimidine strand (OD7) in duplex OD6/OD7 and in the purine strand (OD8) in duplex OD8/OD9. The OD1-QMP1 conjugate was incubated with OD6/OD7 and OD8/OD9 separately and the denaturing gels are shown below (Figure 4.7). Either polypyrimidine or polypurine strands were radiolabeled to prepare totally 4 duplex samples. All of them were incubated with the conjugates and then analyzed by gel electrophoresis. The results indicated that the alkylation yield increased when there was an adjacent guanine to QM in the target sequence. When the polypurine strand was radiolabeled, the yield reached around 20% after a 5 day incubation with guanine adjacent to the binding region (OD8) compared to around 10% yield when no guanine was present (Figure 4.7). The results agreed with our prediction that adjacent guanine could improve the alkylation yield by promoting alkylation reaction with QM. When the polypyrimidine strand was radiolabeled, cross-linking products with the pyrimidine strand had a lower yield than that of the purine strand. This result also indicated that QM preferred to react with adjacent bases. Target duplex OD8/OD9 provided with the best alkylation efficiency of all three duplex DNAs we studied so far. Thus, this sequence was used for most of the following triplex alkylation studies.

**OD1-QMP1:** 3'.....TTTCTCTTTTTTCTTCT ~~~~~ QMP1  
**OD6:** 3'.....AAAGT AAAGAGAAAAAGAAGA CTTA  
**OD7:** 5'.....TTTCA TTTCTCTTTTTTCTTCT **G**AAT  
**OD8:** 3'.....AAAGT AAAGAGAAAAAGAAGA **G**TTA  
**OD9:** 5'.....TTTCA TTTCTCTTTTTTCTTCT CAAT

**Scheme 4.4** New duplex sequences with adjacent guanine (highlighted in red).

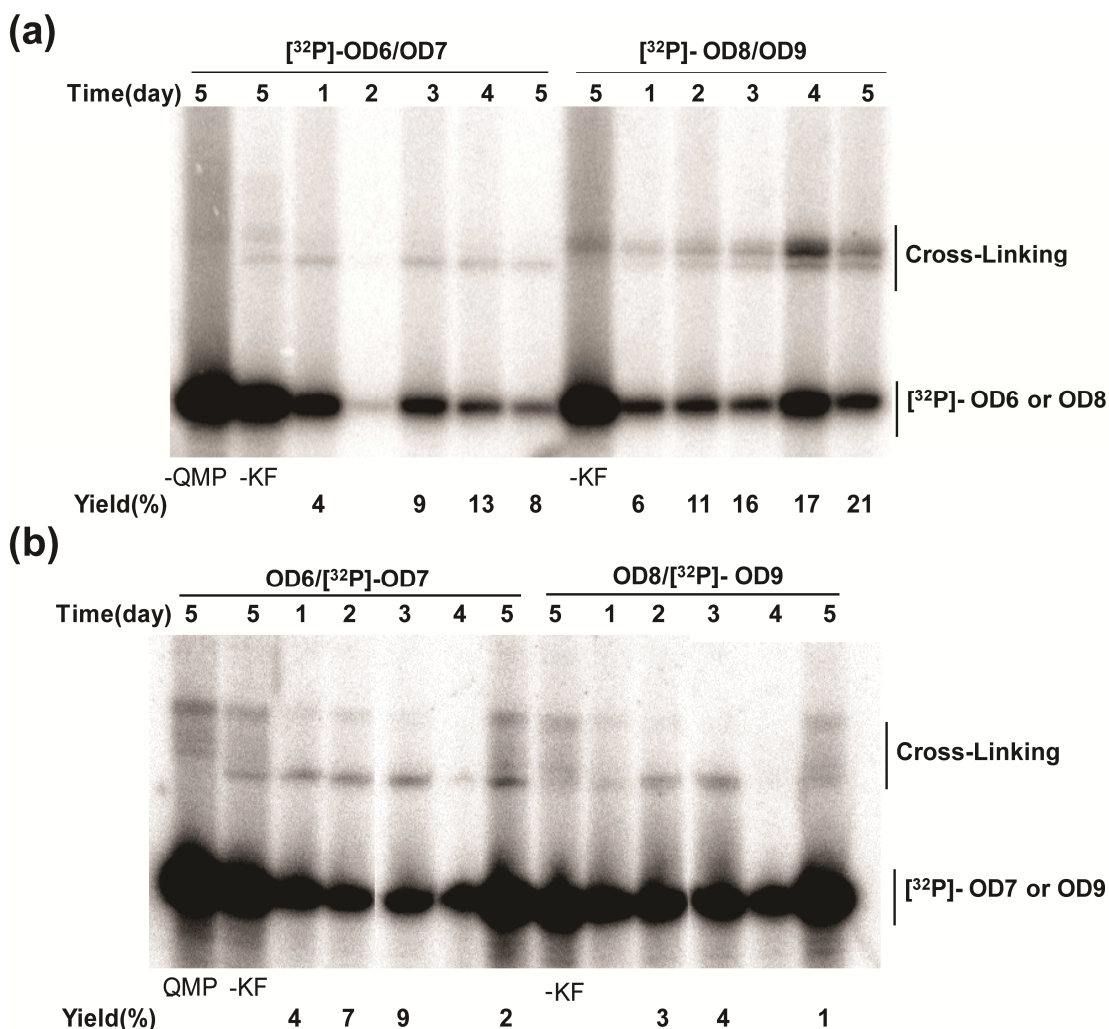


**Figure 4.7** Sequence dependent alkylation by OD1-QMP1. OD1-QMP1 (10.0 μM) was incubated with the indicated duplex sequence (0.05 μM) under standard condition for up to 5 days. Samples were desalted before loading on a denaturing gel. Control samples were either lacking cross-linking agent or KF. Cross-linking products with polypurine strand are showed in gel (a); cross-linking products with polypyrimidine strand were showed in gel (b).

#### 4.2.5 Modified TFO was used to enhance triplex binding

To further increase the alkylation efficiency, a modified TFO (TFO1) was conjugated to the QMP to enhance its binding. TFO1 contained the exact same sequence as OD1 except that the cytosines in the strand were ethylated on their 5 position of the pyrimidine ring. This modification allows triplex formation at neutral condition. It also enhanced the binding by increasing the  $T_m$  of the third strand.<sup>66</sup> The TFO1-QMP1 conjugate was incubated the OD8/OD9 (Scheme 4.5). The alkylation yield reached 27% after 7 days incubation (Figure 4.8). The yield was higher compared to alkylation by OD1-QMP1 conjugate. As expected, the duplex alkylation was improved by incorporating modified bases in the TFO sequence.

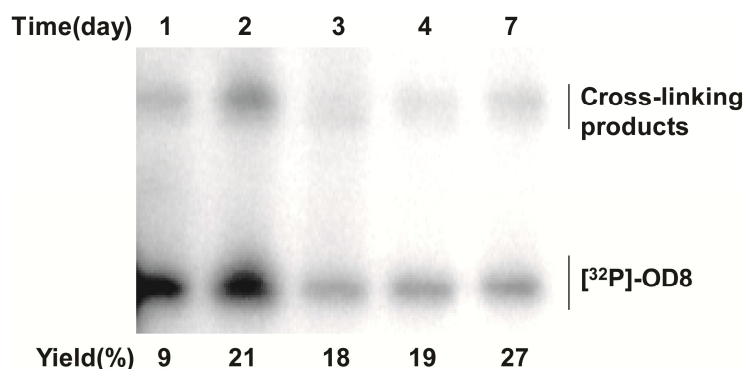
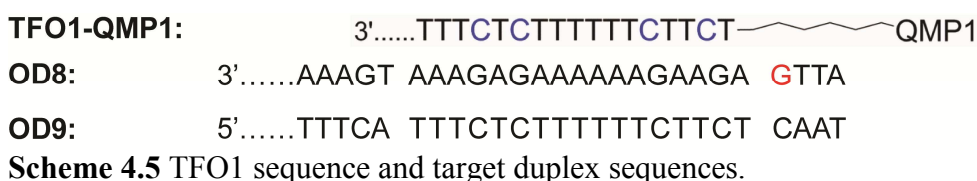


**Figure 4.8** Modified TFO sequences (TFO1) and alkylation of OD8/OD9 with TFO1 linked QMP1. The cytosines showed in blue color in the sequence represent 5-methyl cytosine. Purified TFO1-QMP1 (5.0  $\mu$ M) was incubated with pre-annealed [ $^{32}$ P]-OD8/OD9 (0.05  $\mu$ M) and KF (100 mM) using standard condition for up to 7 days. Samples were desalted before analyzed by the denaturing gel electrophoresis.

#### 4.2.6 DNA-QM1 self-adduct showed limited ability to alkylate the target duplex

In addition to use of the DNA-QMP1 conjugate to alkylate target duplex, alkylation by DNA-QM1 self-adduct was also studied because no chemical or light is

necessary to trigger QM reaction from the self-adduct. QM can be regenerated spontaneously from the reversible self-adducts to promote alkylation of DNA.<sup>31</sup> This property provides a promising future for *in vivo* application since KF used to activate QMP is toxic to cells. OD1-QM1 self-adduct used for triplex alkylation was purified through HPLC before incubating with the target duplex. As a result, the fluoride ion was removed and no extra desalting step was necessary before gel analysis. The TFO1-QM1 self-adduct was incubated with duplex OD8/OD9 alternatively at pH 5 and pH 7 to check for its pH effect. However, no obvious alkylation was observed under either condition (Figure 4.9).

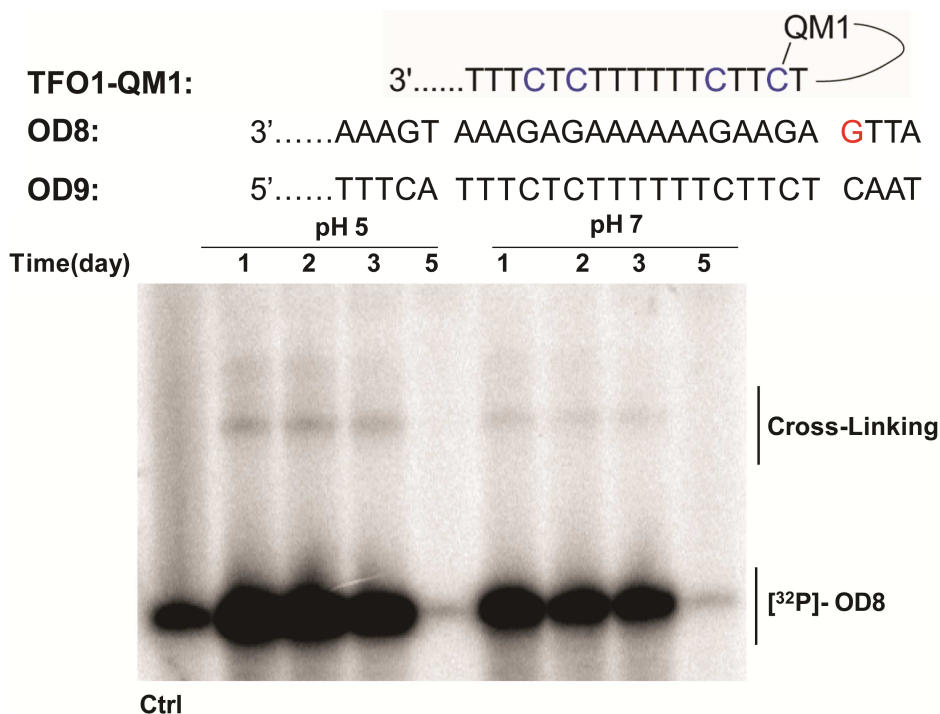


**Figure 4.9** Alkylation of duplex DNA by the TFO1-QM1 self-adduct. TFO1-QM1 self-adduct was prepared by incubating the TFO1-QMP1 conjugate with KF for 24 hours and the products was purified by HPLC. Pre-annealed double strand [<sup>32</sup>P]-OD8/OD9 (0.05 μM) and purified TFO1-QM1 (5.00 μM) were mixed in MES buffer (20 mM) with NaCl (150 mM) and MgCl<sub>2</sub> (2.5 mM) at pH 5 and pH 7. Samples were incubated under ambient condition for up to 5 days and then analyzed by denaturing gel without any further treatment. The control sample contained only OD8/OD9 in incubation buffer for 5 days.

The experiments discussed in section 4.2.4 showed that the OD1-QMP1 conjugate can successfully alkylate the target duplex with decent yield. This confirmed the formation of the triple helix between the chosen TFO and target duplex. The reasons that the alkylation yield of the TFO1-QM1 self-adduct was so low might be the limited reactivity of QM released from the self-adduct. Or, the DNA-QM self-adduct might not be thermodynamically favored to bind and react with the duplex based on the folded structure. TFO needs to be correctly folded for QM to react with the base in the TFO sequence. If QM reacted with cytosine close to the 3' terminus, the resulting DNA-QM self-adduct may not be able to bind tightly to the duplex sequence because of limited bases positioned correctly for hydrogen bonding (Figure 4.10). In order to solve this issue, another modified TFO with a 15 base polypyrimidine sequence and an unpaired adenine at the 5' end was designed (TFO2, Scheme 4.6). TFO2 contains the sequence that can still bind to the duplex target. The modification on 5' end should be helpful since QM can only react with the cytosine in the pyrimidine strand.<sup>80</sup> The added adenine can provide a strong nucleophilic site to react with QM. The reversible self-adducts formed with this site regenerate the QM readily.<sup>45</sup> Addition of adenine increased the chance of generating self-adduct with a less folded sequence since QM can react with adenine and cytosine that are close to itself (5' terminus). Besides, the unpaired adenine can also act as a linker between DNA and QMP which may extend the distance for QM to reach for possible nucleophiles. The TFO2-QM1 self-adduct was incubated with pre-annealed OD4/OD5 for up to 4 days. Duplex OD4/OD5 was used to provide an adjacent guanine. No obvious increase of alkylation products was observed (Figure 4.11). This

result indicated that third strand binding of the self-adduct to the duplex was not the problem for the low alkylation yield.

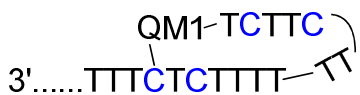


**Figure 4.10** Possible folded structure of a TFO-QM1 self-adduct. Bases that are folded during self-adduct formation could not bind to dsDNA to form triplex.

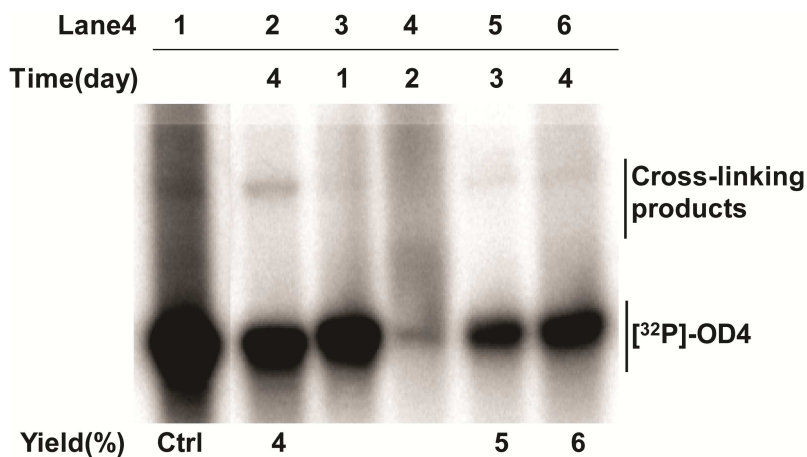
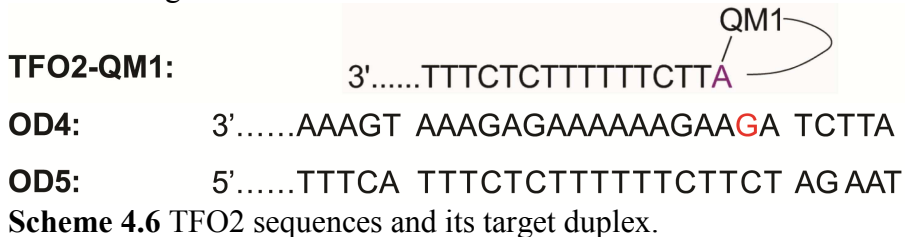


**Figure 4.11** Alkylation of duplex DNA by TFO2-QM1 self-adducts. TFO2 sequence is listed above and contains the unpaired adenine. The TFO2-QM1 (10.0  $\mu$ M) self-adduct was generated *in situ* and [ $^{32}$ P]-OD4/OD5 (0.05  $\mu$ M) was added. Samples were incubated in MES (20 mM) with NaCl (150 mM) and MgCl<sub>2</sub> (2.5 mM) at pH 5. A P6 column was used to desalt samples before analysis by the denaturing gel electrophoresis. Lane 1 was a control with only [ $^{32}$ P]-OD4/OD5 in the buffer for 4 days. The sample of lane 2 contained 100 equiv. of the self-adduct (5.00  $\mu$ M). Samples from lane 3 through lane 6 contained 200 equiv. of the self-adduct (10.0  $\mu$ M).

Modifications on the target sequences were also tested to promote the alkylation of the QM. An unpaired guanine adjacent to the QM was added into the sequence since no hydrogen bonding has to be broken when reacting with the QM.

Thus, the energy barrier for the alkylation was lowered and the reaction kinetics were increased. As a result, DNA alkylation product was likely to be produced. Based on this idea, new duplex targets were designed from the original sequence (Scheme 4.7). They all contain the same 17-base TFO binding region but differ in the position of unpaired guanines. Duplex OD10/OD11 and OD12/OD13 have three extra bases (GCG) which are not paired in the sequence. Duplex OD14/OD15 and OD16/OD17 contain one unpaired G. Both OD1-QMP1 conjugate and OD1-QM1 self-adducts were incubated at room temperature for 6 days and around 20% alkylation was detected for samples treated with OD1-QMP1. However, alkylation by the OD1-QM1 self-adduct produced less than 5% alkylation (Figure 4.11). One possible reason for this result is that the extra bases added in the target sequence cannot be reached by the QM since the bulge part was likely to be positioned outside the major groove of the duplex structure. In order to provide an unpaired guanine within the DNA double helix structure, another target duplex (OD16/OD18) with an abasic site was prepared. The guanine (highlighted in red) in OD16 that is adjacent to the binding region next for QMP has no base to form hydrogen bonding in the opposite strand. As a result, the guanine is placed within the double helical structure and no hydrogen bonding needs to be broken if react with QM. However, alkylation yield of this duplex with an abasic site was still low (<2%) after a 6 day incubation. (The gel is included in the appendix Figure 19, Page 106). The low yield obtained with the newly designed targets suggested that the modifications we introduced to the duplex did not improve the alkylation yield very much. Other ways were needed to help with the alkylation by DNA-QM self-adduct.





**Scheme 4.7** Modified duplex sequences for QM alkylation. Adjacent guanine bases were showed in red. The purple uracil indicates the abasic site.

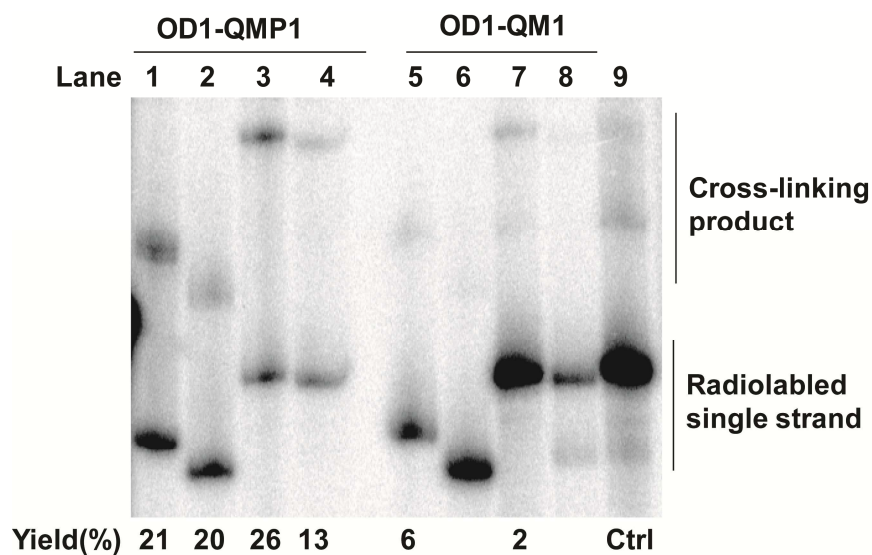


**Figure 4.12** Alkylation of the modified sequences: [<sup>32</sup>P]-OD10/OD11 (Lane 1 and 5); [<sup>32</sup>P]-OD12/OD13 (Lane 2 and 6); [<sup>32</sup>P]-OD14/OD15 (Lane 3 and 7); [<sup>32</sup>P]-OD16/OD17 (Lane 4 and 8). Both the OD1-QMP1 conjugate and the OD1-QM1 self-adduct were incubated with the target duplex for 6 days under standard condition and then analyzed by denaturing gel after desalting. Only purine strand was radiolabeled to check for the cross-linking products.

#### 4.2.7 DNA-QM2 self-adducts showed good ability for duplex DNA alkylation

Alkylation of double strand DNA by the DNA-QM1 self-adduct was observed but with very limited yield compared to the alkylation by the conjugates. Triplex formation with the target sequence was confirmed with alkylation products produced by OD1-QMP1 conjugates. Available nucleophiles were provided to promote alkylation. However, neither enhanced binding of the third strand nor preferred nucleophiles for QM improved the alkylation yield. This suggested that the DNA-QM self-adduct itself might be the major issue responsible for the low alkylation efficiency. The QM1 released from the self-adduct might have limited reactivity with the bases. Therefore, a new QM that could be generated and regenerated more readily than QM1 might help with the alkylation. As introduced in Chapter 2 and 3, an electron rich quinone methide precursor (QMP2) was synthesized and coupled to DNA to promote the kinetics of the single strand alkylation. QM2 was regenerated from OD1-QM2 self-adduct faster than OD1-QM1 species (Figure 3.5). With this fast regeneration and increased reactivity, OD1-QM2 should react with the duplex targets with higher efficiency than OD1-QM1.

The OD1-QM2 self-adduct was prepared and purified under standard condition and then added to OD8/OD9. Samples were incubated using standard conditions at room temperature for 1-7 days. OD1-QM1 self-adduct samples were also included as a control. When the OD1-QM2 self-adduct was used, a maximal target alkylation of 20% was produced in 3 days (Figure 4.13). In contrast, cross-linking product was barely observed on the gel using the OD1-QM1 self-adduct with the same target sequence. This result showed a better alkylation ability of the OD1-

QM2 self-adduct over the OD1-QM1 self-adduct. This improvement in alkylation might be due to the fact that quinone methide intermediate was released more readily to react with nucleophilic sites on DNA. Time dependent alkylation study showed that the maximal alkylation was reached within 4 days of incubation (Figure 4.14).

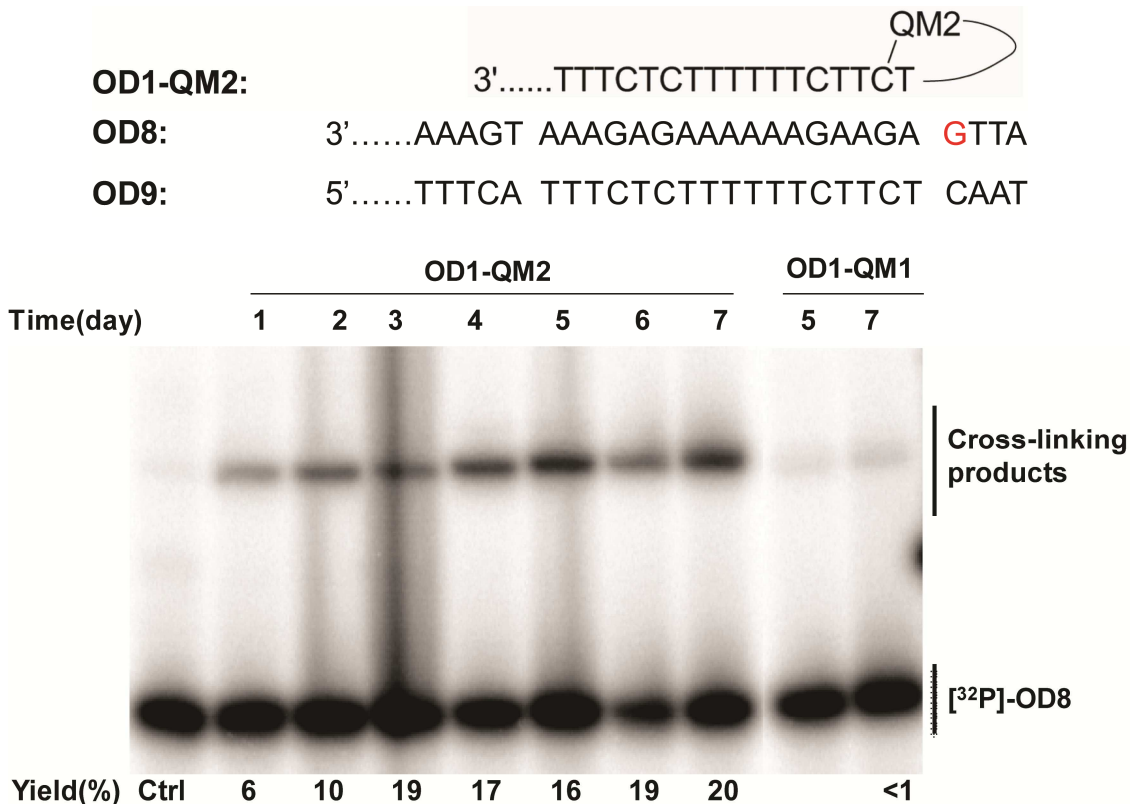


**Figure 4.13** Alkylation of target duplex by OD1-QM2 and OD1-QM1 self-adducts. The self-adducts were prepared from the corresponding conjugates and added to the [<sup>32</sup>P]-OD8/OD9 (0.5 μM) in 100 fold excess (5.0 μM). Samples were incubated under standard condition. Control sample was included that only [<sup>32</sup>P]-OD8/OD9 was present in solution for 7 days.

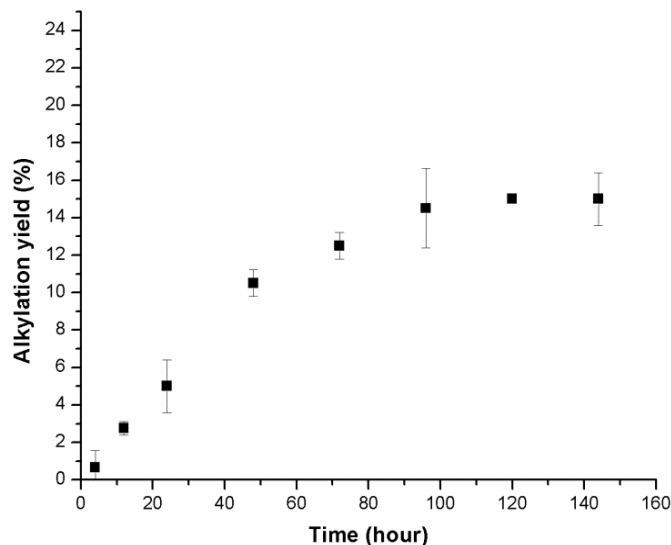


**Figure 4.14** Alkylation over time plot with OD1-QM2 and [<sup>32</sup>P]-OD8/OD9. The data in the plot represent the average value of two experiments and error of the data represents the range of the yield.

#### 4.2.8 Concentration dependent alkylation by OD1-QM2 self-adduct

In order to learn the minimal concentration of OD1-QM2 necessary for alkylation, a concentration dependent experiment was performed. Previous study of alkylation through triplex formation showed that a 200 fold excess of the DNA linked alkylating agent was necessary to support a maximal yield of 30% within 3 days.<sup>79</sup> Thus, a range of the OD1-QM2 self-adduct concentration was incubated with the double strand [<sup>32</sup>P]-OD8/OD9 for 5 days at room temperature. The results (Figure 4.15) indicated that as low as a 10 fold excess of the self-adduct was enough for QM to obtain a maximal yield of target alkylation of 12%. All future experiments contained a 50 fold excess of the OD1-QM2 self-adduct to ensure the optimized condition for alkylation. However, the amount of the alkylation reagents used is still only 25% of the amount reported previously.<sup>79</sup> The reduced amount of alkylating

agent is consistent with the enhanced alkylation property of this electron rich quinone methide.

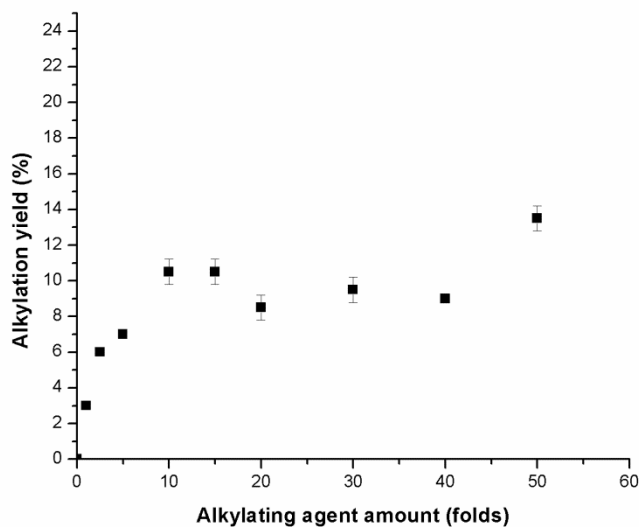
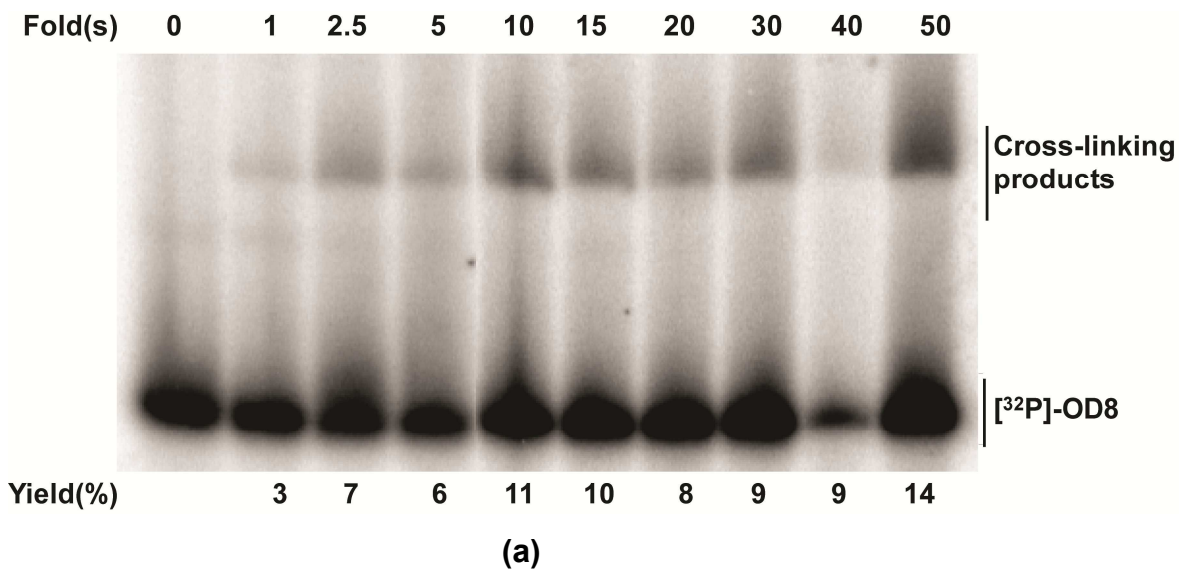


**Figure 4.15** Dosage dependent alkylation results. Samples were prepared following the standard procedure. (a) Different amount of OD1-QM2 was incubated with [<sup>32</sup>P]-OD8/OD9 (0.05 μM) for 5 days and then analyzed by denaturing gel. (b) Alkylation yield over self-adduct plot. Data in the plot with error were averaged value by 2 experimental results. Data without error were from one time experiment. The error represents the range of the data.

#### **4.2.9 Sequence and temperature effect on alkylation of target duplex by OD1-QM2 self-adduct**

The OD1-QM2 self-adduct was incubated with different target dsDNAs to measure the efficiency of alkylation. The experimental results confirmed that the QM preferred to react with an adjacent guanine. The OD1-QM2 self-adduct was incubated with pre-annealed duplex [<sup>32</sup>P]-OD4/OD5, [<sup>32</sup>P]-OD6/OD7, OD6/[<sup>32</sup>P]-OD7, [<sup>32</sup>P]-OD8/OD9 separately (Figure 4.16). Cross-linking products were observed with strand of OD7 and OD8 in which a guanine is next to the QM. When incubating the self-adduct with duplex OD4/OD5, no cross-linking products were evident on the gel for either strand since there was no adjacent guanine in the strand. Alkylation presented by this gel was lower than normal (around 15% after 4 days incubation) because the self-adducts were only incubated with target duplex for 2 days. Therefore, the adjacent guanine next to QM can promote alkylation through triplex formation.

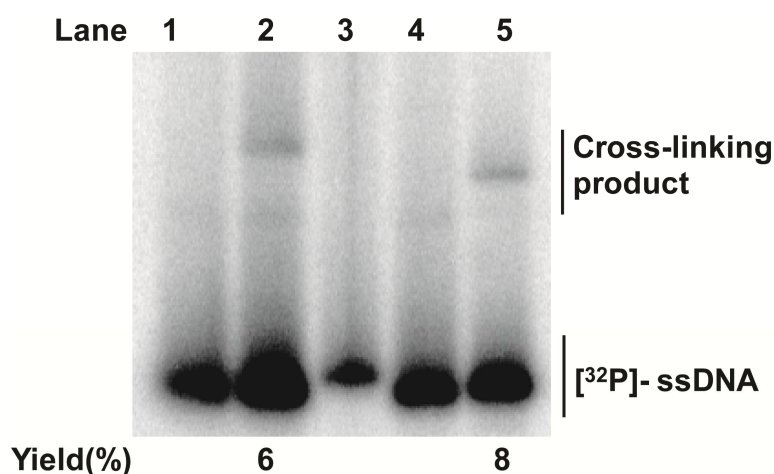
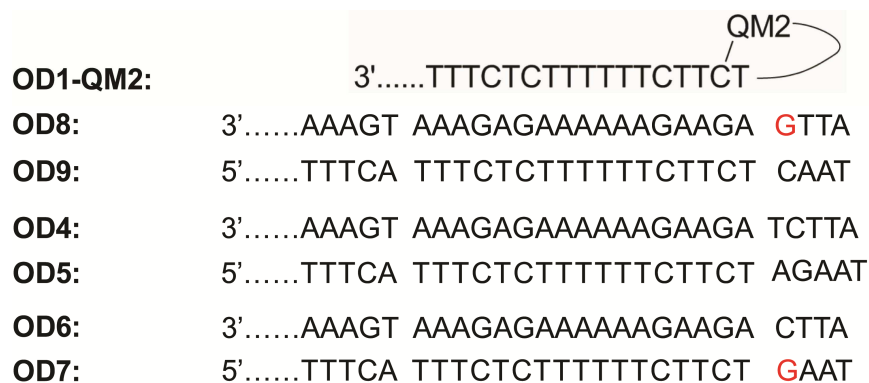


**Figure 4.16** Alkylation of different duplex sequences by OD1-QM2. Samples were incubated under standard condition for 2 days. Lane 1: OD8/O9 control; Lane 2: [<sup>32</sup>P]-OD8/OD9; Lane 3: [<sup>32</sup>P]-OD4/OD5; Lane 4: [<sup>32</sup>P]-OD6/OD7; Lane 5: OD6/[<sup>32</sup>P]-OD7.

The effect of temperature on alkylation of the dsDNA through a triple helix structure was also studied to check the QM2 activity at body temperature. Triple helical structures are usually stabilize with decrease temperature.<sup>81</sup> However, QM reacts more efficiently at room temperature than at lower temperature.<sup>80</sup> The temperature effect on single strand alkylation also confirmed this (Figure 4.17). Alkylation was observed when incubating the OD1-QMP1 conjugate with complementary ssDNA OD2 at room temperature (Lane 1, 3 and 5). However, the same amount of the above DNA samples did not yield evident alkylation when

incubating in the same buffer condition at 4 °C (Lane 2 and 4). This also indicated a slow generation of QM from its precursor at a lower temperature. So the triplex samples were all incubated at room temperature for best results. However, when the electron rich OD1-QMP2 conjugate aqueous solution was examined after stored at -18 °C for 3 months, a peak corresponding to its self-adduct was showed on MALDI spectrum (Figure 4.18). This gradual formation of self-adduct suggested that QMP2 could be activated to generate QM even without addition of fluoride due to the highly reactivity.

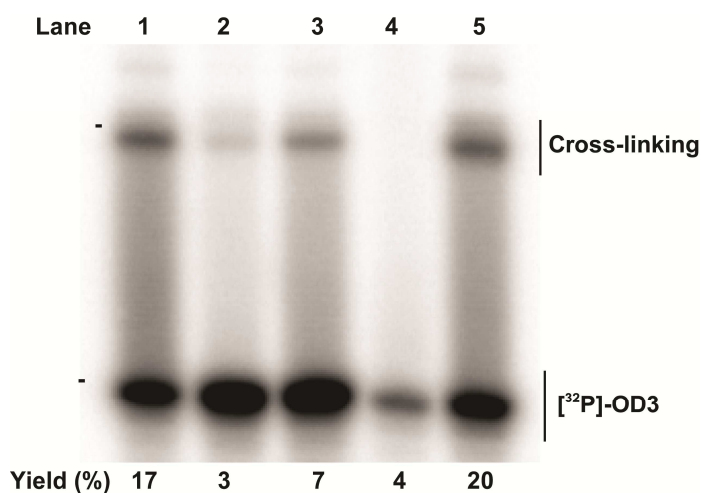


**Figure 4.17** Alkylation of OD2 by OD1-QMP1 at different temperature. OD1-QMP1 (6.6  $\mu$ M) was added to [ $^{32}$ P]-OD2 (6  $\mu$ M) in MES (20 mM). KF (100 mM) was applied to initiate the reaction. Samples were incubated for 4 days under: Lane 1: pH 6; rt; Lane 2: pH 6; 4 °C; Lane 3: pH 7; 4 °C; Lane 4: pH 7; rt with NaCl (150 mM) and MgCl<sub>2</sub> (10 mM); Lane 5: pH 7, rt.



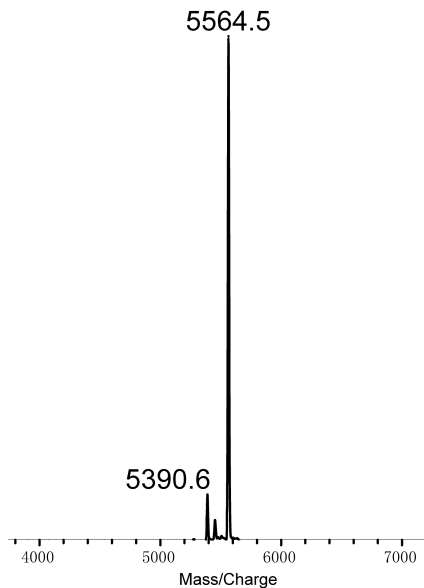


**Figure 4.18** MALDI data of OD1-QMP2 conjugated after stored at -18 °C in water for 3 months. The major peak was the conjugate (calculated: 5564.5; observed: 5564.5); but the self-adduct also appeared (calculated: 5392.7; observed: 5390.6)

Inspired by this reactivity, we proposed that an increase of temperature could enhance the ability of QM2 to alkylate its target. Both the OD1-QMP2 conjugate and the OD1-QM2 self-adduct were incubated with OD8/OD9 in 4 °C, 21 °C (room temperature) and 37 °C. The samples were incubated for up to 4 days and then loaded on the denaturing gel without any further treatment. According to the gel results (Figure 4.19), the alkylation using the OD1-QM2 self-adduct provided the best yield when samples were incubated under 37 °C (Lane 3). No alkylation was apparent for the sample incubated at 4 °C (Lane 4) which was likely to indicate a very slow reaction. For the samples using the OD1-QMP2 conjugate, alkylation was observed even without adding KF. The highest yield was also achieved with samples incubated under 37 °C. Alkylation yield of 26% was achieved after 4 days incubation of the OD1-QMP2 conjugates with target duplex. This is so far the best yield ever

observed for QM alkylation through triplex system. Since no fluoride was necessary to trigger the alkylation reaction of the QMP, the DNA-QMP conjugate might be directly applied in a biological system. Further studies to check the reproducibility of the temperature effect are necessary.

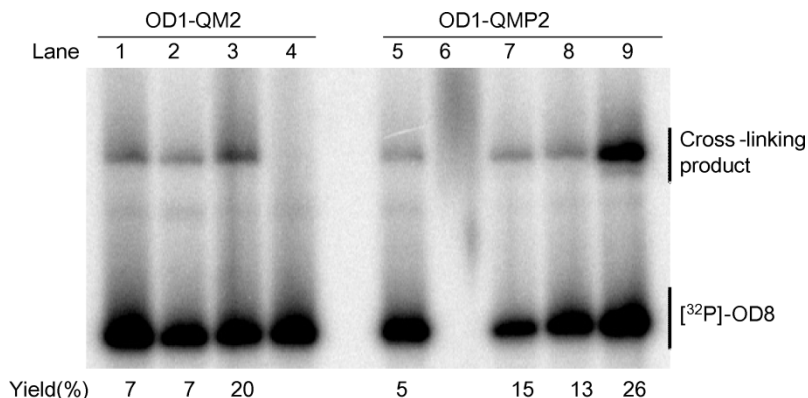


**Figure 4.19** Temperature effect on duplex alkylation. OD1-QM2 (50 equiv.) was incubated with [<sup>32</sup>P]-OD8/OD9 (Lane 1-4) in MES buffer (20 mM, pH 5) with NaCl (150 mM) and MgCl<sub>2</sub> (2.5 mM). OD1-QMP2 (50 equiv.) was incubated with [<sup>32</sup>P]-OD8/OD9 (Lane 5~9) with the same buffer with or without KF (100 mM). Lane 1: (-)KF, rt., 3 days; Lane 2: (-)KF, 4 °C, 1 day, then rt. 2 days; Lane 3: (-)KF, 37 °C, 3 days; Lane 4: (-)KF, 4 °C, 2 days; Lane 5: (-)KF, rt., 3 days; Lane 6: (+)KF, rt., 3 days; Lane 7: (-)KF, rt., 4 °C 1 day, then rt. 2 days; Lane 8: (-)KF, 37 °C 2 days; Lane 9: (-)KF, 37 °C 4 days. Samples were analyzed by the denaturing gel without any further treatment.

### 4.3 Conclusion

Both QMP1 and QMP2 were conjugated to a TFO strand and successfully delivered to the selected duplex DNA through triplex formation. All samples were incubated in acidic buffer at room temperature. In order to display a distinct alkylation products band on the denaturing gel, samples had to be desalted to remove Mg<sup>2+</sup> and F<sup>-</sup> in the solution, which interrupted the DNA migration on the gel. The formation of alkylation products using the DNA-QMP1 conjugate was observed when targets contained an adjacent guanine. The adjacent guanine on the polypurine strand

of the duplex, which binds to the TFO, provided the best yield. The maximal yield was 21% achieved after a 5-day incubation. The alkylation yield could also be increased by enhancing the third strand binding with a modified TFO1 containing methyl cytosines to replace regular cytosine in the sequence. The maximal yield was increased to 27% after 7 days incubation.

Although duplex alkylation was observed with the DNA-QMP1 conjugate, its self-adduct showed almost no alkylation with the target dsDNA. A modified TFO sequence with an unpaired adenine to form a reversible adduct with QM failed to improve alkylation yield. Target sequences were also modified to provide with adjacent guanine without hydrogen bonding for a lower the energy barrier of the alkylation reaction. The alkylation yield was not improved with this modification either.

An electron rich QMP2 was coupled to the TFO and its self-adduct was generated for alkylation. The OD1-QM2 self-adduct successfully alkylated the target duplex in a relative high yield (20%) and the maximal yield was achieved in 3 days. Concentration dependent study showed that as low as a 10 fold excess of alkylating agent was necessary to achieve the maximal alkylation yield. This amount of alkylation agents used was  $\frac{1}{4}$  of what was reported previously in triplex alkylation.<sup>79</sup> Preliminary study on the temperature effect suggested that electron rich QMP2 could be activated at 37 °C without fluoride. This enhanced alkylation efficiency provided by the electron rich QM2 self-adduct will allow for its future application in living cell for mutagenesis study.

#### ***4.4 Materials and Methods***

**Materials:** All single stranded DNA were purchased from IDT (Coralville, IA).

Aqueous solutions were prepared with distilled, deionized water with a resistivity of 18.0 M $\Omega$ . T4 polynucleotide kinase (PNK) was obtained from New England Biolabs (Ipswich, MA). [ $\gamma$ -<sup>32</sup>P]-ATP was purchased from Perkin-Elmer (Waltham, MA). Micro bio-spin columns with bio-gel P-6 was purchased from Bio-Rad (Hercules, CA). Single strand DNA with an abasic site was obtained from Yang Liu of the Rokita group.

**Preparation of double strand DNA:** Duplex DNA was prepared by annealing two complementary single strands. The indicated strand (100 nM) was radioabled at its 5' terminus using standard protocols. Both radiolabeled strand and its complementary strand (200 nM) were mixed in 40 mM 4-morpholineethanesulfonate (MES, pH 5) with 5 mM MgCl<sub>2</sub>, 300 mM NaCl or the specified salt concentration. The mixture was heated to 90 °C for 3 minutes and allowed to cool to room temperature over more than 3 hours. The solution was stored in the -20 °C freezer for future use.

**Alkylation of target duplex by TFO-QMP conjugate/TFO-QM self-adduct:** The TFO linked alkylation agent was added to the duplex solution. For samples using the TFO-QMP conjugate, the reaction was initiated by addition of aqueous KF (100 mM). Final concentrations were 0.5  $\mu$ M duplex DNA, 2.5  $\mu$ M alkylation agent (DNA-QMP conjugate or self-adduct), 2.5 mM MgCl<sub>2</sub>, 150 mM NaCl, 20 mM MES (pH 5). Duplex was radiolabeled at the specified strand. Alkylation agent concentration varied as specified. Samples were then incubated under room temperature for

indicated period of time. Electrophoresis loading solution (0.05% xylene cyanol and 0.05% bromphenol blue in formamide) was added in equal volume which also quenched the reaction when the incubation time was finished. Products were analyzed by denaturing gel electrophoresis (20% acrylamide/7 M urea) with standard TBE buffer (Tris-Borate-EDTA) and quantified by phosphoimagery using imagequant software. Alkylation yields were calculated based on the radioactivity of the product and overall radioactivity of the sample. Samples requiring desalting used the Micro bio-spin columns with bio-gel P-6 following the factory provided procedure.

## Chapter 5: Conclusion

As a small molecule alkylating agent, quinone methide attracted our attention not only because of it could alkylate bases in the DNA to form alkylation products, but also because of its ability to form reversible covalent bonds with the strong nucleophiles of the bases. As a result, the QM can be regenerated from reversible adducts spontaneously for alkylation without the need of any triggering chemicals or energy source. In the target promoted alkylation process, QM was delivered to the target DNA sequence by a DNA-QM self-adduct and alkylation products were formed.<sup>31</sup> However, the reaction was slow. Seven days were necessary for the DNA-QM self-adduct to reach a maximal alkylation yield of 20% when alkylating a complementary single strand DNA. This was too slow for application in a biological system since DNA repair processes may fix the alkylation before it could affect the DNA activity. Therefore, it was necessary to accelerate the reaction by creating a more reactive quinone methide. This dissertation presents the program of designing and synthesizing an electron rich quinone methide precursor and measuring how fast the reaction is accelerated by this increased electron density. Investigation of the optimized condition for duplex alkylation by DNA-QMP and DNA-QM through triplex structure formation is also discussed.

Substitution effects of an QM described by others indicated that the presence of an electron rich donating group in the quinone methide precursor would facilitate the generation of QM from QMP and its regeneration from the adducts.<sup>35</sup> Attempts of synthesizing a QMP2 were made to produce silyl protected quinone methide precursor with increased electron density. Although QMP2 has a similar structure to QMP1,

previous synthesis scheme of QMP1 was not applicable to this new precursor because of the modification. The reactions used to construct QMP1 including formation of benzylic hydroxyl group and generation of benzylic acetate group from protected hydroxyl group were not working on similar substrates with an electron donating group present. Therefore, synthesis of the QMP2 was finally achieved through a novel six-step procedure. An aldehyde starting material was used to avoid constructing the benzylic hydroxyl group under basic condition with heat, which is notorious for its low yield (<20%) and difficult separation due to multiple products formation.<sup>45</sup> In comparison, the reduction reaction yielded single product with high yield (>80%) and the aldehyde group did not need to be protected during synthesis since it was not evolved in reactions of other steps. The overall yield for previous 4-step synthesis plan (Figure 2.2) is around 3.5% while the overall yield for QMP2 (Figure 2.7) is around 4.2% after 6 steps. The new synthesis route is more efficient and the synthetic study of the electron rich QMP2 provides important experiences and references for future synthesis design.

The electron rich QMP2 generates QM much faster to form its self-adduct than the conventional QMP1 as we predicted. Target alkylation of single strand DNA is also accelerated. Alkylation using QMP2 required less than half amount of time (3 days) for maximal yield compared to 7 days required for QMP1. This improvement on alkylation speed of DNA linked QM should make the alkylation process more effective for future *in vivo* study.

Alkylation of a duplex DNA using DNA-QMP conjugates and DNA-QM self-adducts through triplex formation was also studied. Alkylation products were

observed using DNA-QMP1 conjugates incubating with target duplex. Adjacent guanine in the target sequence is very important for alkylation which is consistent with previous results.<sup>82</sup> However, the DNA-QM1 self-adduct showed limited ability in duplex alkylation due to its slow kinetics of QM regeneration from its self-adduct. Thus, DNA-QM2 self-adduct was tested for alkylation. Alkylation products were observed and maximal yield was reached within 4 days. The best yield around 20% was achieved by incubation of the self-adduct with target duplex containing an adjacent guanine. This is the first time that alkylation of a dsDNA is observed with a DNA-QM self-adduct. Compared to target alkylation with a single strand DNA, the third strand binding is weaker than dsDNA but the alkylation provides a similar yield in a shorter time using the electron rich QMP2. The alkylation yield could be further improved with increased temperature (at 37 °C) and the DNA-QMP2 conjugate showed ability to alkylate the duplex at 37 °C without KF. These results demonstrate the advantages of using QMP2 to alkylate duplex DNA and prepare the DNA-QM2 self-adduct for future applications in cells.

Above all, the electron rich QMP2 solved a major issue of DNA alkylation by DNA-QM self-adducts. It speeded up the single strand alkylation process. It also increased the alkylation yield of target dsDNA. These improvements made the self-adduct species ready for in cell application. Compared to psoralen, another commonly used DNA cross-linking agent, the DNA-QM has several advantages. No chemical or light is necessary to initiate the alkylation since QM can be released from the self-adduct spontaneously. In contrast, UV-radiation is required for psoralen reaction which might cause some side-effects from other light initiated reactions in the cell.



Psoralen required AT base pair for cross-linking and this may limit the target sequence selection. The adjacent guanine required for optimized alkylation of QM is convenient to construct in the polypurine binding strand. However, psorlen provides the maximal yield in shorter time (around 15 min) than QM which is also the reason why it was widely used in the cell.<sup>83</sup> For the future direction of this research work, TFO linked electron rich quinone methide self-adducts could be applied to the *Hprt* gene and its alkylation can be analyzed by the gene targeting assay developed by Seidman's group which is used to measure the mutation caused by alkylation.<sup>44</sup>

Detailed study is necessary for temperature effect on duplex alkylation using DNA-QMP2 conjugates. If the conjugate was confirmed to be reactive at body temperature without the use of KF, it could be applied directly to the cells. This provides an alternative method for QMP activation. The use of the DNA-QMP2 conjugate can further increase the alkylation yield from the use of self-adduct since all the QM generated from precursor could have the chance to alkylate the target DNA. In contrast, only the reversible adducts of the DNA-QM self-adducts would regenerate the QM to alkylate the target sequence. Successful activation of QMP at body temperature could also lead to a new direction for study of the quinone methide precursor.

# Appendix

## Chapter 2

NMR spectra of the compounds in QMP2 synthesis (Figure 2.7)

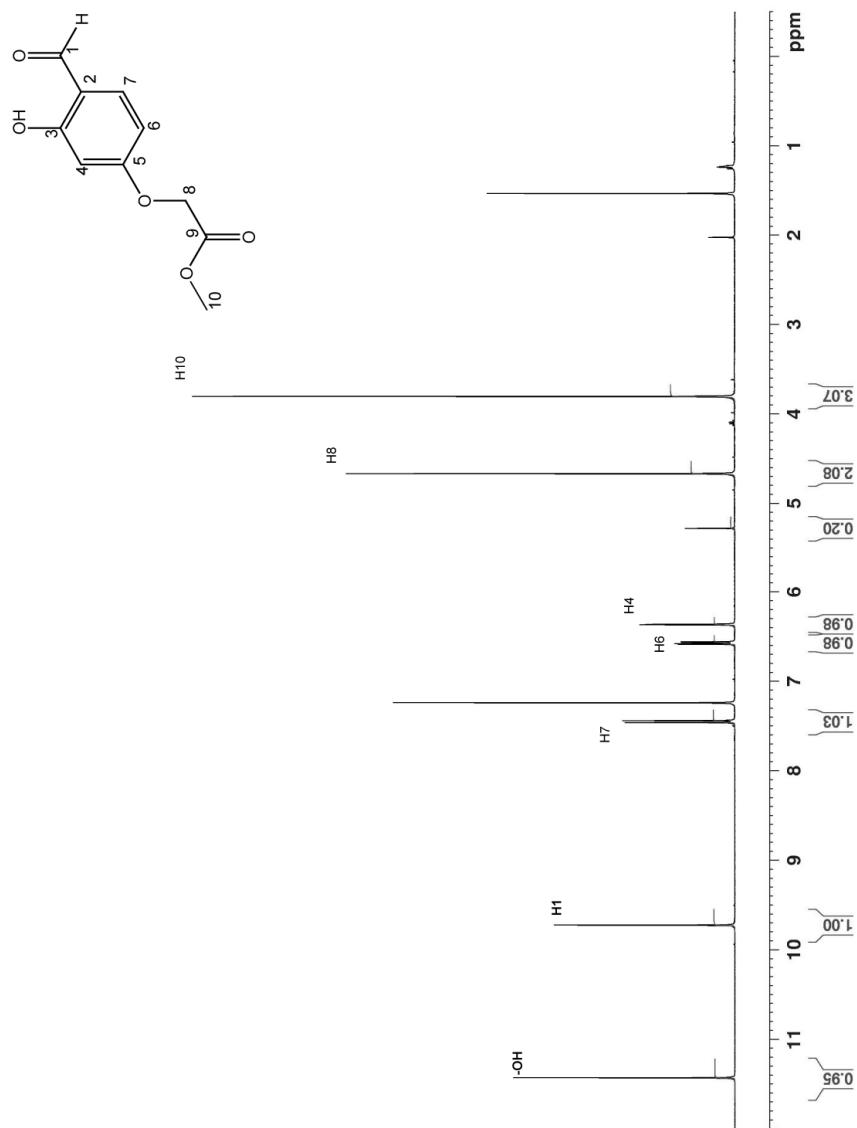


**Figure 1** <sup>1</sup>H NMR of compound 12 in CDCl<sub>3</sub> at 400 MHz.

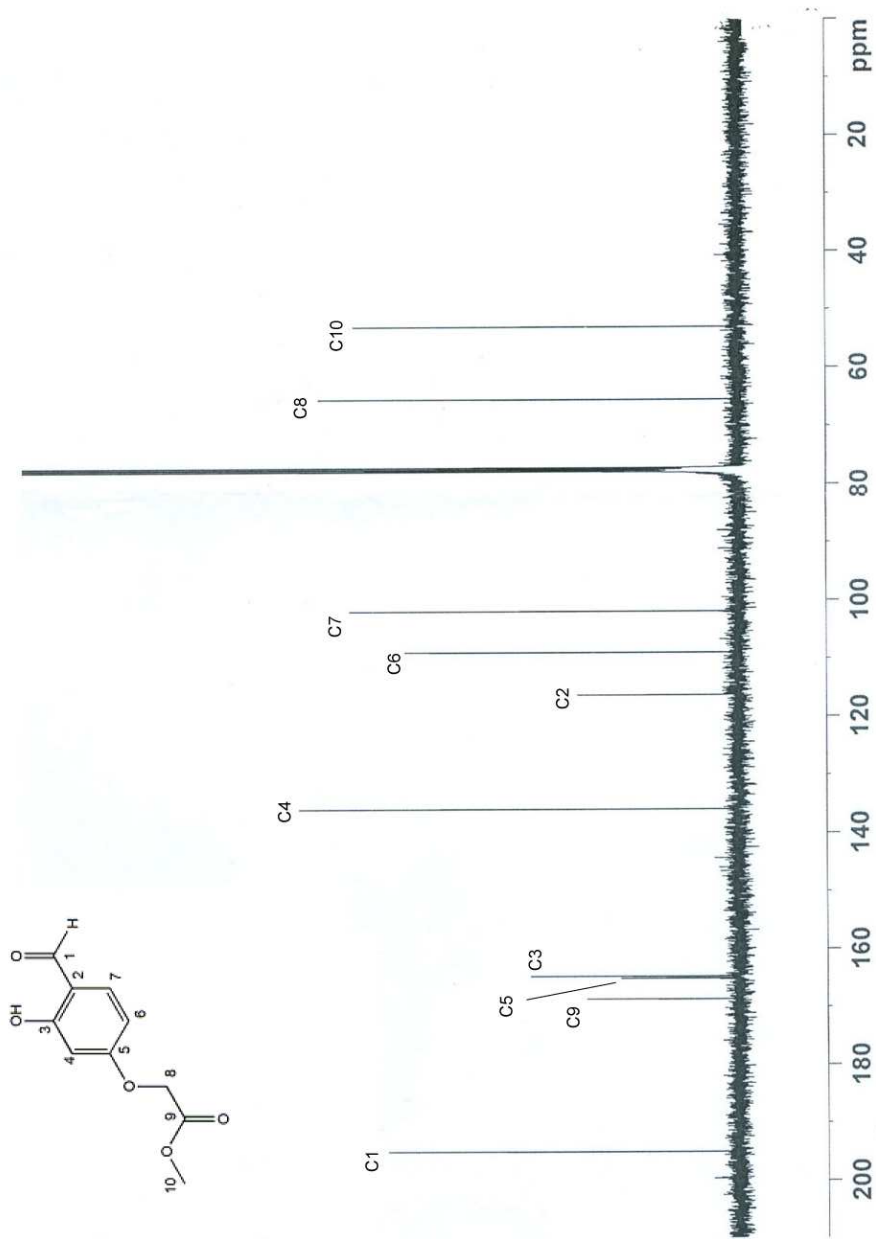


**Figure 2**  $^{13}\text{C}$  NMR of compound 12 in  $\text{CDCl}_3$  at 400 MHz.

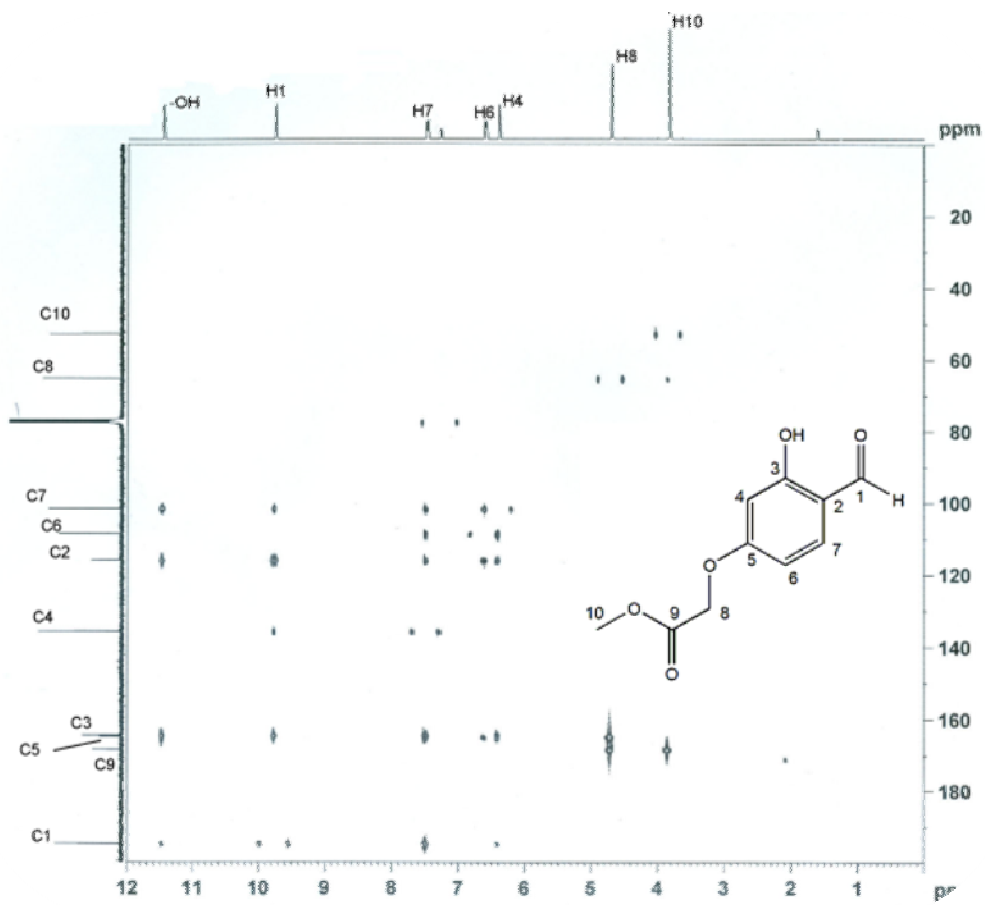
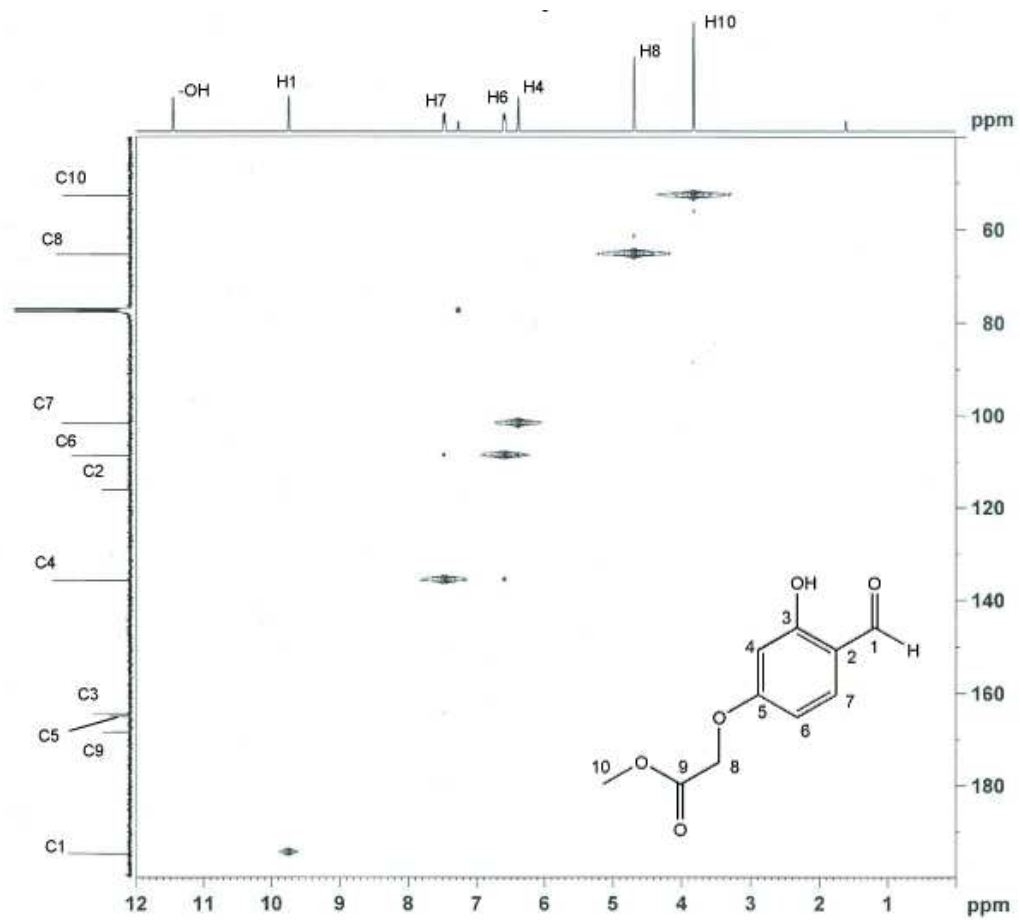
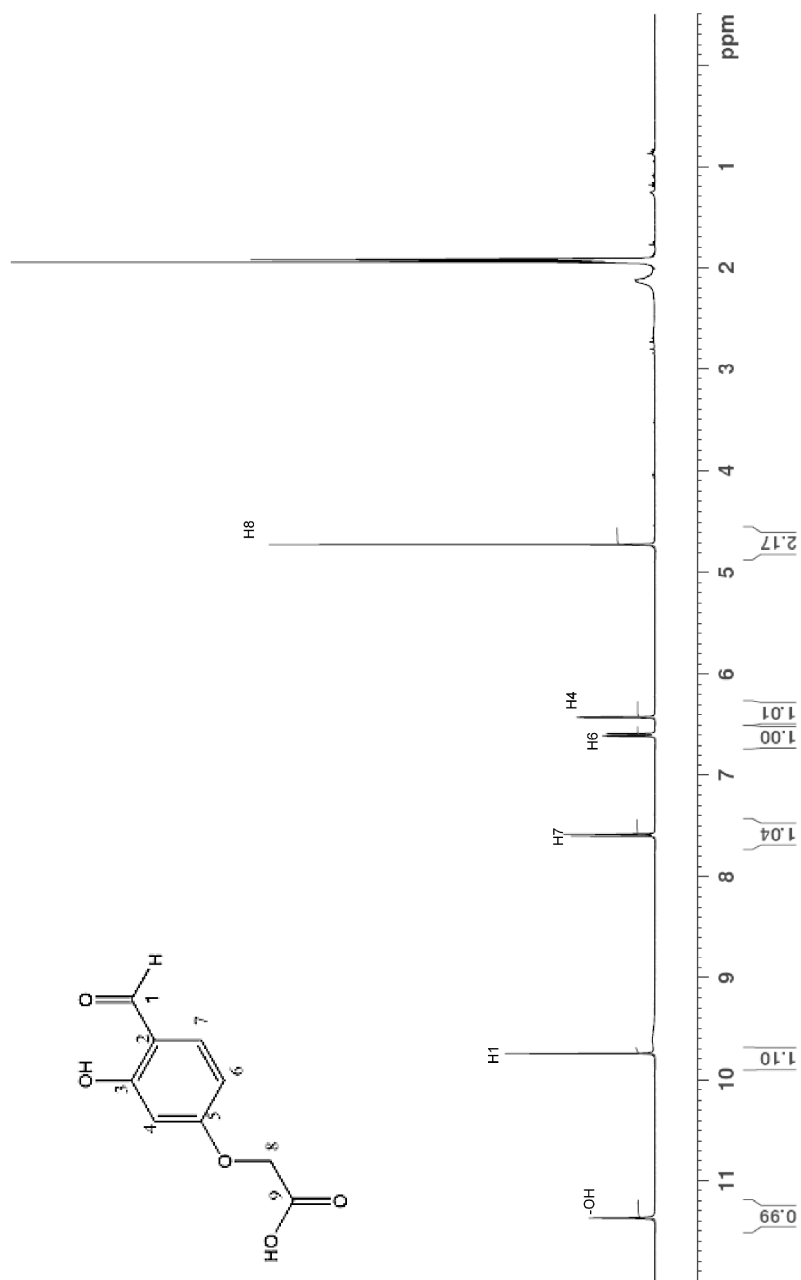


Figure 3  $^1\text{H}$ - $^{13}\text{C}$  HMBC of compound 12 in  $\text{CDCl}_3$  at 400 MHz.



**Figure 4**  $^1\text{H}$ - $^{13}\text{C}$  HSQC of compound **12** in  $\text{CDCl}_3$  at 400 MHz.



**Figure 5**  $^1\text{H}$  NMR of compound **18** in  $\text{CD}_3\text{CN}$  at 400 MHz.

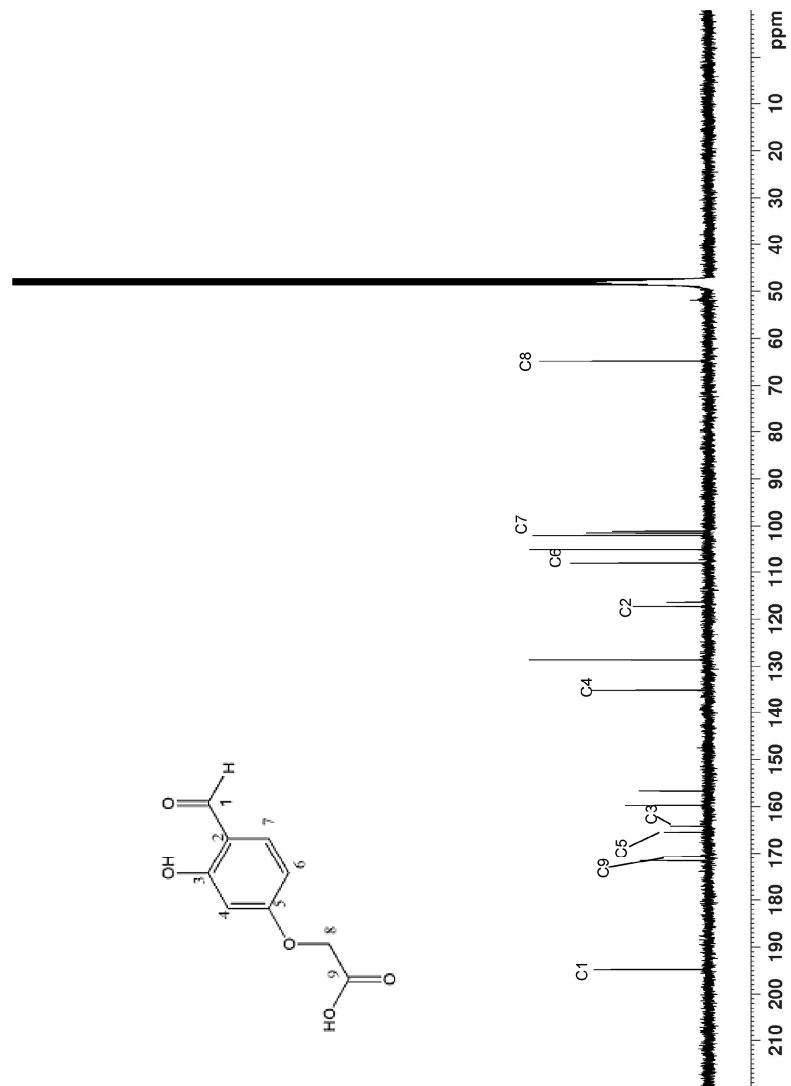


**Figure 6**  $^{13}\text{C}$  NMR of compound **18** in  $\text{CD}_3\text{CN}$  at 500 MHz.

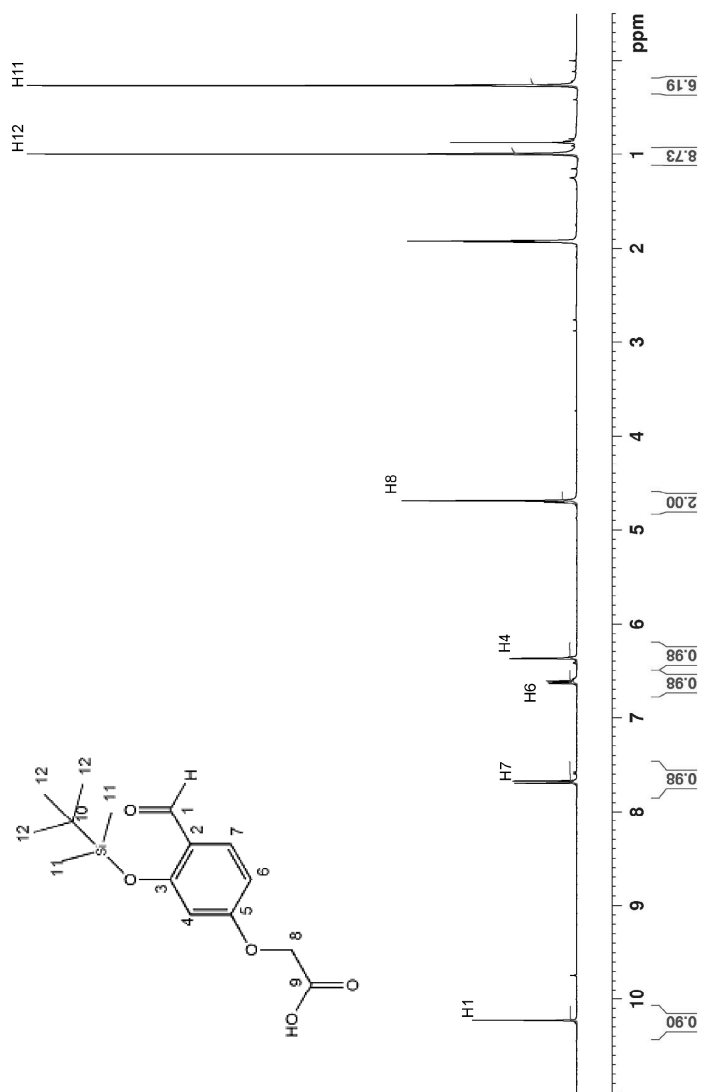


**Figure 7** <sup>1</sup>H NMR of compound **19** in CD<sub>3</sub>CN at 400 MHz



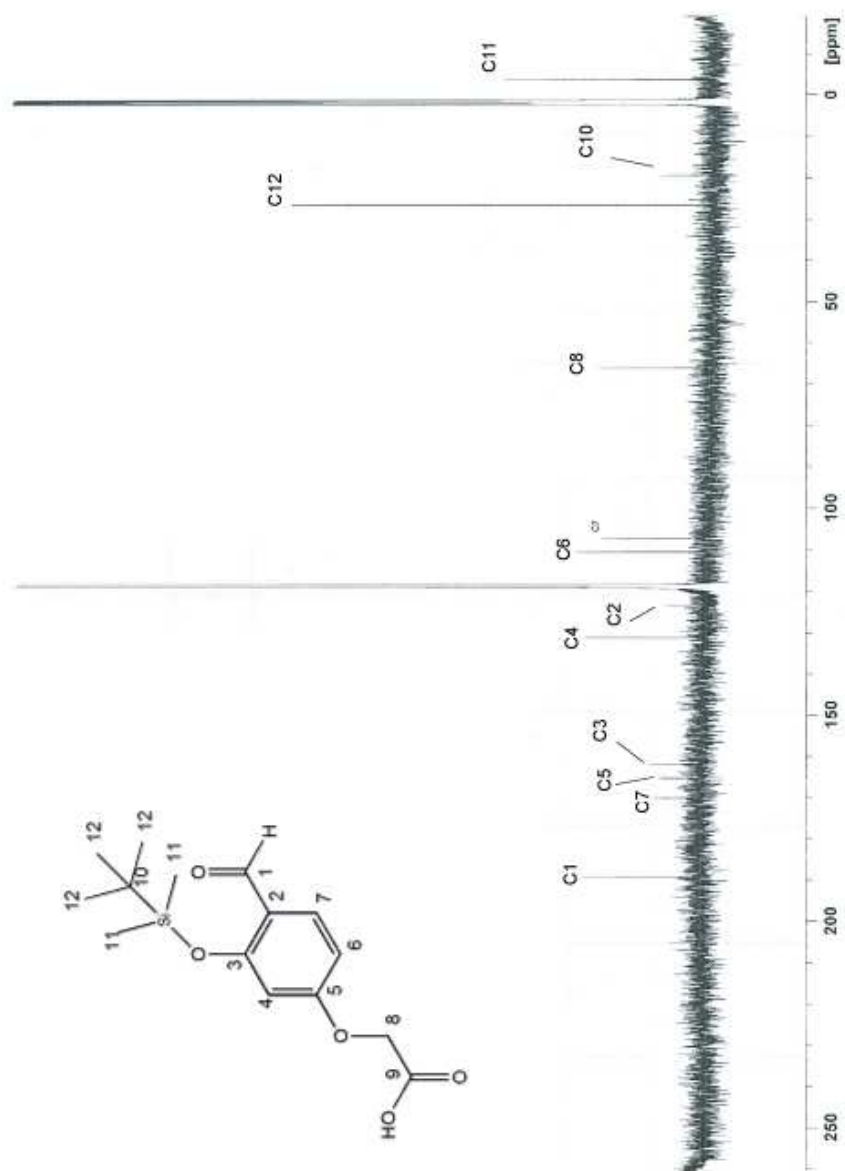


**Figure 8**  $^{13}\text{C}$  NMR of compound **19** in  $\text{CD}_3\text{CN}$  at 500 MHz.

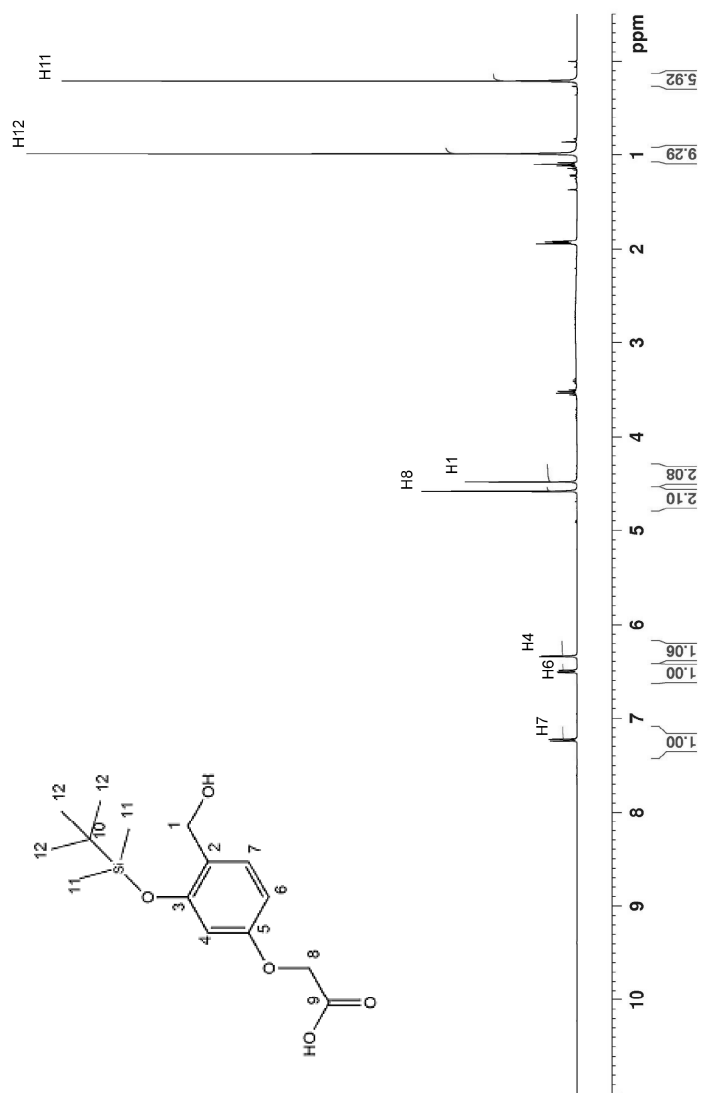


**Figure 9** <sup>1</sup>H NMR of compound **20** in CD<sub>3</sub>CN at 400 MHz.

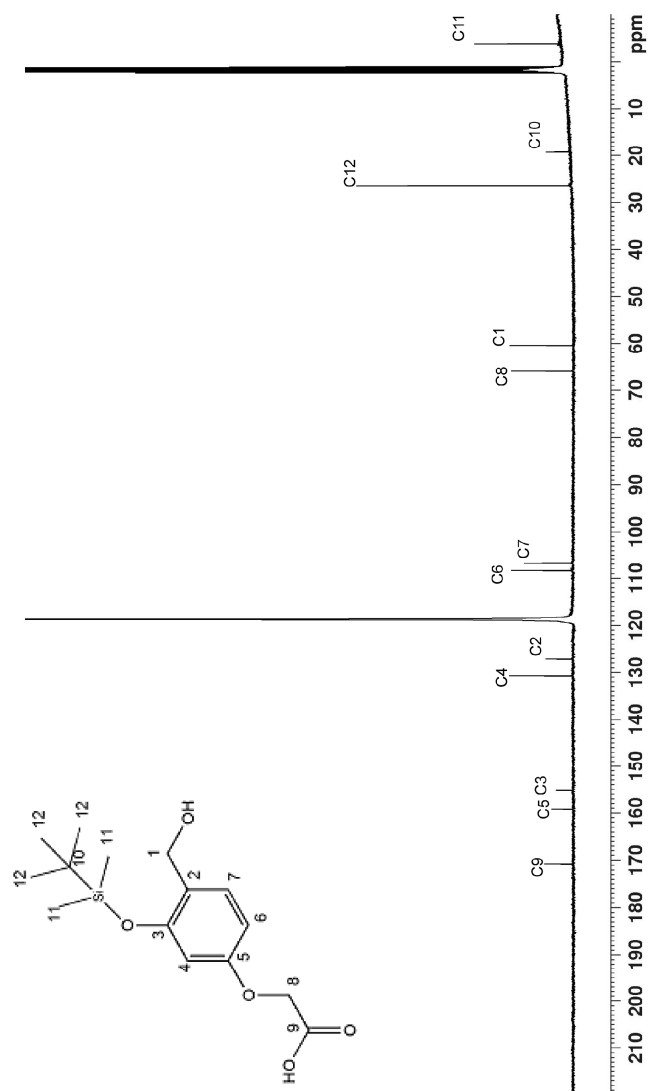


**Figure 10**  $^{13}\text{C}$  NMR of compound **20** in  $\text{CD}_3\text{CN}$  at 400 MHz.

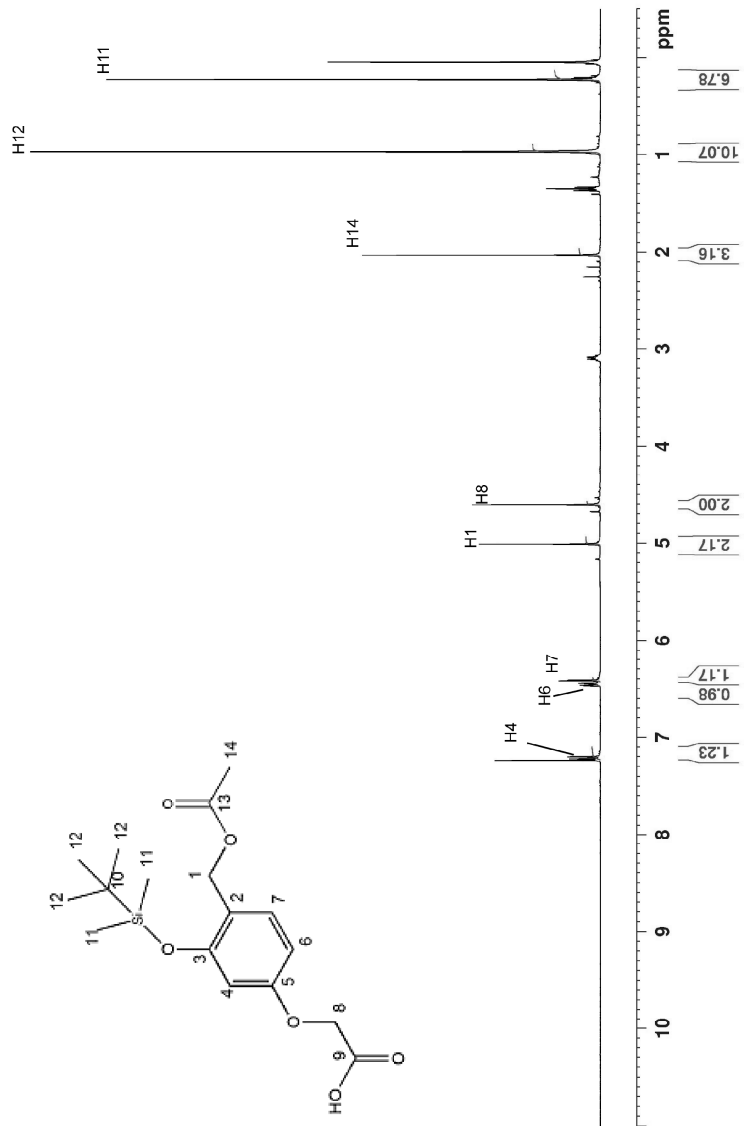


**Figure 11** <sup>1</sup>H NMR of compound 17 in CDCl<sub>3</sub> at 400 MHz.

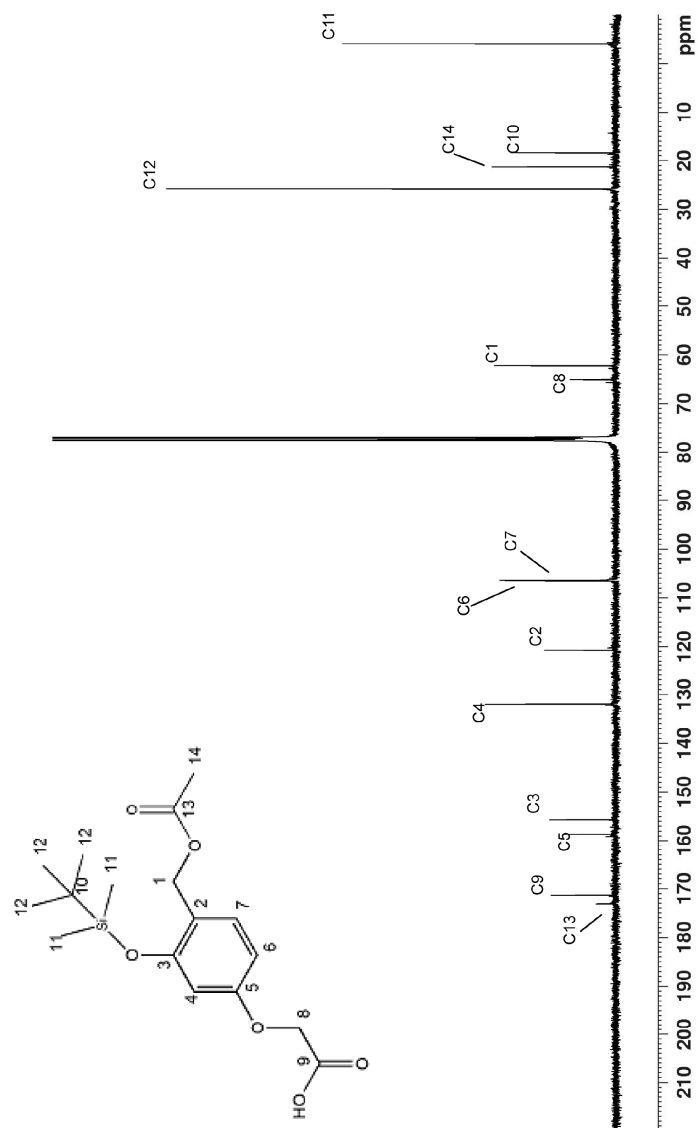


**Figure 12**  $^{13}\text{C}$  NMR of compound 17 in  $\text{CDCl}_3$  at 400 MHz.

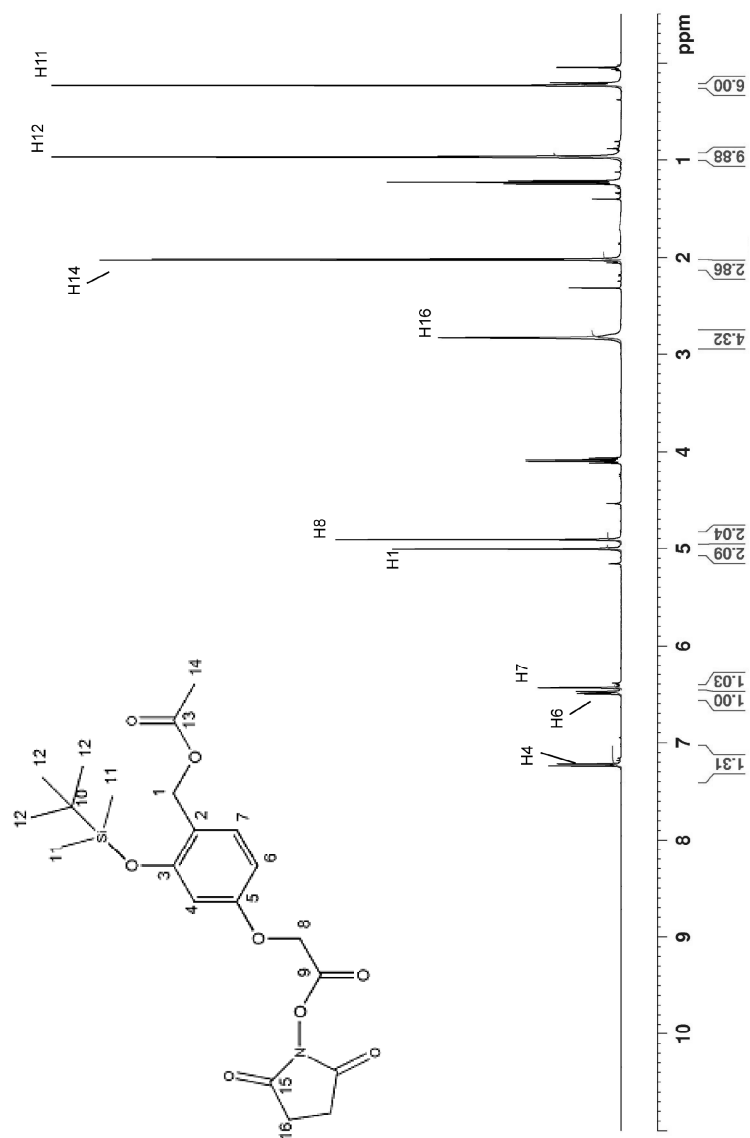
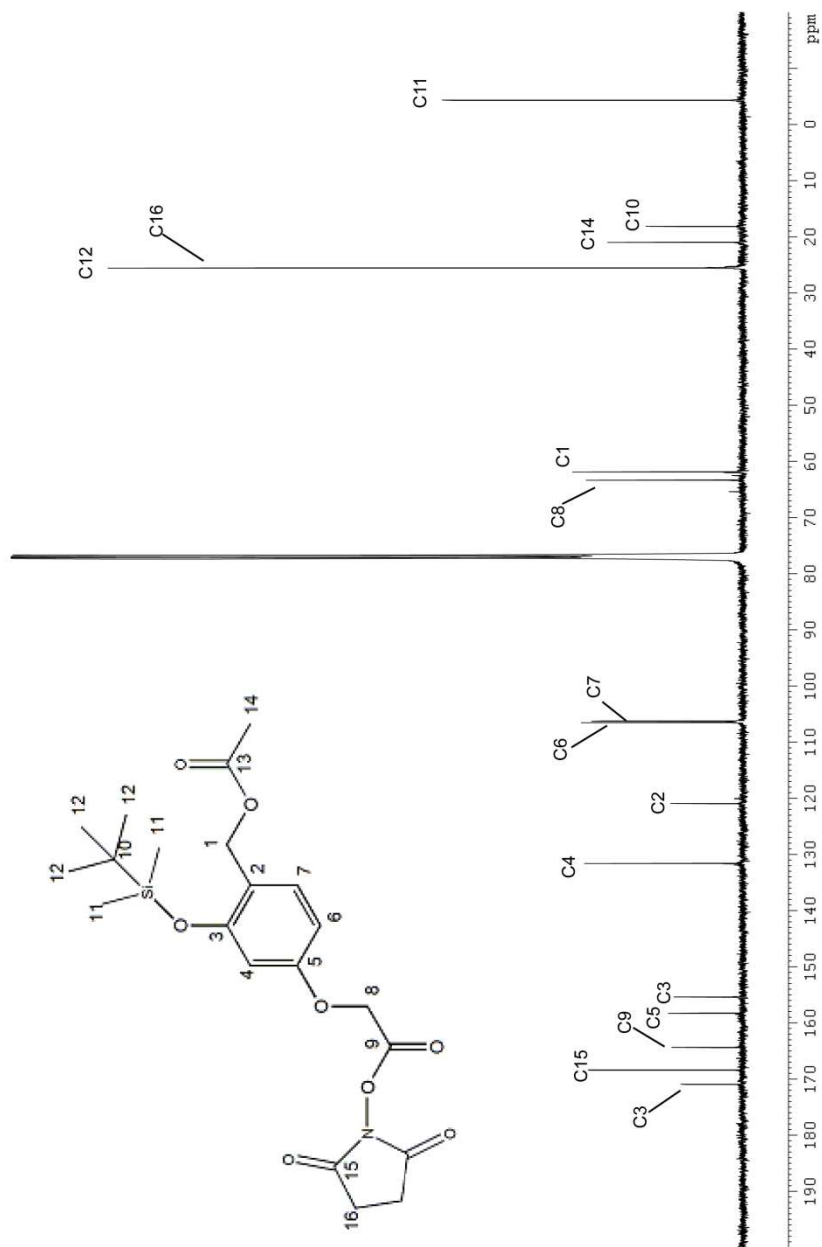
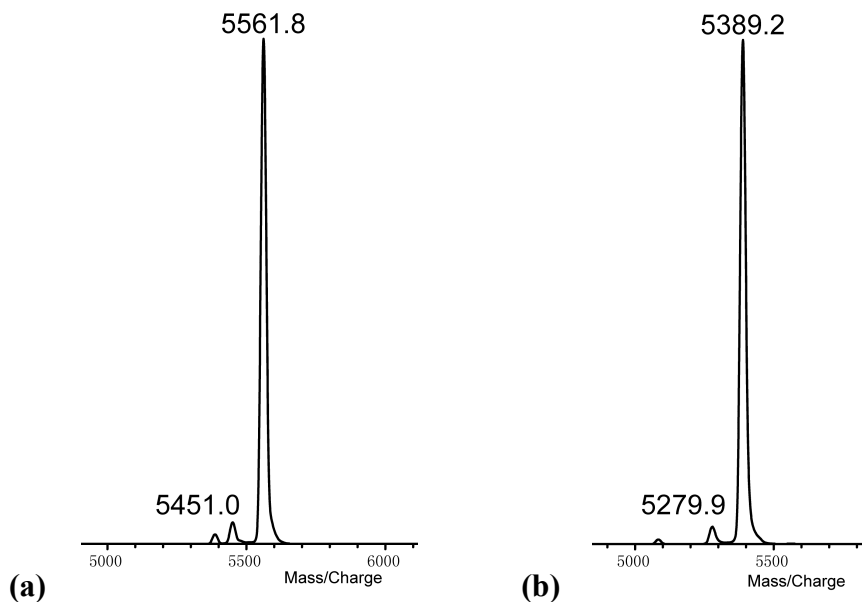


Figure 13 <sup>1</sup>H NMR of QMP2 in CDCl<sub>3</sub> at 400 MHz.



**Figure 14**  $^{13}\text{C}$  NMR of **QMP2** in  $\text{CD}_3\text{CN}$  at 500 MHz.

### Chapter 3



**Figure 15** MALDI of (a) OD1-QMP1 conjugate: calculated mass was 5562.5, found by MALDI was 5561.8; (b) OD1-QM1 self-adduct: calculated mass was 5388.7, found by MALDI was 5389.2.

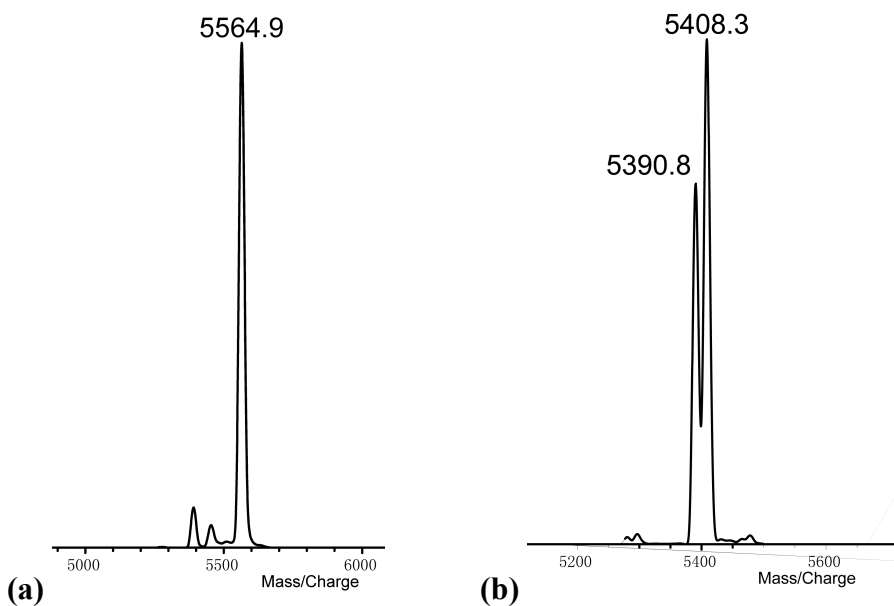


**Figure 16** MALDI of (a) OD1-QMP2 conjugate: calculated mass was 5564.5, found by MALDI was 5564.9; (b) OD1-QM2 self-adduct: calculated mass was 5392.7, found by MALDI was 5390.8. The mass peak 5408.3 corresponds to OD1-QM2 water adduct (calculated: 5409.7).



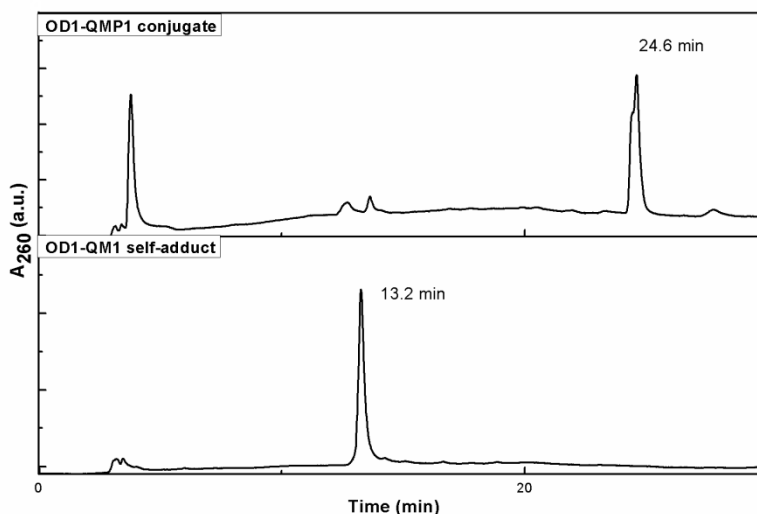


**Figure 17** HPLC separation of OD1-QMP1 conjugate (24.6 min peak) and OD1-QM1 self-adduct (13.2 min peak). Samples were eluted with a linear gradient of 10-55% acetonitrile in aqueous triethylammonium acetate (50 mM, pH 5.0) at 1 ml/min in 30 min. Retention time of the conjugate and self-adduct are consistent with literature value.<sup>31</sup>

#### Chapter 4

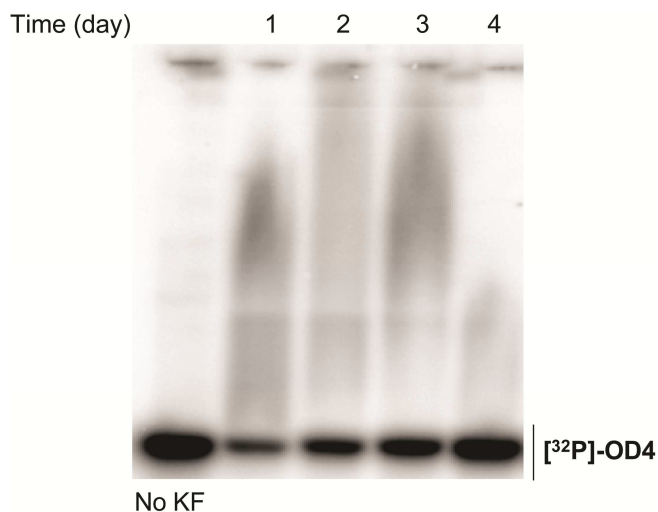


**Figure 18** Alkylation of target duplex OD4/OD5 by OD1-QMP1. [<sup>32</sup>P]-OD4/OD5 (0.1 μM) was pre-annealed in MES buffer. OD1-QMP1 (10.0 μM) was added to the duplex (0.05 μM) and KF (100 mM) was used to activate the QM. The sample was incubated in MES buffer (20 mM, pH 5) with NaCl (150 mM) and MgCl<sub>2</sub> (10 mM) under ambient conditions for 0~4 days. EDTA was added to the samples before analysis by 20% polyacrylamide denaturing gel. Ctrl: single strand [<sup>32</sup>P]-OD4 in the incubation buffer for 4 days. No distinct alkylation band was observed.

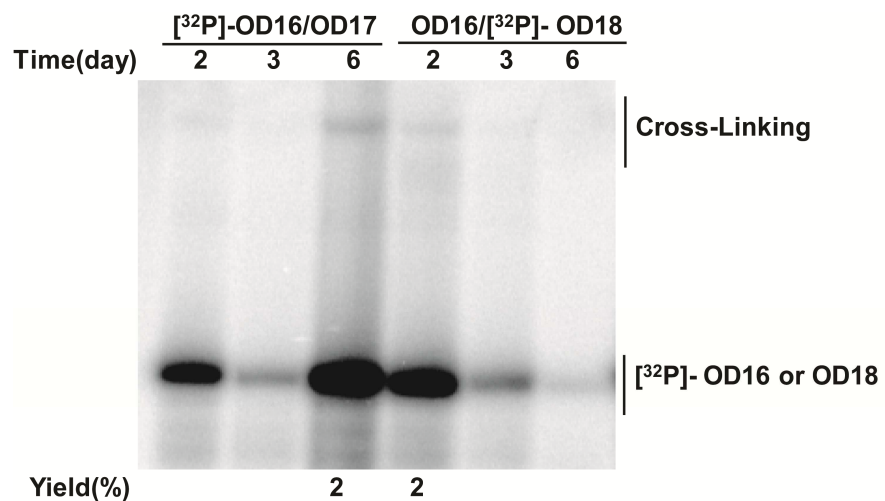


**Figure 19** Alkylation of duplex with an unpaired adjacent guanine by OD1-QM1 self-adduct. Purified OD1-QM1 (10.0  $\mu\text{M}$ ) was incubated with  $[^{32}\text{P}]\text{-OD16/OD17}$  (0.05  $\mu\text{M}$ ) and  $\text{OD16}/[^{32}\text{P}]\text{-OD18}$  (0.05  $\mu\text{M}$ ) separately. Samples were incubated under standard conditions for 2, 3 and 6 days. Samples were analyzed by denaturing gel without any further treatment. Alkylation yield of 2% was observed for this target sequence.

## References

- (1) Franklin, R. E.; Gosling, R. G., Molecular Configuration in Sodium Thymonucleate, *Nature* **1953**, *171*, 740-741.
- (2) Voet, D. V. J. G. *Biochemistry* New York, 1990.
- (3) Berg, J. M., Tymoczko, J. L. , Stryer L. *Biochemistry*; 5 ed.; W H Freeman: New York, 2002.
- (4) Cech, T. R., Self-Splicing of Group I Introns, *Annu. Rev. Biochem* **1990**, *59*, 543.
- (5) Rajski, S. R.; Williams, R. M., DNA Cross-Linking Agents as Antitumor Drugs, *Chem. Rev. (Washington, DC, U. S.)* **1998**, *98*, 2723-2795.
- (6) Hopkins, P. B.; Millard, J. T.; Woo, J.; Weidner, M. F.; Kirchner, J. J.; Sigurdsson, S. T.; Raucher, S., Sequence Preferences of DNA Interstrand Cross-Linking Agents - Importance of Minimal DNA Structural Reorganization in the Cross-Linking Reactions of Mechlorethamine, Cisplatin, and Mitomycin-C, *Tetrahedron* **1991**, *47*, 2475-2489.
- (7) Gniazdowski, M. C., C., The Effects of DNA Covalent Adducts on in Vitro Transcription,, *Chem. Rev.* **1996**, *96*, 619.
- (8) Caffieri, S.; Lucchini, V.; Rodighiero, P.; Miolo, G.; Dallacqua, F., 3,4-Photocycloadducts and 4',5'-Photocycloadducts between 4'-Methylangelicin and Thymine from DNA, *Photochem. Photobiol.* **1988**, *48*, 573-577.
- (9) Dedon, P. C.; Plataras, J. P.; Rouzer, C. A.; Marnett, L. J., Indirect Mutagenesis by Oxidative DNA Damage: Formation of the Pyrimidopurinone

- Adduct of Deoxyguanosine by Base Propenal, *Proc. Natl. Acad. Sci. U. S. A.* **1998**, *95*, 11113-11116.
- (10) Kim, H. Y. H.; Voehler, M.; Harris, T. M.; Stone, M. P., Detection of an Interchain Carbinolamine Cross-Link Formed in a CpG Sequence by the Acrolein DNA Adduct  $\gamma$ -OH-1,N<sup>2</sup>-Propano-2'-Deoxyguanosine, *J. Am. Chem. Soc.* **2002**, *124*, 9324-9325.
- (11) Plastaras, J. P.; Riggins, J. N.; Otteneder, M.; Marnett, L. J., Reactivity and Mutagenicity of Endogenous DNA Oxopropenylating Agents: Base Propenals, Malondialdehyde, and N-Epsilon-Oxopropenyllysine, *Chem. Res. Toxicol.* **2000**, *13*, 1235-1242.
- (12) Kozekov, I. D., Nechev, L.V., Sanchez, A., Harris, C.M., Lloyd, R.S., Harris, T.M., Interchain Cross Linking of DNA Mediated by the Principal Adduct of Acrolein., *Chem. Res. Toxicol.* **2001**, *14*, 1482-1485.
- (13) Weinert, E. E., Quinone Methide Alkylation of DNA: Understanding Reactivity through Reversibility, Trapping, and Substituent Effects, Doctoral Dissertation, University of Maryland, College Park, 2006.
- (14) Dale L. Boger, W. Y., Reversibility of the Duocarmycin a and Sa DNA Alkylation Reaction, *J. Am. Chem. Soc.* **1993**, *115*, 9872.
- (15) Boger, D. L.; Garbaccio, R. M., Shape-Dependent Catalysis: Insights into the Source of Catalysis for the CC-1065 and Duocarmycin DNA Alkylation Reaction, *Acc. Chem. Res.* **1999**, *32*, 1043-1052.

- (16) Warpehoski, M. A., Harper, D.E., Mitchell, M.A., Monroe, T.J. , Reversibility of the Covalent Reaction of CC-1065 and Analogues with DNA, *Biochemistry* **1992**, *31*, 2502-2508.
- (17) Thompson DC, T. J., Sugumaran M, Moldéus P., Biological and Toxicological Consequences of Quinone Methide Formation, *Chem Biol Interact.* **1993**, *86*, 129.
- (18) Modica, E.; Zanaletti, R.; Freccero, M.; Mella, M., Alkylation of Amino Acids and Glutathione in Water by O-Quinone Methide. Reactivity and Selectivity, *J. Org. Chem.* **2001**, *66*, 41-52.
- (19) Richter, S. N.; Maggi, S.; Mels, S. C.; Palumbo, M.; Freccero, M., Binol Quinone Methides as Bisalkylating and DNA Cross-Linking Agents, *J. Am. Chem. Soc.* **2004**, *126*, 13973-13979.
- (20) Diao, L.; Yang, C.; Wan, P., Quinone Methide Intermediates from the Photolysis of Hydroxybenzyl Alcohols in Aqueous Solution, *J. Am. Chem. Soc.* **1995**, *117*, 5369-5370.
- (21) Padwa, A.; Dehm, D.; Oine, T.; Lee, G. A., Competitive Keto-Enolate Photochemistry in 3-Phenylisocoumaranone System, *J. Am. Chem. Soc.* **1975**, *97*, 1837-1845.
- (22) Rosenau, T.; Habicher, W. D., Novel Tocopherol Compounds. 1. Bromination of  $\alpha$ -tocopherol - Reaction Mechanism and Synthetic Applications, *Tetrahedron* **1995**, *51*, 7919-7926.
- (23) Moore, R. F.; Waters, W. A., Some Products Formed from Phenolic Inhibitors During the Autoxidation of Cumene, *J. Chem. Soc.* **1954**, 243-246.

- (24) Warpehoski, M. A. H., laurence H., Sequence Selectivity of DNA Covalent Modification, *Chem. Res. Toxicol.* **1988**, *1*, 315-333.
- (25) Wang, P.; Song, Y.; Zhang, L.; He, H.; Zhou, X., Quinone Methide Derivatives: Important Intermediates to DNA Alkylating and DNA Cross-Linking Actions, *Curr. Med. Chem.* **2005**, *12*, 2893-2913.
- (26) Tomasz, M., Mitomycin C: Small, Fast and Deadly (but Very Selective), *Chemistry & Biology* **1995**, *2*, 575-579.
- (27) Das, A., Tang, K.S., Gopalakrishnan, S., Waring, M.J., Tomasz, M., Reactivity of Guanine at M(5)Cpg Steps in DNA: Evidence for Electronic Effects Transmitted through the Base Pairs, *Chem. Biol.* **1999**, *6*, 461.
- (28) Thomas, M. G.; Lawson, C.; Allanson, N. M.; Leslie, B. W.; Bottomley, J. R.; McBride, A.; Olusanya, O. A., A Series of 2(Z)-2-Benzylidene-6,7-Dihydroxybenzofuran-3 2h -Ones as Inhibitors of Chorismate Synthase, *Bioorg. Med. Chem. Lett.* **2003**, *13*, 423-426.
- (29) Pande, P.; Shearer, J.; Yang, J.; Greenberg, W. A.; Rokita, S. E., Alkylation of Nucleic Acids by a Model Quinone Methide, *J. Am. Chem. Soc.* **1999**, *121*, 6773-6779.
- (30) Veldhuyzen, W. F.; Lam, Y. F.; Rokita, S. E., 2'-Deoxyguanosine Reacts with a Model Quinone Methide at Multiple Sites, *Chem. Res. Toxicol.* **2001**, *14*, 1345-1351.
- (31) Zhou, Q.; Rokita, S. E., A General Strategy for Target-Promoted Alkylation in Biological Systems, *Proc. Natl. Acad. Sci. U. S. A.* **2003**, *100*, 15452-15457.

- (32) Lewis, M. A., Yoerg, D.G., Bolton, J.L., Thompson, J.A., Alkylation of 2'-Deoxynucleosides and DNA by Quinone Methides Derived from 2,6-Di-Tert-Butyl- 4-Methylphenol., *Chem. Res. Toxicol.* **1996**, *9*, 1368-1374.
- (33) Weinert, E. E.; Frankenfield, K. N.; Rokita, S. E., Time-Dependent Evolution of Adducts Formed between Deoxynucleosides and a Model Quinone Methide, *Chem. Res. Toxicol.* **2005**, *18*, 1364-1370.
- (34) Wang, H.; Wahl, M. S.; Rokita, S. E., Immortalizing a Transient Electrophile for DNA Cross-Linking, *Angew. Chem., Int. Ed.* **2008**, *47*, 1291-1293.
- (35) Weinert, E. E.; Dondi, R.; Colloredo-Melz, S.; Frankenfield, K. N.; Mitchell, C. H.; Freccero, M.; Rokita, S. E., Substituents on Quinone Methides Strongly Modulate Formation and Stability of Their Nucleophilic Adducts, *J. Am. Chem. Soc.* **2006**, *128*, 11940-11947.
- (36) Weinert, E. E., Quinone Methide Alkylation of DNA: Understanding Reactivity through Reversibility, Trapping, and Substituent Effects, Doctoral Thesis, University of Maryland, 2006.
- (37) Felsenfeld, G.; Rich, A., Studies on the Formation of 2-Stranded and 3-Stranded Polyribonucleotides, *Biochim. Biophys. Acta* **1957**, *26*, 457-468.
- (38) Jain, A.; Wang, G.; Vasquez, K. M., DNA Triple Helices: Biological Consequences and Therapeutic Potential, *Biochimie* **2008**, *90*, 1117-1130.
- (39) Singleton, S. F.; Dervan, P. B., Influence of pH on the Equilibrium Association Constants for Oligodeoxyribonucleotide-directed Triple Helix Formation at Single DNA Sites *Biochemistry* **1992**, *31*, 10995-11003.

- (40) Beal, P. A.; Dervan, P. B., 2nd Structural Motif for Recognition of DNA by Oligonucleotide-Directed Triple-Helix Formation *Science* **1991**, *251*, 1360-1363.
- (41) Cheng, A. J.; Vandyke, M. W., Oligodeoxyribonucleotide Length and Sequence Effects on Intermolecular Purine-Purine-Pyrimidine Triple-Helix Formation *Nucleic Acids Res.* **1994**, *22*, 4742-4747.
- (42) Hampel, K. J.; Crosson, P.; Lee, J. S., Polyamines Favor DNA Triplex Formation at Neutral pH, *Biochemistry* **1991**, *30*, 4455-4459.
- (43) Gaddis S.S. , W. Q., Thames H. D. , DiGiovanni J. , Walborg E. F. , MacLeod M. C. , Vasquez K. M., A Web-Based Search Engine for Triplex-Forming Oligonucleotide Target Sequences, *Oligonucleotides* **2006**, *16*, 196-201.
- (44) Majumdar, A.; Puri, N.; Cuenoud, B.; Natt, F.; Martin, P.; Khorlin, A.; Dyatkina, N.; George, A. J.; Miller, P. S.; Seidman, M. M., Cell Cycle Modulation of Gene Targeting by a Triple Helix-Forming Oligonucleotide, *J. Biol. Chem.* **2003**, *278*, 11072-11077.
- (45) Veldhuyzen, W. F.; Shallop, A. J.; Jones, R. A.; Rokita, S. E., Thermodynamic Versus Kinetic Products of DNA Alkylation as Modeled by Reaction of Deoxyadenosine, *J. Am. Chem. Soc.* **2001**, *123*, 11126-11132.
- (46) Weinert, E. E.; Frankenfield, K. N.; Rokita, S. E., Time-Dependent Evolution of Adducts Formed between Deoxynucleosides and a Model Quinone Methide, *Chem. Res. Toxicol.* **2005**, *18*, 1364-1370.
- (47) Corey, E. J.; Venkates.A, Protection of Hydroxyl Groups as Tert-Butyldimethylsilyl Derivatives, *J. Am. Chem. Soc.* **1972**, *94*, 6190-&.



- (48) Chen, G.; Tokunaga, N.; Hayashi, T., Rhodium-Catalyzed Asymmetric 1,4-Addition of Arylboronic Acids to Coumarins: Asymmetric Synthesis of (*R*)-Tolterodine, *Org. Lett.* **2005**, *7*, 2285-2288.
- (49) Al-Maharik, N.; Botting, N. P., A New Short Synthesis of Coumestrol and Its Application for the Synthesis of [6,6a,11a-<sup>13</sup>C<sub>3</sub>]Coumestrol, *Tetrahedron* **2004**, *60*, 1637-1642.
- (50) Gustin, J. L., Vent Sizing for the Phenol Plus Formaldehyde Reaction, *Org. Process Res. Dev.* **2006**, *10*, 1263-1274.
- (51) Kraus, G. A.; Nguyen, T.; Bae, J.; Hostetter, J.; Steadham, E., Synthesis and Antitubercular Activity of Tricyclic Analogs of Puupehenone, *Tetrahedron* **2004**, *60*, 4223-4225.
- (52) Li, J.; Rush Iii, T. S.; Li, W.; DeVincentis, D.; Du, X.; Hu, Y.; Thomason, J. R.; Xiang, J. S.; Skotnicki, J. S.; Tam, S.; Cunningham, K. M.; Chockalingam, P. S.; Morris, E. A.; Levin, J. I., Synthesis and Sar of Highly Selective Mmp-13 Inhibitors, *Bioorg. Med. Chem. Lett.* **2005**, *15*, 4961-4966.
- (53) Laganis, E. D.; Chenard, B. L., Metal Silanolates - Organic Soluble Equivalents for O-2, *Tetrahedron Lett.* **1984**, *25*, 5831-5834.
- (54) Ganem, B.; Small, V. R., Ferric-Chloride in Acetic-Anhydride - Mild and Versatile Reagent for Cleavage of Ethers, *J. Org. Chem.* **1974**, *39*, 3728-3730.
- (55) Hornberger, K. R.; Hamblett, C. L.; Leighton, J. L., Total Synthesis of Leucascandrolide A, *J. Am. Chem. Soc.* **2000**, *122*, 12894-12895.
- (56) Shirali, A.; Sriram, M.; Hall, J. J.; Nguyen, B. L.; Guddneppanavar, R.; Hadimani, M. B.; Ackley, J. F.; Siles, R.; Jelinek, C. J.; Arthasery, P.; Brown,

- R. C.; Murrell, V. L.; MeMordie, A.; Sharma, S.; Chaplin, D. J.; Pinney, K. G., Development of Synthetic Methodology Suitable for the Radiosynthesis of Combretastatin A-1 (CA1) and Its Corresponding Prodrug CA1P, *J. Nat. Prod.* **2009**, *72*, 414-421.
- (57) Veldhuyzen, W. F.; Pande, P.; Rokita, S. E., A Transient Product of DNA Alkylation Can Be Stabilized by Binding Localization, *J. Am. Chem. Soc.* **2003**, *125*, 14005-14013.
- (58) Demyttenaere, J.; Van Syngel, K.; Markusse, A. P.; Vervisch, S.; Debenedetti, S.; De Kimpe, N., Synthesis of 6-Methoxy-4H-1-Benzopyran-7-ol, a Character Donating Component of the Fragrance of *Wisteria Sinensis*, *Tetrahedron* **2002**, *58*, 2163-2166.
- (59) Cincinelli, R.; Dallavalle, S.; Nannei, R.; Carella, S.; De Zani, D.; Merlini, L.; Penco, S.; Garattini, E.; Giannini, G.; Pisano, C.; Vesci, L.; Carminati, P.; Zuco, V.; Zanchi, C.; Zunino, F., Synthesis and Structure-Activity Relationships of a New Series of Retinoid-Related Biphenyl-4-ylacrylic Acids Endowed with Antiproliferative and Proapoptotic Activity, *J. Med. Chem.* **2005**, *48*, 4931-4946.
- (60) Corey, E. J.; Venkateswarlu, A., Protection of Hydroxyl Groups as Tert-Butyldimethylsilyl Derivatives, *J. Am. Chem. Soc.* **1972**, *94*, 6190-6191.
- (61) Laganis, E. D.; Chenard, B. L., Metal Silanolates: Organic Soluble Equivalents for O-2, *Tetrahedron Lett.* **1984**, *25*, 5831-5834.
- (62) Hornberger, K. R.; Hamblett, C. L.; Leighton, J. L., Total Synthesis of Leucascandrolide A, *J. Am. Chem. Soc.* **2000**, *122*, 12894-12895.

- (63) Mangas-Sanchez, J.; Rodriguez-Mata, M.; Busto, E.; Gotor-Fernandez, V.; Gotor, V., Chemoenzymatic Synthesis of Rivastigmine Based on Lipase-Catalyzed Processes, *J. Org. Chem.* **2009**, *74*, 5304-5310.
- (64) Liu, Y.; Rokita, S. E., Inducible Alkylation of DNA by a Quinone Methide-Peptide Nucleic Acid Conjugate, *Biochemistry* **2012**, *51*, 1020-1027.
- (65) Felsenfeld, G.; Davies, D. R.; Rich, A., Formation of a 3-Stranded Polynucleotide Molecule, *J. Am. Chem. Soc.* **1957**, *79*, 2023-2024.
- (66) Xodo, L. E.; Manzini, G.; Quadrifoglio, F.; Vandermarel, G. A.; Vanboom, J. H., Effect of 5-Methylcytosine on the Stability of Triple-Stranded DNA— a Thermodynamic Study, *Nucleic Acids Res.* **1991**, *19*, 5625-5631.
- (67) Krawczyk, S. H.; Milligan, J. F.; Wadwani, S.; Moulds, C.; Froehler, B. C.; Matteucci, M. D., Oligonucleotide-Mediated Triple Helix Formation Using an N3-Protonated Deoxycytidine Analog Exhibiting pH-Independent Binding within the Physiological Range, *Proc. Natl. Acad. Sci. U. S. A.* **1992**, *89*, 3761-3764.
- (68) Majumdar, A.; Khorlin, A.; Dyatkina, N.; Lin, F. L. M.; Powell, J.; Liu, J.; Feiz, Z. Z.; Khripine, Y.; Watanabe, K. A.; George, J.; Glazer, P. M.; Seidman, M. M., Targeted Gene Knockout Mediated by Triple Helix Forming Oligonucleotides, *Nat. Genet.* **1998**, *20*, 212-214.
- (69) Alam, M. R.; Majumdar, A.; Thazhathveetil, A. K.; Liu, S. T.; Liu, J. L.; Puri, N.; Cuenoud, B.; Sasaki, S.; Miller, P. S.; Seidman, M. M., Extensive Sugar Modification Improves Triple Helix Forming Oligonucleotide Activity in Vitro but Reduces Activity in Vivo, *Biochemistry* **2007**, *46*, 10222-10233.

- (70) Asensio, J. L.; Carr, R.; Brown, T.; Lane, A. N., Conformational and Thermodynamic Properties of Parallel Intramolecular Triple Helices Containing a DNA, RNA, or 2'-OMeDNA Third Strand, *J. Am. Chem. Soc.* **1999**, *121*, 11063-11070.
- (71) Chan, P. P.; Glazer, P. M., Triplex DNA: Fundamentals, Advances, and Potential Applications for Gene Therapy, *J. Mol. Med.* **1997**, *75*, 267-282.
- (72) Moser, H. E.; Dervan, P. B., Sequence-Specific Cleavage of Double Helical DNA by Triple Helix Formation, *Science* **1987**, *238*, 645-650.
- (73) Landgraf, R.; Chen, C. H. B.; Sigman, D. S., Oligonucleotide-Directed Nucleic-Acid Scission by Micrococcal Nuclease, *Biochemistry* **1994**, *33*, 10607-10615.
- (74) Giovannangeli, C.; Montenaygarestier, T.; Rougee, M.; Chassignol, M.; Thuong, N. T.; Helene, C., Single-Stranded-DNA as a Target for Triple-Helix Formation, *J. Am. Chem. Soc.* **1991**, *113*, 7775-7777.
- (75) Wang, S. H.; Kool, E. T., Recognition of Single-Stranded Nucleic-Acids by Triplex Formation - the Binding of Pyrimidine-Rich Sequences, *J. Am. Chem. Soc.* **1994**, *116*, 8857-8858.
- (76) Samadashwily, G. M.; Mirkin, S. M., Trapping DNA-Polymerases Using Triplex-Forming Oligodeoxyribonucleotides, *Gene* **1994**, *149*, 127-136.
- (77) Puri, N.; Majumdar, A.; Cuenoud, B.; Natt, F.; Martin, P.; Boyd, A.; Miller, P. S.; Seidman, M. M., Targeted Gene Knockout by 2'-O-Aminoethyl Modified Triplex Forming Oligonucleotides, *J. Biol. Chem.* **2001**, *276*, 28991-28998.

- (78) Puri, N.; Majumdar, A.; Cuenoud, B.; Natt, F.; Martin, P.; Boyd, A.; Miller, P. S.; Seidman, M. M., Minimum Number of 2'-O-(2-Aminoethyl) Residues Required for Gene Knockout Activity by Triple Helix Forming Oligonucleotides, *Biochemistry* **2002**, *41*, 7716-7724.
- (79) Zhou, Q. B.; Pande, P.; Johnson, A. E.; Rokita, S. E., Sequence-Specific Delivery of a Quinone Methide Intermediate to the Major Groove of DNA, *Bioorg. Med. Chem.* **2001**, *9*, 2347-2354.
- (80) Pande, P.; Shearer, J.; Yang, J.; Greenberg, W. A.; Rokita, S. E., Alkylation of Nucleic Acids by a Model Quinone Methide, *J. Am. Chem. Soc.* **1999**, *121*, 6773-6779.
- (81) Shindo, H.; Torigoe, H.; Sarai, A., Thermodynamic and Kinetic Studies of DNA Triplex Formation of an Oligohomopyrimidine and a Matched Duplex by Filter Binding Assay, *Biochemistry* **1993**, *32*, 8963-8969.
- (82) Zhou, Q.; Pande, P.; Johnson, A. E.; Rokita, S. E., Sequence-Specific Delivery of a Quinone Methide Intermediate to the Major Groove of DNA. [Erratum to Document Cited in Ca135:354282], *Bioorg. Med. Chem.* **2002**, *10*, 2089.
- (83) Ping, Y. H.; Rana, T. M., Mechanism of Site-Specific Psoralen Photoadducts Formation in Triplex DNA Directed by Psoralen-Conjugated Oligonucleotides, *Biochemistry* **2005**, *44*, 2501-2509.